



Universiteit
Leiden
The Netherlands

Plant Agc protein kinases orient auxin-mediated differential growth and organogenesis

Galván Ampudia, C.S.

Citation

Galván Ampudia, C. S. (2009, December 15). *Plant Agc protein kinases orient auxin-mediated differential growth and organogenesis*. Retrieved from <https://hdl.handle.net/1887/14506>

Version: Corrected Publisher's Version

License: [Licence agreement concerning inclusion of doctoral thesis in the Institutional Repository of the University of Leiden](#)

Downloaded from: <https://hdl.handle.net/1887/14506>

Note: To cite this publication please use the final published version (if applicable).

**Plant AGC protein kinases orient auxin-mediated
differential growth and organogenesis**

Carlos Samuel Galván Ampudia

**Plant AGC protein kinases orient auxin-mediated
differential growth and organogenesis**

Proefschrift

Ter verkrijging van
de graad van Doctor aan de Universiteit Leiden,
op gezag van Rector Magnificus Prof. mr. P. F. van der Heijden,
volgens besluit van het College voor Promoties
te verdedigen op dinsdag 15 december 2009
klokke 10.00 uur

door

Carlos Samuel Galván Ampudia

geboren te Monterrey (México) in 1978

Promotiecommissie

Promotor: Prof. Dr. P.J.J. Hooykaas

Co-promotor: Dr. R. Offringa

Overige leden: Prof. Dr. L. Bögre
Prof. Dr. M. Janson
Dr. C.S. Testerink
Prof . Dr. J. Memelink

CONTENTS		Page
<i>Chapter 1</i>	Plant evolution: AGC kinases tell the auxin tale	9
<i>Chapter 2</i>	Getting back in TOUCH: calcium-dependent feed back on auxin transport	31
<i>Chapter 3</i>	PINOID signaling regulated by small calcium binding Proteins	63
<i>Chapter 4</i>	Fine tuning PINOID action by PDK1-mediated phosphorylation	95
<i>Chapter 5</i>	AGC3 kinases orient plant development by directing PIN polar targeting	119
Summary		151
Samenvatting		157
<i>Curriculum vitae</i>		163
<i>Publication list</i>		164

CHAPTER 1

Plant evolution: AGC kinases tell the auxin tale

Carlos S. Galván-Ampudia and Remko Offringa

Modified from Galván-Ampudia and Offringa (2007), *Trends Plant Sci* **12**, 541-547

Summary

The signaling molecule auxin is a central regulator of plant development, which instructs tissue and organ patterning, and couples environmental stimuli to developmental responses. Here, we discuss the function of PINOID (PID) and the phototropins, members of the plant specific AGCVIII protein kinases, and their role in triggering and regulating development by controlling PIN-FORMED (PIN) auxin transporter-generated auxin gradients and maxima. We propose that the *AGCVIII* kinase gene family evolved from an ancestral phototropin gene, and that the co-evolution of PID-like and PIN gene families marks the transition of plants from water to land. We hypothesize that the PID-like kinases function in parallel to, or downstream of, the phototropins to orient plant development by establishing the direction of polar auxin transport.

Plant development directed by the hormone auxin

The development of flowering plants is dualistic: on one hand, it follows strict programs producing uniform flowers and embryos; on the other hand, it can be flexible, particularly during vegetative development. In view of the predominantly sessile nature of plants, this flexible development is crucial to enable adaptation to changes in the environment. The plant hormone auxin is well recognized as a central regulator of both flexible growth responses, like tropisms, and strict developmental programs, such as organ formation and patterning [1-5]. A characteristic of this signaling molecule is that it is actively transported in a directional manner, e.g. from young developing aerial organs to the root system. This polar auxin transport (PAT) generates auxin maxima and gradients that are instrumental in directing growth and in positioning the formation of new organs. The chemiosmotic hypothesis proposed in the 1970s for auxin transport predicted that asymmetrically-distributed auxin efflux carriers are the drivers of PAT. Two types of proteins have now been acknowledged as auxin efflux carriers. Firstly, the PIN family of transporters was identified through the *Arabidopsis pin-formed* and *ethylene-insensitive root 1* mutants that phenocopied wild-type plants grown on PAT inhibitors. These mutants led to the cloning of respectively *PIN1* and *PIN2*, and the subsequent identification of 6 other *PIN* genes in the *Arabidopsis* genome. The PIN1-type proteins PIN1, 2, 3, 4 and 7 show different, tissue- and cell-type specific asymmetric subcellular localization at the plasma membrane, and play crucial roles in phyllotaxis, tropic growth and embryo patterning [6]. PIN5, 6 and 8 were found to localize to the endoplasmatic reticulum, where they may be involved in regulating auxin homeostasis in the cytosol. The PIN1-type auxin-efflux carriers have been characterized as central rate-limiting components that determine the direction of auxin transport through their asymmetric subcellular localization [6-10]. In addition, several multi-drug-resistant/P-glycoprotein (MDR/PGP)-type ATP-binding cassette (ABC) proteins were shown to act as auxin efflux carriers [11]. In contrast to PIN proteins, MDR/PGP proteins in most cases do not show a pronounced asymmetric subcellular localization, and it is as yet unclear whether they are part of the PIN-dependent or another parallel auxin transport pathway [6;11].

What determines and regulates the polar subcellular localization of the PIN membrane proteins and thereby the direction of polar auxin transport? By using the vesicle trafficking inhibitor brefeldin A (BFA) in combination with different cytoskeleton inhibitors, Geldner and coworkers showed that PIN1-loaded vesicles cycle via the actin cytoskeleton between plasma membrane and endosomal compartments [12]. Treatment with BFA blocks the exocytosis step, resulting in the accumulation of PIN proteins in BFA compartments. Analogous to animal vesicle trafficking, an ADP ribosylation factor - GTP exchange factor (ARF-GEF) named GNOM was identified as the BFA sensitive component in the recycling of PIN1 vesicles to the plasma membrane [13]. PIN1 is randomly distributed at the plasma membrane in cells of *gnom* mutant embryos [14], suggesting that the initiation of recycling by the GNOM ARF-GEF is required to maintain, rather than to determine PIN polarity.

The only component in the polar targeting of PIN proteins that has so far been identified is the PINOID (PID) protein kinase [15]. The *PID* gene was identified through *Arabidopsis pid* loss-of-function mutants that phenocopy the *pin1* mutant. The phenotype of the *pid* mutant already suggested a role for PID as a regulator of PAT [16;17]. More recently, it was shown that PID is necessary for proper apical localization of PIN1 proteins in epidermal cells of the inflorescence meristem, which is required to generate auxin maxima in the meristem that are initiation points for lateral organ formation. In *pid* loss-of-function mutants, PIN1 localizes at the basal membrane, which deprives the meristem of auxin, and prevents the initiation and positioning of new lateral organs, thus resulting in the pin-shaped inflorescences that are characteristic for the *pid* mutant [15]. The action of PID does not seem to be restricted to the polar targeting of PIN1, as overexpression of *PID* results in a basal-to-apical (bottom-to-top) switch of PIN1 as well as PIN2 and PIN4 in root meristem cells. The fact that different PIN proteins are apicalized in response to PID and that *PID* expression is upregulated by auxin, suggests that PID is involved in feedback control of PAT [15;16;18-20].

A previous comparison of the PID protein kinase with known kinases indicated that it classifies to the plant-specific AGCVIII protein serine-threonine kinases [16;21]. AGC kinases are named after protein kinase A (PKA), cyclic GMP-dependent protein kinase (PKG) and protein kinase C (PKC), three classes of animal protein kinases that are

involved in receptor-mediated growth factor signal transduction. We have performed a detailed bioinformatics analysis of the *Arabidopsis* AGCVIII kinase family, which besides PID, also comprises the well-known phototropins [22], and have studied their evolutionary origin and function in plant development. We hypothesize that AGCVIII kinases evolved from an ancestral phototropin, and that the acquisition of PID and the PIN transporters in plant evolution marks the transition of plants from water to land. Below we summarize the data that support our hypothesis.

The plant-specific characteristics of the AGCVIII kinases

The *Arabidopsis* genome encodes 37 AGC kinases, of which 23 classify to the AGCVIII group (Figure 1). Flowering plants do not have the typical animal PKA, PKC and PKG kinases. The AGCVIII kinases might therefore represent plant orthologs of these animal kinases.

One characteristic of members of the AGCVIII subfamily is the substitution of the conserved DFG motif in subdomain VII of the catalytic domain for DFD (Figure 2a). The DFD triplet is not plant-specific and defines a class of AGC protein kinases that can be found in all eukaryotes. Another characteristic is the presence of an amino acid insertion between the conserved subdomains VII and VIII of the catalytic domain (VII–VIII insertion), which ranges from 36 to 90 residues in the *Arabidopsis* family members (Figure 2a and b). The insertion in combination with the DFD triplet is specific for the plant AGC group of protein kinases. Recent data suggest a role for the VII–VIII insertion in the subcellular localization of these protein kinases [23].

Phylogeny of the *Arabidopsis* AGCVIII kinases

To determine the evolutionary relationships between the members of the *Arabidopsis* AGCVIII subfamily, the sequences corresponding to the catalytic domain were used to construct an AGCVIII-specific phylogenetic tree (Figure 2b). A previous phylogenetic analysis using the full-length amino acid sequences of the plant AGC kinases indicated that they classified into two groups [24]. However, in our analysis, we found that AGCVIII kinases classify into four distinct groups that we named AGC1–AGC4 (Figure 2).

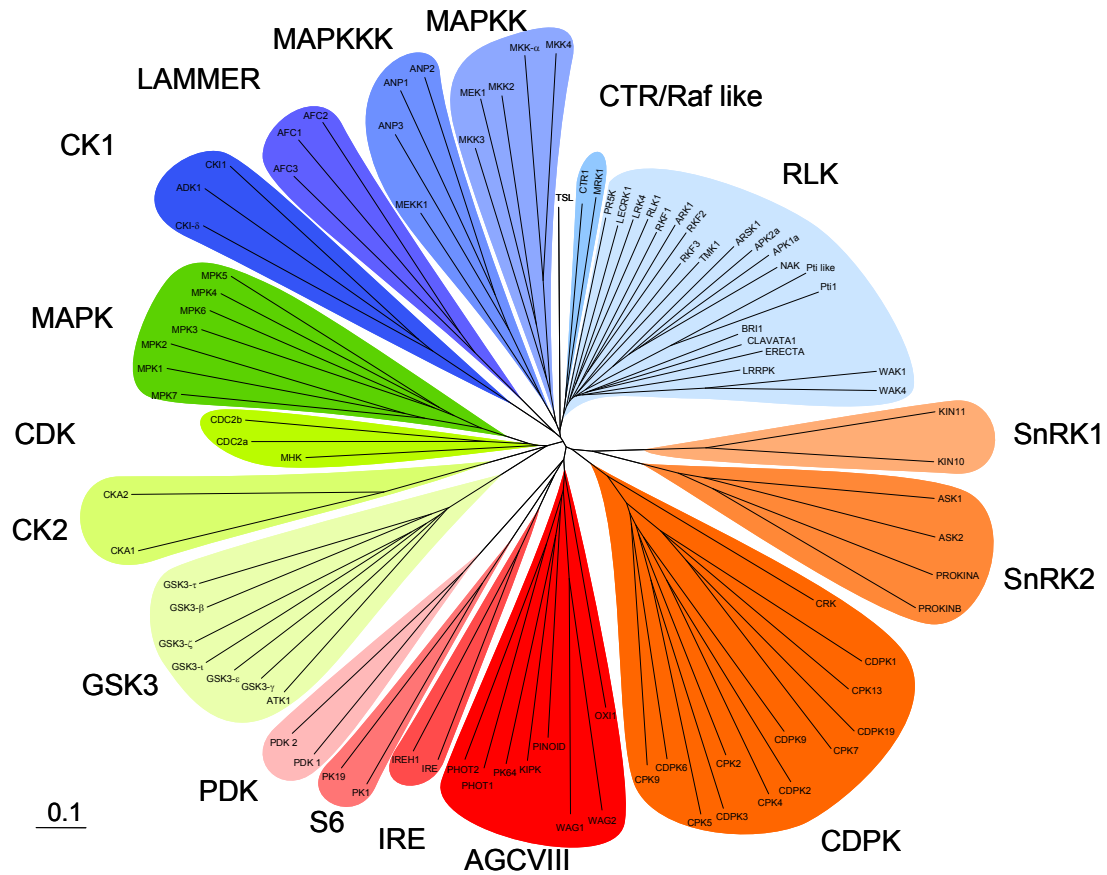


Figure 1. Phylogenetic tree of the *Arabidopsis* protein serine–threonine kinases. To visualize the position of PID and its relatives within the *Arabidopsis* kinome, 109 protein kinase sequences were selected from the TAIR database (<http://www.Arabidopsis.org/>), representing almost all of the known protein kinase subfamilies. A phylogenetic tree was constructed based on the amino acid sequences corresponding to the protein kinase catalytic domains: in red the AGC subfamily, in orange the CaMK subfamily, in green the CMGC subfamily and in blue the “Others” subfamily.

The largest group (AGC1) is formed by 13 putative protein kinases and comprises orthologues of the first protein kinases to be identified in plants, for example, *Phaseolus vulgaris* protein kinase 1 (PvPK1) [25].

The AGC4 group is formed by the phototropins PHOT1 and PHOT2, which are characterized by an N-terminal photoreceptor domain with two chromophore-binding LOV domains and a C-terminal protein kinase domain [26]. PID, AGC3-4, WAG1 and WAG2 (“wag” after the phenotype of the corresponding mutants, which have an enhanced sinusoidal growth of the root, also known as root waving [27]) form the third

group (AGC3). The kinases within these three subgroups share conserved residues within the VII–VIII insertion, including a conserved AEP triplet that is located close to subdomain VIII (Figure 2a). Interestingly, this AEP triplet is not found in the four remaining kinases that form the AGC2 group, which demonstrates that they are more distantly related to phototropins than was previously thought [24] (Figure 2).

The genes encoding AGCVIII members are not clustered or do not show a clear organization in the *Arabidopsis* genome [23] (Figure 2b). Five of the genes do not contain an intron, whereas the other 18 genes contain one or more introns. Interestingly, one intron is found in members of all four groups at a conserved position in the region encoding kinase subdomain VIa (Figure 2b), indicating that the *AGCVIII* genes originate from a single ancestral kinase. *AtPHOT1* and *AtPHOT2* carry multiple introns at identical positions, corroborating their relatedness.

In conclusion, our analysis of the *Arabidopsis* AGCVIII kinases shows that they classify into four groups, and indicates that the encoding gene family originated from a single ancestral kinase gene through multiple independent duplication steps. Interestingly, each group seems to perform a different function in plants, with AGC1 kinases having a role in cell organization [28], AGC2 kinases in stress responses [29;30], AGC3 kinases in the regulation of PAT [16;31] and AGC4 kinases in chloroplast avoidance and phototropism [32;33]. The last two subgroups have clear links with PAT and will therefore be discussed in more detail.

Phototropins - remnants of the ancestral plant AGCVIII kinase

Phototropins, which constitute the AGC4 group, were discovered through a screen for *Arabidopsis* mutants that lack directive growth of the hypocotyl of dark-grown seedlings towards a blue light source [33]. This screen identified several non-phototropic mutants, one of which is mutated in the gene encoding the blue light receptor PHOT1 [22;33]. The *Arabidopsis* genome also encodes a homologue of PHOT1 known as PHOT2 [22]. PHOT1 is the major player in the phototropic growth of seedling hypocotyls and roots at low fluence rate conditions (low intensity light), while PHOT2 functions in triggering the auxin-mediated phototropic response under high fluence rate conditions (high intensity

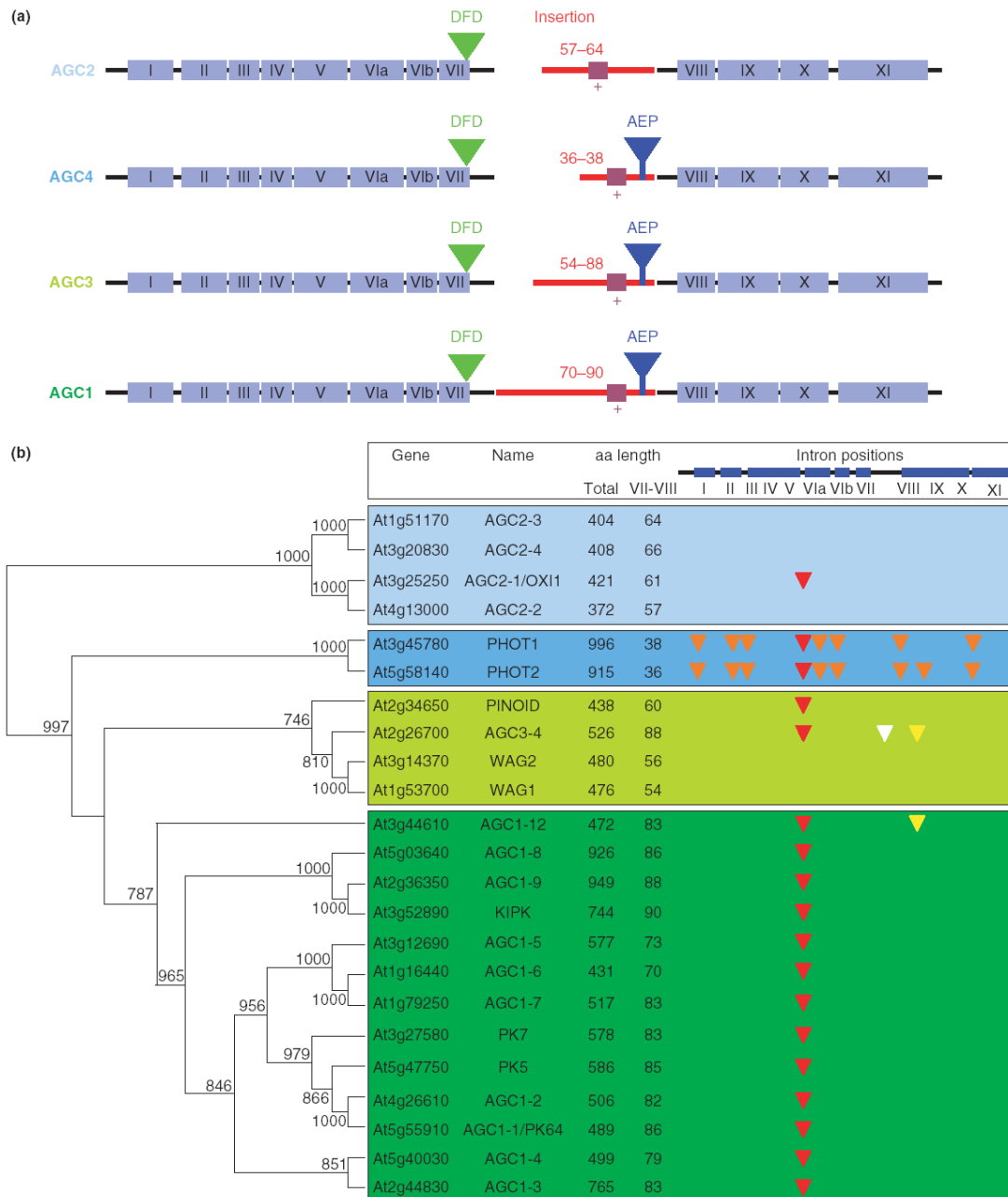


Figure 2. The *Arabidopsis* AGCVIII protein kinase family.

(a) Schematic representation of the catalytic kinase domain of the *Arabidopsis* AGCVIII protein kinases. The eleven conserved subdomains of the catalytic kinase domain are represented as blue boxes labeled with Roman numbers. The (length of the) amino acid insertion between sub-domains VII and VIII (red), the typical DFD (Asp-Phe-Asp) signature in sub-domain VII (green), the conserved basic pocket (purple), and the AEP (Ala-Glu-Pro) triplet close to sub-domain VIII (blue) are indicated.

Figure 2 (continued)

(b) Phylogenetic tree of the 23 *Arabidopsis* AGCVIII protein kinases based on an alignment of their catalytic kinase domains subdivides the *Arabidopsis* AGCVIII kinases into four distinct groups. A comparison of the total protein size, the length of the VII-VIII insertion and the intron positions within the region coding for the catalytic domain is indicated. The positions of the highly conserved intron (red arrowheads) and the more variable introns (orange and yellow arrowheads) are indicated.

light). Moreover, the PHOTs have been found to function redundantly in blue-light-induced chloroplast movement and stomatal opening [26]. Phototropins are the only members of the AGCVIII family so far identified in unicellular green algae. Therefore, they might represent the first descendants of the ancestral AGCVIII protein kinase. The *PHOT* gene of the green alga *Chlamydomonas* can partially restore phototropism, chloroplast positioning and stomatal opening in response to blue light when expressed in the *Arabidopsis phot1 phot2* double mutant [34], indicating that phototropin function and signaling is conserved in plants and algae. A comparison of catalytic kinase domains of 31 selected phototropin-related proteins from 14 representative plant species revealed two major groups (Figure 3): (i) the PHOT1-like proteins that are characterized by the conserved CLTSCKPQ signature in the VII–VIII insertion and (ii) the PHOT2-like proteins. Interestingly, genes encoding PHOT2-like photoreceptors are found in all plant groups, whereas the *PHOT1-like* genes are restricted to seed plants (Table 1, Figure 3). Taking all these observations into consideration, we speculate that optimization of light perception mediated by PHOT2-like proteins, e.g. the high fluence rate light avoidance of chloroplasts, is one of the ancient traits in plant evolution. A more detailed analysis and functional characterization of phototropins throughout the plant kingdom should provide further evidence for our hypothesis.

AGC3 kinases direct auxin transport

The PID-containing subgroup (AGC3) is composed of four genes in both *Arabidopsis* and the monocot *Oryza sativa*, and our analysis identified homologous genes in numerous plant species from the moss *Physcomitrella patens* to the monocot *Zea mays*, but not in unicellular algae (Table 1). Apart from PID, two other AGC3 members in *Arabidopsis*

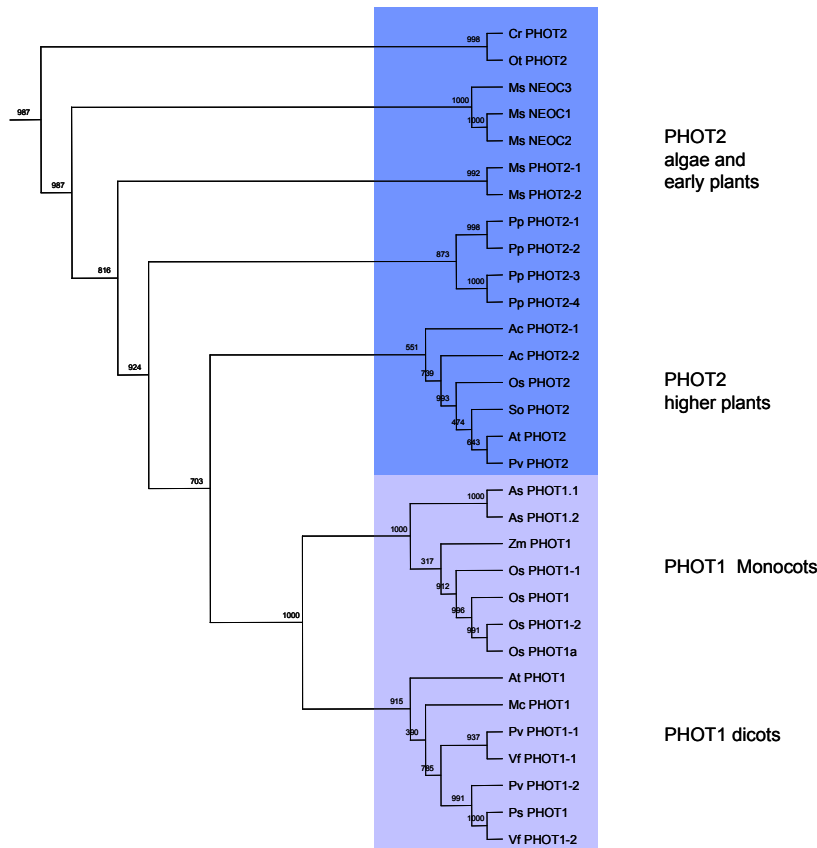


Figure 3. Phototropin phylogeny. *PHOT2-like* genes can be found throughout the plant kingdom, indicating that they represent remnants of an ancestral gene, whereas *PHOT1-like* genes occur only later in plant evolution, in spermatophyta. Alignment of the amino acid sequences of the protein kinase catalytic domain of phototropins of representative plant species identifies two major groups: *PHOT2-like* genes (dark blue) and *PHOT1-like* genes (light blue). Abbreviations: Ac: *Adiantum capillus-veneris* (maidenhair); As: *Avena sativa* (oat); At: *Arabidopsis thaliana* (Mouse-ear cress); Cr: *Chlamydomonas reinhardtii* (a green alga); Mc: *Mesembryanthemum crystallinum* (iceplant); Ms: *Mougeotia scalaris* (a green alga); Os: *Oryza sativa* (rice); Ot: *Ostreococcus tauri* (a green alga); Pp: *Physcomitrella patens* (a moss); Ps: *Pisum sativum* (pea); Pv: *Phaseolus vulgaris* (common bean); So: *Spinacia oleracea* (spinach); Vf: *Vicia faba* (fava bean); Zm: *Zea mays* (maize).

have been characterized in more detail: WAG1 and WAG2. Homologues of *WAG1* were initially discovered in *Cucumis sativus* and *Pisum sativum* as auxin-induced and light-repressed genes [35-38]. Also the *Arabidopsis* *WAG1* and *WAG2* transcript levels were found to be negatively regulated by light [31;38], and it is therefore likely that one or both of the *WAG* genes are auxin-responsive, similar to the *Cucumis sativus* homologue *CsPK3* or the *PID* gene in *Arabidopsis* [16;35]. Loss-of-function mutations in *WAG1* or

Table 1. Overview of the occurrence of the AGCVIII kinases and the PIN auxin efflux carriers in different representatives of the plant kingdom

Family	Genus	PIN ^c	AGC4 ^c				
			PHOT2	PHOT1	AGC3 ^c	AGC1 ^c	AGC2 ^c
Chlorophyta (Green Algae)	<i>Ostreococcus</i> ^a	-	+	-	-	-	-
	<i>Chlamydomonas</i> ^b	-	+	-	-	-	-
	<i>Mougeotia</i> ^b	-	+	-	-	-	-
Embryophyta							
Bryophytes (Mosses)	<i>Physcomitrella</i> ^b	+	+	-	+	+	?
Pteridophytes (Ferns)	<i>Adiantum</i> ^b	+	+	-	+	?	?
Spermatophyta (Seed plants)							
Gymnosperms	<i>Pinus</i> ^b	+	+	+	+	+	+
Monocots	<i>Oryza</i> ^a	+	+	+	+	+	+
	<i>Zea</i> ^b	+	+	+	+	+	+
Dicots	<i>Medicago</i> ^a	+	+	+	+	+	+
	<i>Arabidopsis</i> ^a	+	+	+	+	+	+

^a complete genome sequence is available. ^b analysis is based on EST databases. ^c + present, - absent, ? Predicted to be present but not found in databases.

WAG2 result in weak root waving phenotypes, and double mutants show a constitutive root waving phenotype, and root curling is more resistant to the PAT inhibitor 1-naphthylphthalamic acid (NPA). As root waving is clearly linked to PAT [27], and the PAT-inhibitor resistant root curling phenotype is characteristic for mutants in PAT [39], it is likely that the WAG kinases, similar to PID, are involved in the regulation of auxin transport [27;31].

To confirm this possible functional relatedness, we analyzed the subcellular localization of WAG1, WAG2 and PID in *Arabidopsis thaliana* protoplasts (Figure 4a-c), and found that all three kinases localize predominantly to the plasma membrane; however, WAGs can also be found in the nucleus. Our observations are partially in contrast to those of Zegzouti and co-workers, who concluded that the WAG kinases are localized in the nucleus [23]. As their conclusion was based on the expression of fusions with the green fluorescent protein (GFP) in yeast cells, our own observations on functional YFP fusions expressed in *Arabidopsis* protoplasts are more likely to reflect the subcellular localization of the WAG kinases *in planta*.

The plasma membrane localization, together with the phenotypes observed on the loss-of function mutants and the similarity in amino acid sequence between PID and the

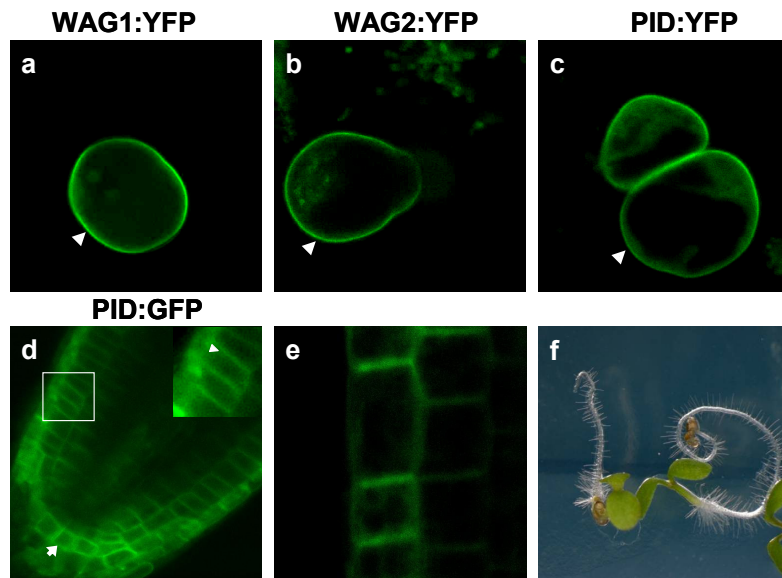


Figure 4. PID, WAG1 and WAG2 are plasma membrane-associated kinases. (a-c) C-terminal fusions of PID, WAG1 and WAG 2 with yellow fluorescent protein (YFP) localize to the plasma membrane (arrow head) in *Arabidopsis* protoplasts. (d and e) Confocal sections of two independent transgenic lines overexpressing PID:GFP (35S::PID:GFP). (d) Root tip showing non-polar membrane localization of PID in the columella cells (arrow) and apico-basal localization in the epidermal cell layer (inset, arrow head). (e) Detail of the root epidermis, in the distal elongation zone (between the root tip and the elongation zone), showing apical membrane localization of PID. (f) The 35S::PID:GFP seedlings show agravitropic growth and the primary root meristem collapses, demonstrating that the fusion protein is functional.

WAG kinases, suggest that these kinases act in the same or in a parallel pathway to regulate the PAT machinery.

Fine tuning PID-dependent polar localization of PIN proteins

The PID protein kinase is the first, and for now only, identified determinant of the polar targeting of PIN proteins [15]. PID kinase activity is regulated by three factors: (i) by phosphorylation of the catalytic activation loop by 3-phosphoinositide-dependent kinase 1 (PDK1), which enhances PID kinase activity [23;40]; (ii) by phosphorylated phosphatidylinositols (PIP2) and phosphatidic acid (PA), phospholipids that bind PID most strongly and most likely enable its association with the plasmamembrane [23]; and (iii) by Ca^{2+} binding proteins that bind to PID in a calcium-dependent manner, and regulate its kinase activity [41]. At the plasmamembrane, PID partially co-localizes with

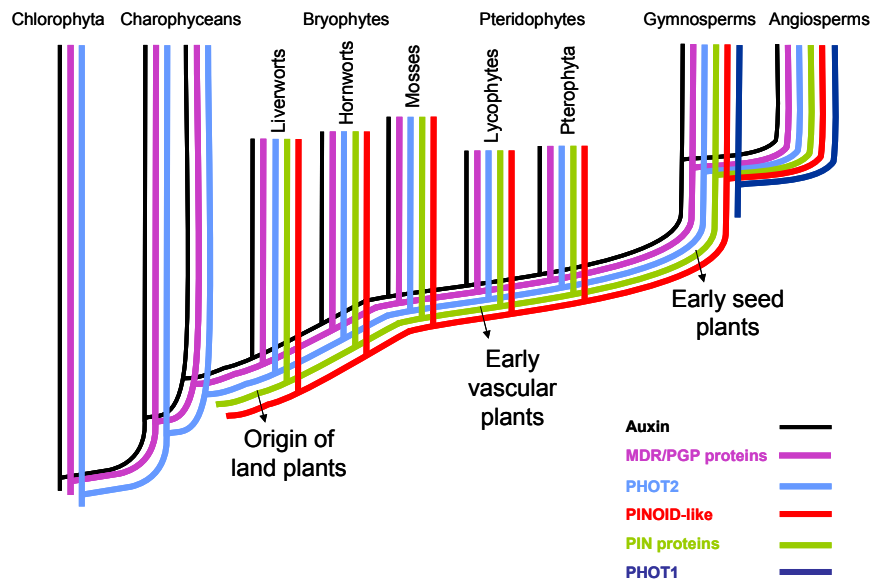


Figure 5. The phototropins and the AGC3 kinases recapitulate plant evolution. Phylogenetic tree of the plant kingdom, depicting the presence of genes involved in auxin biosynthesis, or genes encoding phototropins, AGC3 (PINOID-like) kinases, MDR/PGP transporters and PIN proteins. Auxin and auxin-biosynthesis genes have been identified in a range of green plants, from unicellular algae to angiosperms, as have genes encoding PHOT2-like proteins and MDR/PGP transporter proteins. By contrast, genes encoding the AGC3 kinases and PIN auxin efflux carriers occur only later in evolution in land plants. Therefore, the PHOT2-like proteins probably represent the most ancient AGCVIII protein kinases from which the other AGCVIII kinases evolved. A duplication of the ancestral *PHOT2* gene gave rise to the low-fluence phototropin-encoding *PHOT1* gene, which is found only in spermatophytes

PIN proteins [19;39]. Overexpression of a functional PID:GFP fusion in *Arabidopsis* indicates that the subcellular localization of PID in the root meristem is cell-type specific (Figure 4d-f). In columella cells, PID shows random non-polar localization (Figure 4d), similar to PIN3 [42], whereas in the epidermal cell layer, PID shows apico-basal polarity (Figure 4d inset and e) that partially overlaps with PIN2 [15;39]. Recently evidence was found for direct phosphorylation of PIN proteins by PID [39]. How exactly this phosphorylation affects the polar subcellular localization of PIN proteins is still unknown. It is likely, however, that PID-dependent polar targeting of PINs is tightly regulated by a combined action of PDK1, phospholipids and calcium binding proteins.

The evolution of auxin-dependent plant development: AGC kinases tell the tale

From an evolutionary perspective, the phototropins and AGC3 kinases seem to recapitulate plant evolution (Figure 5). It is unsurprising that *PHOT2-like* genes represent the most ancient AGCVIII protein kinases, because the optimization of photosynthesis in response to light intensities in the first eukaryotic photosynthetic cells was a crucial trait in plant evolution. The essential function of *PHOT2-like* genes has been well conserved and our analysis indicates that *PHOT2-like* genes are found in representative species throughout the plant kingdom (Figure 5). In contrast, *PHOT1-like* genes are only found in spermatophytes, indicating that PHOT1-mediated tropic growth in response to low fluence rate light evolved later as an important determinant of proper development of soil-born germinating seedlings (Figure 5).

As for auxin-dependent processes, a tryptophan-dependent biosynthesis pathway has been found in green and brown algae (Chlorophytes and Charophytes) [43]. In contrast, no genes encoding PID, PID-like kinases or PIN auxin efflux carriers have been identified in the green algal genomes of *Chlamydomonas* or *Ostreococcus* (Table 1) and, although auxin transport seems to regulate directional growth and patterning in the brown algae [43], there is no clear evidence for PIN-dependent auxin efflux in these early plant forms [43]. In fact, auxin transport in Charophytes might well be mediated by the MDR/PGP type of transporters, that are found through the entire plant kingdom (Figure 5), and like PIN proteins, exhibit auxin efflux activity and sensitivity to PAT inhibitors [6;11;43].

Genes encoding homologs of the AGC3 kinases and PIN auxin efflux carriers have been identified in the moss *Physcomitrella* [44] (www.cosmoss.com), and in many other land plants (Figure 5, Table 1). This together with the demonstrated functional relationship between PID and PINs [15] suggest that these two gene families co-evolved, and that AGC3 kinase-regulated PIN-dependent PAT might have played an important role in the adaptation of plants during the transition from water to land (Figure 5, Table 1). In conclusion, there is a strong correlation between the known functions of the AGC3 and AGC4 kinases in plant development, and their distribution throughout the plant kingdom, which suggests that new AGC kinases might have been acquired during most critical steps in plant evolution.

Concluding Remarks and future perspectives

Although there is much information about how differential auxin distribution couples environmental stimuli to developmental responses, such as directional growth, it is still unclear how the different components in the PAT pathway work coordinately to orient this auxin-directed plant development. Two subgroups of the AGCVIII protein kinases are directly involved in this process. On one hand, light-activated phototropins induce rapid Ca^{2+} release into the cytosol and initiate differential auxin transport leading to auxin accumulation in the cell layers at the dark side of the hypocotyl [42]. On the other hand, PID, and possibly other AGC3 kinases, direct PAT by determining the correct polar localization of PIN proteins during embryo development and organ formation in the shoot apical meristem.

Although none of the AGC3 kinases has been directly connected to phototropic growth, the observation that the activity of PID is regulated by interacting calcium-binding proteins [41] suggests that these kinases might be downstream components of the phototropin signal-transduction pathway. Whether the other AGC3 kinases, like PID, direct PAT through direct phosphorylation of PIN proteins, whether one or more AGC3 kinases affect the subcellular PIN localization during phototropism, and whether there is a link between PHOT-induced calcium release and regulation on the activity of AGC3 kinases through calcium binding proteins are key questions to be addressed by future research.

In conclusion, based on the data presented here, we propose that those AGCVIII kinases that play an essential role in plant development, recapitulate plant evolution. Phototropins represent the most ancient AGCVIII kinase forms that regulate highly conserved processes in plants like optimization of light perception and AGC3 kinases co-evolved with PIN auxin transporters in multicellular plants during their colonization of land, and act together, possibly downstream of the phototropins, to orient plant development by establishing the directionality of auxin transport.

Outline of this thesis

The role of PID as determinant of PIN polarity has been well established, and it has been shown now that PID acts via direct phosphorylation of the central hydrophilic loop in PIN proteins [39]. In order to phosphorylate PIN proteins PID has to be active and to localize close to its phospho targets at the plasmamembrane. Previous studies have shown that PID subcellular localization is dependent on the tissue in which it is expressed [19;39]. Likely candidates to regulate the activity and localization of this kinase are the PID interacting proteins PDK1 and the calcium binding proteins PID BINDING PROTEIN1 (PBP1) and TOUCH3 (TCH3) [40-41]. The aim of the research described in this thesis was 1) to further elucidate the role of TCH3, PBP1 and PDK1 as upstream regulators of PID, and 2) to investigate whether other plant AGC kinases are also involved in regulating PIN polarity.

Previous studies have shown that PID interacts in a calcium-dependent manner with TCH3 and PBP1, thereby providing the first molecular link between calcium and polar auxin transport [41]. **Chapter 2** shows the inhibitory effect of TCH3 on PID kinase activity and provides evidence for auxin-dependent sequestration of PID from the plasma membrane to the cytosol. The results suggest that TCH3 is part of a negative feedback loop that regulates PID activity. **Chapter 3** describes the functional characterization of PBP1 in *Arabidopsis*. The presented analysis is consistent with the previous hypothesis of PBP1 as an enhancer of PID kinase activity.

The third known PID interactor, PDK1, phosphorylates the catalytic activation loop of PID, enhancing its kinase activity [40]. **Chapter 4** describes the effect of this protein on PID subcellular localization. In *Arabidopsis thaliana* protoplasts, PDK1 was found to induce translocation of PID from the plasma membrane to endomembrane compartments and microtubules (MT). Replacing the PDK1 phosphorylation targets in PID by alanine made PID non-responsive to PDK1, suggesting that the PDK1-dependent phosphorylation status of PID determines its subcellular localization. Based on these results we propose a model for the role of PDK1 and phospholipids in modulating PID-dependent polar targeting of PIN proteins.

The two closely related AGC3 kinases, named WAG1 and WAG2, share similarity with PID not only at the sequence level but also in their regulation and action.

Not much is known yet of the fourth AGC3 kinase. **Chapter 5** describes the characterization of AGC3 kinases and their roles during different stages of plant development. The defects observed in the loss and gain-of-function mutants correlate with mislocalization of PIN proteins. Like PID, WAGs phosphorylate PIN proteins and induce basal-to-apical shifts in PIN localization in root cells. However, complementation experiments show that WAG2 and AGC3-4 act differently and are likely to function in parallel pathways during inflorescence development. Here we propose a model in which PID, WAG1 and WAG2 act together and in parallel to establish apical and lateral PIN polarity to form a plant compass dictating directionality of the polar auxin transport.

Reference list

1. Benkova E, Michniewicz M, Sauer M, Teichmann T, Seifertova D, Jurgens G, Friml J: **Local, efflux-dependent auxin gradients as a common module for plant organ formation.** *Cell* 2003, **115**:591-602.
2. Friml J, Vieten A, Sauer M, Weijers D, Schwarz H, Hamann T, Offringa R, Jurgens G: **Efflux-dependent auxin gradients establish the apical-basal axis of *Arabidopsis*.** *Nature* 2003, **426**:147-153.
3. Muday GK: **Auxins and tropisms.** *J.Plant Growth Regul.* 2001, **20**:226-243.
4. Reinhardt D, Frenz M, Mandel T, Kuhlemeier C: **Microsurgical and laser ablation analysis of interactions between the zones and layers of the tomato shoot apical meristem.** *Development* 2003, **130**:4073-4083.
5. Sabatini S, Beis D, Wolkenfelt H, Murfett J, Guilfoyle T, Malamy J, Benfey P, Leyser O, Bechtold N, Weisbeek P, Scheres B: **An auxin-dependent distal organizer of pattern and polarity in the *Arabidopsis* root.** *Cell* 1999, **99**:463-472.
6. Vieten A, Sauer M, Brewer PB, Friml J: **Molecular and cellular aspects of auxin-transport-mediated development.** *Trends Plant Sci.* 2007, **12**:160-168.
7. Petrasek J, Mravec J, Bouchard R, Blakeslee JJ, Abas M, Seifertova D, Wisniewska J, Tadele Z, Kubes M, Covanova M, Dhonukshe P, Skupa P, Benkova E, Perry L, Krecek P, Lee OR, Fink GR, Geisler M, Murphy AS, Luschnig C, Zazimalova E, Friml J: **PIN proteins perform a rate-limiting function in cellular auxin efflux.** *Science* 2006, **312**:914-918.
8. Wisniewska J, Xu J, Seifertova D, Brewer PB, Ruzicka K, Blilou I, Rouquie D, Benkova E, Scheres B, Friml J: **Polar PIN localization directs auxin flow in plants.** *Science* 2006, **312**:883.
9. Tanaka H, Dhonukshe P, Brewer PB, Friml J: **Spatiotemporal asymmetric auxin distribution: a means to coordinate plant development.** *Cell Mol. Life Sci.* 2006, **63**:2738-2754.
10. Zazimalova E, Krecek P, Skupa P, Hoyerova K, Petrasek J: **Polar transport of the plant hormone auxin - the role of PIN-FORMED (PIN) proteins.** *Cell Mol. Life Sci.* 2007, **64**:1621-1637.
11. Geisler M, Murphy AS: **The ABC of auxin transport: the role of p-glycoproteins in plant development.** *FEBS Lett.* 2006, **580**:1094-1102.
12. Geldner N, Friml J, Stierhof YD, Jurgens G, Palme K: **Auxin transport inhibitors block PIN1 cycling and vesicle trafficking.** *Nature* 2001, **413**:425-428.

13. Geldner N, Anders N, Wolters H, Keicher J, Kornberger W, Muller P, Delbarre A, Ueda T, Nakano A, Jurgens G: **The *Arabidopsis* GNOM ARF-GEF mediates endosomal recycling, auxin transport, and auxin-dependent plant growth.** *Cell* 2003, **112**:219-230.
14. Steinmann T, Geldner N, Grebe M, Mangold S, Jackson CL, Paris S, Galweiler L, Palme K, Jurgens G: **Coordinated polar localization of auxin efflux carrier PIN1 by GNOM ARF GEF.** *Science* 1999, **286**:316-318.
15. Friml J, Yang X, Michniewicz M, Weijers D, Quint A, Tietz O, Benjamins R, Ouwerkerk PB, Ljung K, Sandberg G, Hooykaas PJ, Palme K, Offringa R: **A PINOID-dependent binary switch in apical-basal PIN polar targeting directs auxin efflux.** *Science* 2004, **306**:862-865.
16. Benjamins R, Quint A, Weijers D, Hooykaas P, Offringa R: **The PINOID protein kinase regulates organ development in *Arabidopsis* by enhancing polar auxin transport.** *Development* 2001, **128**:4057-4067.
17. Bennett SRM, Alvarez J, Bossinger G, Smyth DR: **Morphogenesis in pinoid mutants of *Arabidopsis thaliana*.** *Plant J.* 1995, **8**:505-520.
18. Delarue M, Muller P, Bellini C, Delbarre A: **Increased auxin efflux in the IAA-overproducing *sur1* mutant of *Arabidopsis thaliana*: A mechanism of reducing auxin levels?** *Physiol.Plant.* 1999, **107**:120-127.
19. Lee SH, Cho HT: **PINOID positively regulates auxin efflux in *Arabidopsis* root hair cells and tobacco cells.** *Plant Cell* 2006, **18**:1604-1616.
20. Sauer M, Balla J, Luschnig C, Wisniewska J, Reinohl V, Friml J, Benkova E: **Canalization of auxin flow by Aux/IAA-ARF-dependent feedback regulation of PIN polarity.** *Genes Dev.* 2006, **20**:2902-2911.
21. Christensen SK, Dagenais N, Chory J, Weigel D: **Regulation of auxin response by the protein kinase PINOID.** *Cell.* 2000, **100**:469-478.
22. Briggs WR, Beck CF, Cashmore AR, Christie JM, Hughes J, Jarillo JA, Kagawa T, Kanegae H, Liscum E, Nagatani A, Okada K, Salomon M, Rudiger W, Sakai T, Takano M, Wada M, Watson JC: **The phototropin family of photoreceptors.** *Plant Cell* 2001, **13**:993-997.
23. Zegzouti H, Li W, Lorenz TC, Xie M, Payne CT, Smith K, Glenny S, Payne GS, Christensen SK: **Structural and functional insights into the regulation of *Arabidopsis* AGC VIIIa kinases.** *J.Biol.Chem.* 2006, **281**:35520-35530.
24. Bogre L, Okresz L, Henriques R, Anthony RG: **Growth signalling pathways in *Arabidopsis* and the AGC protein kinases.** *Trends Plant Sci.* 2003, **8**:424-431.

25. Lawton MA, Yamamoto RT, Hanks SK, Lamb CJ: **Molecular cloning of plant transcripts encoding protein kinase homologs.** *Proc.Natl.Acad.Sci.USA* 1989, **86**:3140-3144.
26. Celaya RB, Liscum E: **Phototropins and associated signaling: providing the power of movement in higher plants.** *Photochem.Photobiol.* 2005, **81**:73-80.
27. Oliva M, Dunand C: **Waving and skewing: how gravity and the surface of growth media affect root development in *Arabidopsis*.** *New Phytol.* 2007, **176**:37-43.
28. Day IS, Miller C, Golovkin M, Reddy AS: **Interaction of a kinesin-like calmodulin-binding protein with a protein kinase.** *J Biol. Chem.* 2000, **275**:13737-13745.
29. Anthony RG, Henriques R, Helfer A, Meszaros T, Rios G, Testerink C, Munnik T, Deak M, Koncz C, Bogre L: **A protein kinase target of a PDK1 signalling pathway is involved in root hair growth in *Arabidopsis*.** *EMBO J.* 2004, **23**:572-581.
30. Rentel MC, Lecourieux D, Ouaked F, Usher SL, Petersen L, Okamoto H, Knight H, Peck SC, Grierson CS, Hirt H, Knight MR: **OXI1 kinase is necessary for oxidative burst-mediated signalling in *Arabidopsis*.** *Nature* 2004, **427**:858-861.
31. Santner AA, Watson JC: **The WAG1 and WAG2 protein kinases negatively regulate root waving in *Arabidopsis*.** *Plant J.* 2006, **45**:752-764.
32. Jarillo JA, Gabrys H, Capel J, Alonso JM, Ecker JR, Cashmore AR: **Phototropin-related NPL1 controls chloroplast relocation induced by blue light.** *Nature.* 2001, **19**:410:952-954.
33. Liscum E, Briggs WR: **Mutations in the NPH1 locus of *Arabidopsis* disrupt the perception of phototropic stimuli.** *Plant Cell.* 1995, **7**:473-485.
34. Onodera A, Kong SG, Doi M, Shimazaki K, Christie J, Mochizuki N, Nagatani A: **Phototropin from *Chlamydomonas reinhardtii* is functional in *Arabidopsis thaliana*.** *Plant Cell Physiol* 2005, **46**:367-374.
35. Chono M, Nemoto K, Yamane H, Yamaguchi I, Murofushi N: **Characterization of a protein kinase gene responsive to auxin and gibberellin in cucumber hypocotyls.** *Plant Cell Physiol.* 1998, **39**:958-967.
36. Khanna R, Lin X, Watson JC: **Photoregulated expression of the *PsPK3* and *PsPK5* genes in pea seedlings.** *Plant Mol.Biol.* 1999, **39**:231-242.
37. Lin X, Feng XH, Watson JC: **Differential accumulation of transcripts encoding protein kinase homologs in greening pea seedlings.** *Proc.Natl.Acad.Sci.USA* 1991, **88**:6951-6955.

38. Ma J, Khanna R, Fukasawa-Akada T, Poisso J, Deitzer GF, Watson JC: **PK3At (Accession No. AF082391): An *Arabidopsis* homolog of the PsPK3 protein kinase from *Pisum sativum* L.** *Plant Physiol.* 1998, **118**:712.
39. Michniewicz M, Zago MK, Abas L, Weijers D, Schweighofer A, Meskiene I, Heisler MG, Ohno C, Huang F, Weigel D, Meyerowitz EM, Luschnig C, Offringa R, Friml J: **Phosphatase 2A and PID kinase activities antagonistically mediate PIN phosphorylation and apical/basal targeting in *Arabidopsis*.** *Cell* 2007, **130**:1-13.
40. Zegzouti H, Anthony RG, Jahchan N, Bogre L, Christensen SK: **Phosphorylation and activation of PINOID by the phospholipid signaling kinase 3-phosphoinositide-dependent protein kinase 1 (PDK1) in *Arabidopsis*.** *Proc.Natl.Acad.Sci.USA* 2006, **103**:6404-6409.
41. Benjamins R, Galvan Ampudia CS, Hooykaas PJ, Offringa R: **PINOID-mediated signaling involves calcium-binding proteins.** *Plant Physiol.* 2003, **132**:1623-1630.
42. Friml J, Wisniewska J, Benkova E, Mendgen K, Palme K: **Lateral relocation of auxin efflux regulator PIN3 mediates tropism in *Arabidopsis*.** *Nature* 2002, **415**:806-809.
43. Cooke TJ, Poli D, Sztein AE, Cohen JD: **Evolutionary patterns in auxin action.** *Plant Mol.Biol.* 2002, **49**:319-338.
44. Decker EL, Frank W, Sarnighausen E, Reski R: **Moss systems biology en route: phytohormones in *Physcomitrella* development.** *Plant Biol (Stuttg)* 2006, **8**:397-405.
45. Benjamins R. **Functional analysis of the PINOID protein kinase in *Arabidopsis thaliana*.** 2004. Institute of Biology, Leiden University, The Netherlands. Ref Type: Thesis/Dissertation

CHAPTER 2

Getting back in TOUCH: calcium-dependent feedback on auxin transport

Carlos Samuel Galvan-Ampudia¹, H el ene Robert¹, Karen Sap, Remko Offringa

¹ These authors contributed equally to this manuscript

Summary

Calcium is a broadly used second messenger in signaling pathways. For the specificity of its response, not only the spatio-temporal pattern, but also calcium “receptors” are essential. Earlier studies suggest that the signaling and polar transport of the plant hormone auxin are processes modulated by calcium. PIN efflux carrier-driven auxin transport generates maxima and minima that are essential for plant development. The *Arabidopsis* PINOID (PID) protein serine/threonine kinase has been identified as a determinant in the polar subcellular targeting of PIN proteins, and thereby of the direction of transport. The finding that PID shows a calcium-dependent interaction with the calmodulin-related protein TOUCH3 (TCH3) provided the first molecular link between calcium and auxin transport. Here we show that TCH3 inhibits PID kinase activity by interacting with its catalytic domain, and we provide genetic evidence for the *in vivo* significance of this interaction. Furthermore, we show auxin-dependent sequestration of PID from the plasma membrane to the cytosol in protoplasts upon co-expression of TCH3. In root epidermal cells, where PID and TCH3 are co-expressed, auxin induces rapid and transient dissociation of PID from the plasma membrane away from its phospho-targets, the PIN proteins. This response requires the action of calmodulins and calcium channel. These results suggest that TCH3 is part of a feedback loop that modulates PIN polar targeting by rapid inhibition of PID activity in response to stimuli, such as auxin, that induce cytosolic calcium peaks.

Introduction

Calcium plays an important role as an intracellular second messenger in a variety of signaling pathways. In plants, rapid changes in the cytosolic calcium concentration are required for the transduction of both abiotic signals and biotic stimuli [1]. In order to give an appropriate response, cells need to distinguish the calcium signals produced by these different stimuli. Spatial and temporal patterns of calcium responses, and also the presence of calcium “receptors” or sensors in the cell, are needed to give specificity to the signal [2;3]. The receptor proteins are able to monitor the changes in the calcium concentration by binding calcium through specific domains called EF hands [4]. The conformational changes induced by binding of calcium to these proteins either induces their activation, or enhances their interaction with other proteins that are in turn activated or repressed [2;3;5]. Two main types of sensors are known: the calmodulins (CaMs) and the calcium-dependent protein kinases (CDPKs). CaMs are small proteins with typically four EF-hands without an effector domain. The transmission of the signal occurs through the interaction with a target enzyme to influence its activity [1;6]. The CDPKs combine a calmodulin-like domain with a kinase domain. Binding of calcium directly activates the protein kinase [7].

The phytohormone auxin regulates plant development by controlling basic cellular processes such as cell division, -differentiation and -elongation [8-10]. Several studies suggest that the auxin signaling pathway involves rapid changes in the cytosolic calcium concentration. For example, in wheat protoplasts [11], maize coleoptile cells [12;13], and parsley cells [12] an increase of the cytosolic calcium concentration was detected within minutes after auxin application using calcium fluorescent dyes or ion-sensitive microelectrodes. The observation of an auxin-induced calcium pulse was not limited to protoplasts, but was also observed in intact plant tissues such as maize and pea roots [12].

Ever since the first observations of Darwin on the growth response of Canary grass coleoptiles to unidirectional light [14], it is well-established now that auxin is transported from cell to cell in a polar fashion from its sites of synthesis to its sites of action [15]. This polar auxin transport (PAT) generates auxin maxima and minima that mediate tropic growth responses, and are instructive for embryogenesis, meristem

maintenance and organ positioning [16-19,58]. The mechanism of auxin transport have been widely studied, and PIN transmembrane proteins have been identified as auxin efflux carriers that direct this polar intercellular transport through their asymmetric subcellular localization [20-22]. The plant-specific AGC protein serine/threonine kinase PINOID (PID) was identified as a regulator of auxin transport, and is a determinant in the polar targeting of PIN proteins. PID directs their localization at the apical (shoot facing) cell membrane, by phosphorylation of the PIN central hydrophilic loop [23-25].

Calcium has also been implied as an important signal in the regulation of PAT in sunflower hypocotyls [26], in gravistimulated roots [27] and in the phototropism signaling pathway. The light signal inducing phototropic growth is perceived by the PHOT1 blue receptor kinase. This induces a rapid increase in the cytoplasmic calcium concentration [28;29] and triggers PIN-dependent auxin accumulation at the shaded side, resulting in auxin-dependent changes in gene transcription, and leading to shoot bending toward the light source [30;31]. The function of the rapid calcium response in phototropic growth and the downstream components of the signaling pathway have not yet been characterized.

Our previous finding that PID interacts in a calcium-dependent manner with the calcium-binding proteins PINOID BINDING PROTEIN1 (PBP1) and TOUCH3 (TCH3) provided the first molecular evidence for calcium as a signal transducer in the regulation of auxin transport [32]. TCH3 is a CaM-like protein containing 6 EF-hands, and its corresponding gene was initially identified as a touch-responsive gene [33;34]. Here we present a detailed study of the *in vivo* interaction between PID and TCH3. Using loss- and gain-of-function mutant lines, we confirm *in vitro* observations that TCH3 is a negative regulator of the PINOID kinase activity. This regulation occurs directly by inhibition of the kinase activity, as shown in phosphorylation assays, and by sequestration of PID from the plasma membrane where its phospho-targets are located [25]. Interestingly, auxin treatment also results in rapid transient re-localization of the membrane-associated kinase to the cytosol. We speculate that this occurs through its interaction with TCH3, which is enhanced by the auxin-induced increase in cytosolic calcium.

Results

TCH3 reduces the kinase activity by binding to the catalytic domain of PID

Previously, the calmodulin-like protein TCH3 was identified as a PID-binding protein in a yeast two-hybrid screen. Using *in vitro* pull-down assays it was shown that the kinase-CaM interaction is calcium-dependent [32]. In order to map the TCH3 interaction site in PID, we incubated GST-tagged isolates of full-length PID, the N-terminal domain (aa 2-103), the catalytic domain (aa 75-398) or C-terminal domain (aa 339-438) with crude *E. coli* extracts containing Histidine (His)-tagged TCH3 (Figure 1a). Protein complexes were pulled down with glutathione beads and separated on gel. Western blot analysis using anti-His antibodies showed that TCH3 interacts with full-length PID or with its catalytic domain (Figure 1b, lanes 2 and 4) but not with the N- or C-terminal domains (Figure 1b, lanes 3 and 5) nor with GST alone (Figure 1b, lane 1). Binding to the catalytic domain suggested that TCH3 might affect PID kinase activity. Indeed, previous studies showed that TCH3 reduces the *in vitro* phosphorylation activity of PID using traditional kinase assay with Myelin Basic Protein (MBP) as a substrate [32]. To confirm these results with a wider array of substrates, we incubated a commercial phospho-peptide chip with radiolabelled ATP and PID alone or in the presence of PBP1, a PID positive regulator [32], or of both PBP1 and TCH3. For a quantitative comparison of the differences in PID activity, we focused on the phosphorylation intensity of four peptides, one of which represented a phospho-target in MBP. PID efficiently phosphorylated all four peptides (Figures 2a and 2d), and in presence of PBP1 the phosphorylation intensity was significantly increased (Figures 2b and 2d), which corroborated the role of PBP1 as positive regulator of PID [32]. When TCH3 was added to the last mix, the phosphorylation intensity was reduced to even below the level of PID alone (Figures 2c and 2d). These data corroborate our previous data that TCH3 is a negative regulator of PID kinase activity *in vitro*, and indicate that TCH3 binding to PID is able to overrule this positive effect of PBP1.

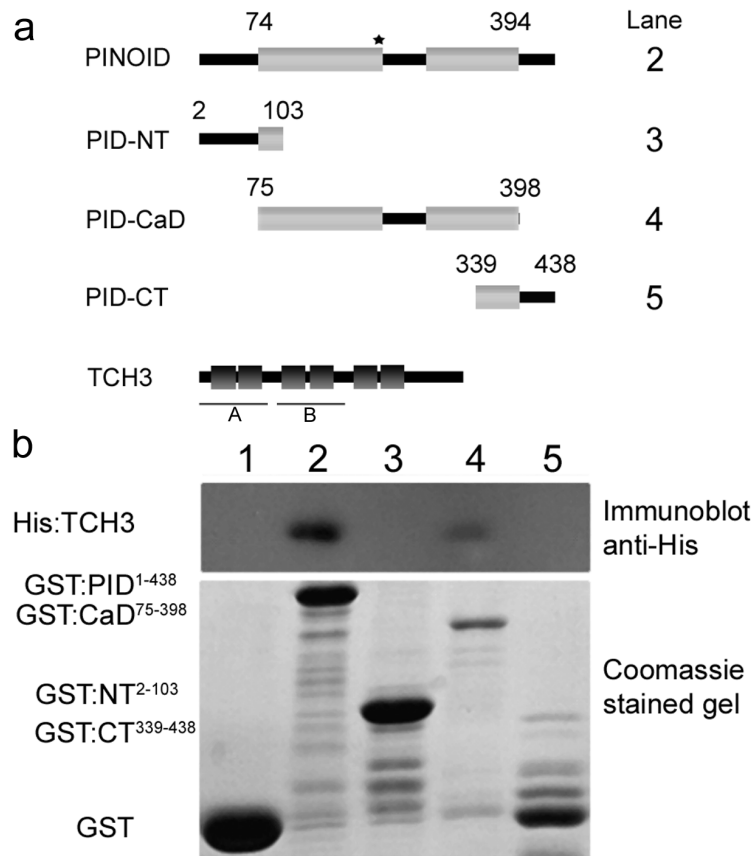


Figure 1. TCH3 interacts with the catalytic domain of PID.

(a) A schematic representation of the proteins used in the *in vitro* pull-down assay. Full-length PID (498 aa) and its deletion mutants: the N-terminal portion (PID-NT, aa 2-103), the catalytic domain (PID-CaD, aa 75-398) and the C-terminal portion (PID-CT, aa 339-438), are shown. The light grey boxes represent the PID catalytic domain (aa 74-394), comprising 11 conserved sub-domains and the amino acid insertion between sub-domain VII and VIII (aa 226-281). The star indicates the DFG to DFD mutation characteristic for the plant-specific AGCVIII protein kinases. The numbers indicated on the right correspond to the lane numbers of the Western blot and Coomassie stained gel in (b). TCH3 (324 aa) is depicted with the six EF-hand domains (aa 12-38, 50-74, 101-127, 139-163, 191-217, 228-253) as dark grey boxes. The lines A and B represent the perfect tandem repeat comprising EF-hand pairs 1-2 and 3-4.

(b) Western blot analysis (top) with anti-His antibodies detects His-tagged TCH3 after pull-down with GST-tagged PID (lane 2) or GST-tagged PID catalytic domain (GST:CaD, lane 4), but not after pull-down with GST-tagged PID N-terminal (GST:NT, lane 3) or C-terminal (GST:CT, lane 5) domains or with GST alone (lane 1). Coomassie stained gel (bottom) showing the input of proteins used in the pull-down assay.

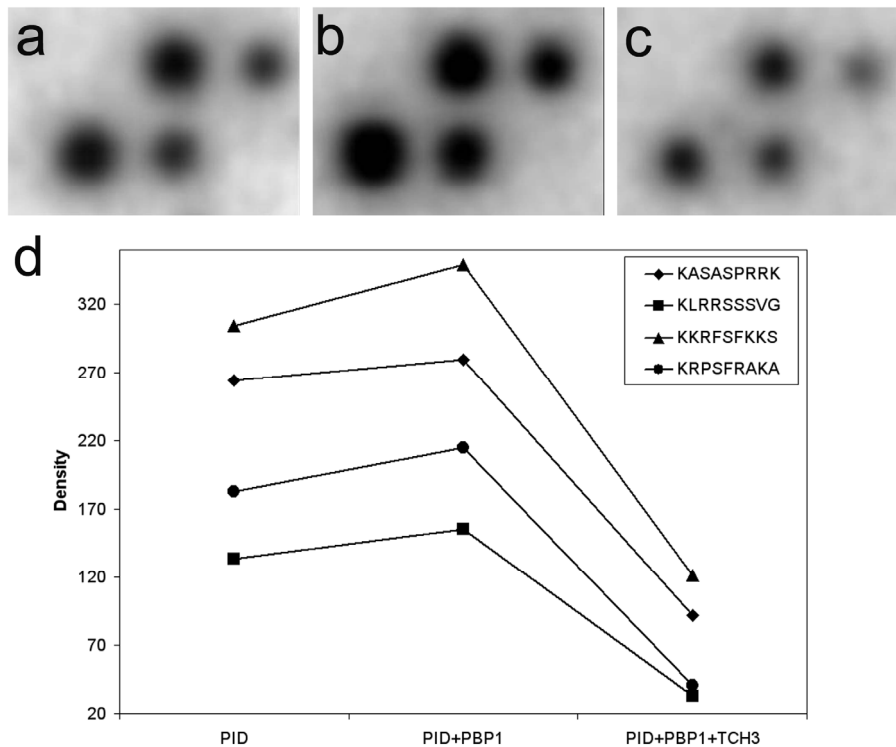


Figure 2. TCH3 reduces PID kinase activity *in vitro*.

(a-c) Kinase assay using a chip where PID alone (a), PID and the positive regulator PBP1 (b), or PID, PBP1 and TCH3 (c) were incubated with radiolabelled ATP.

(d) Quantification of the phosphorylation density of the four peptides shown in (a-c) confirms that TCH3 represses PID kinase activity *in vitro*.

***TCH3* overexpression lines and *tch3* loss-of-function mutants do not show phenotypes**

To further analyze the possible function of TCH3 as a regulator of the PID pathway *in planta*, we obtained the mutant alleles *tch3-2* and *tch3-1* from the SALK collection with a T-DNA inserted at respectively positions -134 and -120 relative to the ATG of *TCH3*. Northern blot analysis indicated that *tch3-2* was a null allele, whereas in *tch3-1* the expression was enhanced (Figure 3a). Another SALK line with a T-DNA insertion at position -71, named *tch3-3*, was found to be a complete knock-out both on Northern and Western blots (J. Braam, pers. com.). Both *tch3-2* and *tch3-3* (J. Braam, pers. com.)

alleles did not show any obvious phenotypes, suggesting that TCH3 is functionally redundant with the most related calmodulin-like proteins CaML9 and CML10 [35].

In order to generate gain-of-function alleles, *TCH3* full-length cDNA was overexpressed in *Arabidopsis* Columbia under the strong *35S* promoter. Despite high expression levels in four independent single locus insertion lines (Figure 3b), no obvious phenotypes were observed in the *35Spro::TCH3* plants. Our analysis focused on auxin-related phenotypes (gravitropic growth, sensitivity to IAA and NPA and lateral root development) and we may have therefore missed phenotypes related to the touch response pathway.

***TCH3* overexpression reduces *PID* gain-of-function root meristem collapse**

The above data suggest that TCH3 provides feedback regulation on the PID kinase activity in response to auxin or other signals that induce rapid changes in the cytosolic calcium concentration. As both loss-of-function and gain-of-function lines did not provide further information, we crossed the *TCH3* overexpression line *35Spro::TCH3-4* with the overexpression line *35Spro::PID-21*. Overexpression of *PID* in the root causes the collapse of the main root meristem, which is triggered by the lack of an auxin maximum due to the basal-to-apical PIN polarity switch [23;24]. This phenotype was observed in only 5 % of the seedlings at 3 days after germination (dag), but occurred in up to 97 % of the seedlings at 6 dag (Figure 3c). Overexpression of *TCH3* significantly reduced the root meristem collapse (Figure 3c) from 75 % to 31 % at 4 dag (Student's t-test, $p < 0.05$), and from 97 % to 81 % at 6 dag (Student's t-test, $p = 0.06$). The levels of *PID* and *TCH3* expression were slightly lower in 5 days old *35Spro::PID-21/35Spro::TCH3-4* seedlings than in *35Spro::PID-21* and *35Spro::TCH3-4* seedlings (Figure 3d), but not enough to explain the difference in timing of the root meristem collapse phenotype between *35Spro::PID-21* and *35Spro::PID-21/35Spro::TCH3-4*. These observations corroborate the proposed role of TCH3 as negative regulator of PID kinase activity [32].

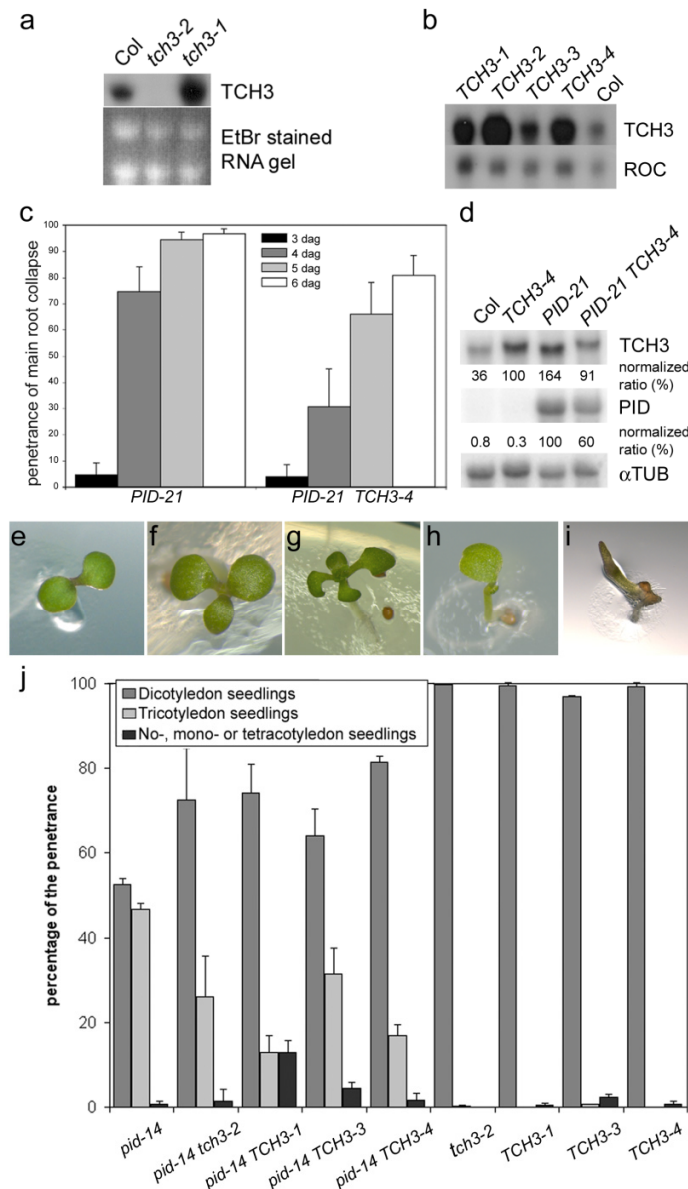


Figure 3: TCH3 is a negative regulator of PID *in vivo*.

(a) Northern blot showing *TCH3* expression in *tch3-2* (SALK_090554) and *tch3-1* (SALK_056345), having a T-DNA insertion at respectively position -134 and -120 relative to the ATG of the *TCH3* gene: *tch3-2* shows no detectable mRNA expression, whereas the expression in *tch3-1* is enhanced. An Ethidium bromide stained RNA gel is shown to compare loading.

(b) Northern blot showing the level of *TCH3* overexpression in five days old seedlings of four independent transgenic lines carrying the *35Spro::TCH3* construct. The blot was first hybridized with the *TCH3* cDNA (top), and subsequently stripped and hybridized with the *ROC* cDNA to show the loading (bottom).

Figure 3. (continued)

(c) The percentage of the main root meristem collapse in the *35Spro::PID-21* and in *35Spro::PID-21/35Spro::TCH3-4* lines. When *TCH3* is overexpressed the root meristem collapse is significantly delayed (Student's t-test, $p < 0.05$).

(d) Northern blot analysis showing the expression level of *TCH3* (top), *PID* (middle) and *α Tubulin* (bottom) in seedlings of the lines used in (c). The same blot was successively hybridized with the *PID*, *TCH3* and *α Tubulin* cDNA. Intensities were quantified using Image Quant and normalized to the corresponding *α Tubulin* sample to compensate for loading differences. The sample with *TCH3* or *PID* overexpression alone was put at 100%.

(e-i) Observed seedling phenotypes, ranging from di- (e) and tri-cotyledon seedlings (f) as seen in the *pid-14* allele, to tetra- (g), mono- (h) and no-cotyledon seedlings (i) as seen in the *pid-14/tch3-2*, and *pid-14/35Spro::TCH3* lines.

(j) The percentage of the penetrance of the aberrant number of cotyledons was analyzed in seedling population of *pid-14+*, *pid-14+/tch3-2*, *pid-14+/35Spro::TCH3-1*, *pid-14+/35Spro::TCH3-3*, *pid-14+/35Spro::TCH3-4*.

***pid* loss-of-function mutant is sensitized to changes in *TCH3* expression**

One of the characteristic defects of *pid* loss-of-function mutants is embryos and seedlings with three cotyledons. The penetrance of this phenotype varies between 10 and 50 % depending on the strength of the mutant allele [23;36;37]. In the *pid-14* allele, 46 % of the homozygous seedlings have three cotyledons (Figures 3f and 3j) and less than 1 % develops a single cotyledon (Figures 3h and 3j). To investigate the influence of *TCH3* on the *pid* embryo phenotype, the *tch3-2* allele and the *35Spro::TCH3-1*, *-3* and *-4* overexpression lines were crossed with *pid-14*, and progeny homozygous for the *tch3-2* loss-of-function or the *35Spro::TCH3* gain-of-function locus and segregating for the *pid-14* allele were scored for cotyledon defects. The percentages were calculated relative to the expected number of *pid-14* homozygous individuals. The *tch3-2* loss-of-function allele did not show aberrant cotyledon phenotypes and in the three *TCH3* overexpressing lines only a few seedlings with one cotyledon were observed (up to 2 % for *35Spro::TCH3-3*, Figure 3j). In all the double mutant lines, the overall penetrance of aberrant cotyledon phenotypes was reduced (17 % to 31 % for the double mutants versus 46 % for *pid-14*, Figure 3j), whereas a significantly higher number of seedlings showed stronger cotyledon defects, such as four cotyledons (< 1 % for *pid-14/35Spro::TCH3-4*, Figure 3g), one cotyledon (ranging from 2 % for *pid-14/tch3-2* and *pid-*

14/35Spro::TCH3-4, up to 10 % for *pid-14/35Spro::TCH3-1*, Figure 3h) or even no cotyledons (3 % for *pid-14/35Spro::TCH3-1*, Figure 3i). Although there is a clear effect of both *TCH3* overexpression and loss-of-function on the severity of the *pid* loss-of-function seedling phenotypes, the data do not indicate a clear negative regulatory function for *TCH3*, as observed in the *in vitro* phosphorylation assays or for the *PID* overexpression-induced root meristem collapse phenotype. No correlation between the level of *TCH3* overexpression and the increase in number of mono-, no- and tetracotyledon seedlings is found. Possibly, during embryo development, a critical balance between the cellular *PID* activity and *TCH3* levels is required for proper cotyledon positioning, and both *TCH3* overexpression and loss-of-function can disturb this balance, as indicated by the significant number of seedlings with defects in cotyledon positioning. The *pid* loss-of-function mutant background is sensitized to changes in *TCH3* expression, which substantiates the functional relationship between the *PID* kinase and *TCH3*.

***TCH3* mediates auxin-dependent sequestration of *PID* from the plasma membrane**

The subcellular localization of *TCH3* was tested by transfecting *Arabidopsis* protoplasts with a *35Spro::TCH3:YFP* construct. The *TCH3:YFP* fusion protein was found to be cytoplasmic (Figure 4a), overlapping with soluble CFP (Figures 4b and 4c). In contrast to soluble CFP (Figure 4b), however, *TCH3:YFP* was excluded from the nucleus (Figures 4b and 4c), and its localization also differed significantly from that of *PID*, which is membrane-associated both in protoplasts (Figure 4e), and *in planta* (Figure 6e) [25;38].

When *35Spro::PID:CFP* and *35Spro::TCH3:YFP* were co-transfected in auxin-starved *Arabidopsis* protoplasts, *PID:CFP* and *TCH3:YFP* did not co-localize and remained at their respective subcellular location, the plasma membrane and the cytoplasm (Figures 4f-h). Interestingly, when cells were cultured in normal auxin-containing medium, *PID* subcellular localization became cytoplasmic in presence of *TCH3* (Figures 4i-k), suggesting that the auxin-dependent interaction with *TCH3* sequesters *PID* from the plasma membrane. The fact that auxin treatment of auxin-starved protoplasts did not lead to *PID* sequestration when *TCH3* was co-transfected (results not shown), suggests

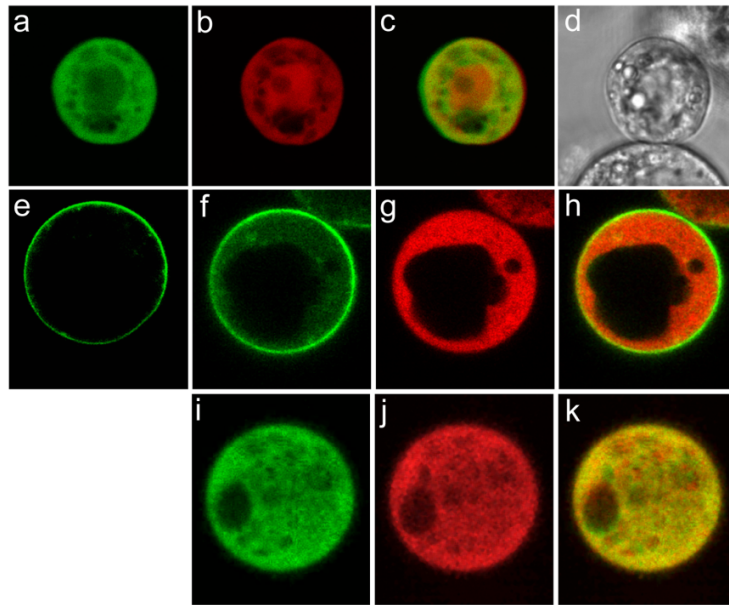


Figure 4. TCH3 and PID co-localization is auxin-dependent.

(a-d) *35Spro::TCH3:YFP* was co-transfected with *35Spro::CFP* in *Arabidopsis* protoplasts. Comparison of the YFP image (a) with the CFP image (b) or the merged image (c) indicates that TCH3 is cytoplasmic and excluded from the nucleus. (d) A transmitted light image of the protoplast in (a-c).

(e) *Arabidopsis* cell suspension protoplast transfected with *35Spro::PID:CFP* shows a plasma membrane localization.

(f-k) Auxin-starved (f-h) or auxin-cultured (i-k) *Arabidopsis* protoplasts co-transfected with *35Spro::PID:CFP* and *35Spro::TCH3:YFP*. Shown are the CFP channel (f, i), the YFP channel (g, j) or the merged image (h, k). PID is membrane localized in auxin-starved protoplasts but co-localizes with TCH3 in the cytoplasm when cells are cultured in presence of auxin.

that protoplasts are desensitized to auxin, and that the sequestration observed in auxin grown protoplasts is probably the result of PID and TCH3 overexpression and constitutively elevated calcium levels.

To confirm the *in vivo* interaction between the two proteins, we checked for the presence of Förster (Fluorescence) Resonance Energy Transfer (FRET) between the CFP and YFP moieties of the co-expressed fusion proteins using confocal lambda scanning [39]. No bleed-through occurred in protoplasts co-expressing CFP and YFP, meaning that YFP was not excited by CFP excitation wavelength (457 nm) and vice versa (data not shown). However, excitation with 457 nm leads to a significant CFP-derived signal at the YFP emission wavelength (527 nm). FRET in the test sample is therefore signified by a

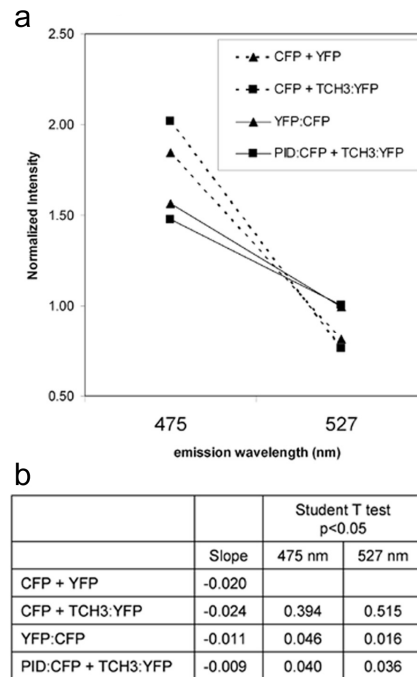


Figure 5. TCH3 interacts with PID *in vivo*.

(a) Graph showing the fluorescence intensities at 475 nm (CFP emission peak) and 527 nm (YFP emission peak) during lambda scanning using an excitation wavelength of 457 nm (donor, CFP) in *Arabidopsis* protoplasts expressing a translational fusion between YFP and CFP (triangle, plain line, positive control), or co-expressing PID:CFP and TCH3:YFP (square, plain line), CFP and TCH3:YFP (square, dotted line, negative control) or CFP and YFP (triangle, dotted line, negative control). The observed quenched intensities at the CFP emission peak and enhanced intensities at the YFP emission peak of the PID:CFP-TCH3:YFP sample are indicative for FRET, and corroborate the *in vivo* interaction between TCH3 and PID.

(b) Table indicating the slope of the curves shown in (a) and the *P*-values of Student's t-tests, in which the 475 nm (CFP) and the 527 nm (YFP) emission intensities of CFP and TCH3:YFP, and YFP:CFP were compared with those of YFP and CFP expressing protoplasts; and of PID:CFP and TCH3:YFP compared with those of TCH3:YFP and *35Spro::CFP*.

quenched signal at the CFP emission wavelength (475 nm) and higher signal at the YFP emission wavelength (527 nm), as compared to control transfections with non-interacting versions of CFP and YFP (*35Spro::CFP* co-transfected either with *35Spro::TCH3:YFP* or with *35Spro::YFP*). Indeed, a significant FRET signal could be detected in protoplasts that co-expressed TCH3:YFP and PID:CFP. The lambda scanning profile matched that of protoplasts expressing the YFP:CFP fusion protein for which FRET is expected (Figures 5a and 5b). These data corroborate our earlier hypothesis that TCH3 sequesters PID from the plasma membrane to the cytoplasm by interaction with the protein kinase.

Auxin-induced calcium-dependent sequestration of PID in root epidermal cells

Previous studies [23;33;40] already indicated that expression patterns of *PID* and *TCH3* overlap, and thus should allow a functional *in vivo* interaction between the two proteins. As shown by a *TCH3pro::TCH3:GUS* translational fusion, *TCH3* is expressed in epidermis cells of the elongation zone of the root tip (Figure 6a), in the vasculature of the root at the root-hypocotyl junction (Figure 6b), in the vasculature and guard cells in leaves and cotyledons (Figure 6c), and at the shoot apical meristem (Figure 6c). As the expression of *TCH3* is auxin responsive, it preferentially accumulates in cells that are part of auxin response maxima, e.g., in the shoot apical meristem and root columella, in vascular tissues in roots, leaves and sepals and in the anthers and stigmas of flowers [33;40]. Upon IAA treatment, *TCH3* expression is strongly induced in the root, where it is extended to the vasculature and the epidermis of the complete root (Figure 6d). *PID* is also auxin responsive and is co-expressed with *TCH3* in the epidermis cells in the elongation zone of the root tip, in the shoot apical meristem and in flowers [23], suggesting a functional interaction between the two proteins in these tissues.

To investigate the biological relevance of the auxin-dependent, *TCH3*-mediated sequestration of *PID* observed in protoplasts, we used the *PIDpro::PID:VENUS* line [25] to study the dynamics of the subcellular localization of *PID* in wild type *Arabidopsis* and *35Spro::TCH3* overexpression epidermis root cells. In both backgrounds, *PID* localized at the membrane (Figures 6e and 6m) [25;38], suggesting that overexpression of *TCH3* alone is not sufficient to trigger the change in *PID* subcellular localization *in planta*.

Upon auxin treatment, however, *PID* was rapidly released in the cytoplasm within 5 minutes of treatment (Figure 6f), and plasma membrane localization was restored 10 minutes after auxin addition (Figures 6g-j). Pre-treatment of seedlings with tetracain (Tc), a calmodulin inhibitor, or lanthanum (La), a calcium channel blocker, did not influence the *PID* localization by itself (Figures 6k and 6s), but did inhibit IAA-induced dissociation of *PID* from the plasma membrane (Figures 6l and 6t). *PID* localization was not influenced by *TCH3* overexpression. These data suggest that this dissociation is dependent on an increase in the cytoplasmic calcium concentration involving plasma membrane calcium channels, and that this calcium signal is translated by one or more

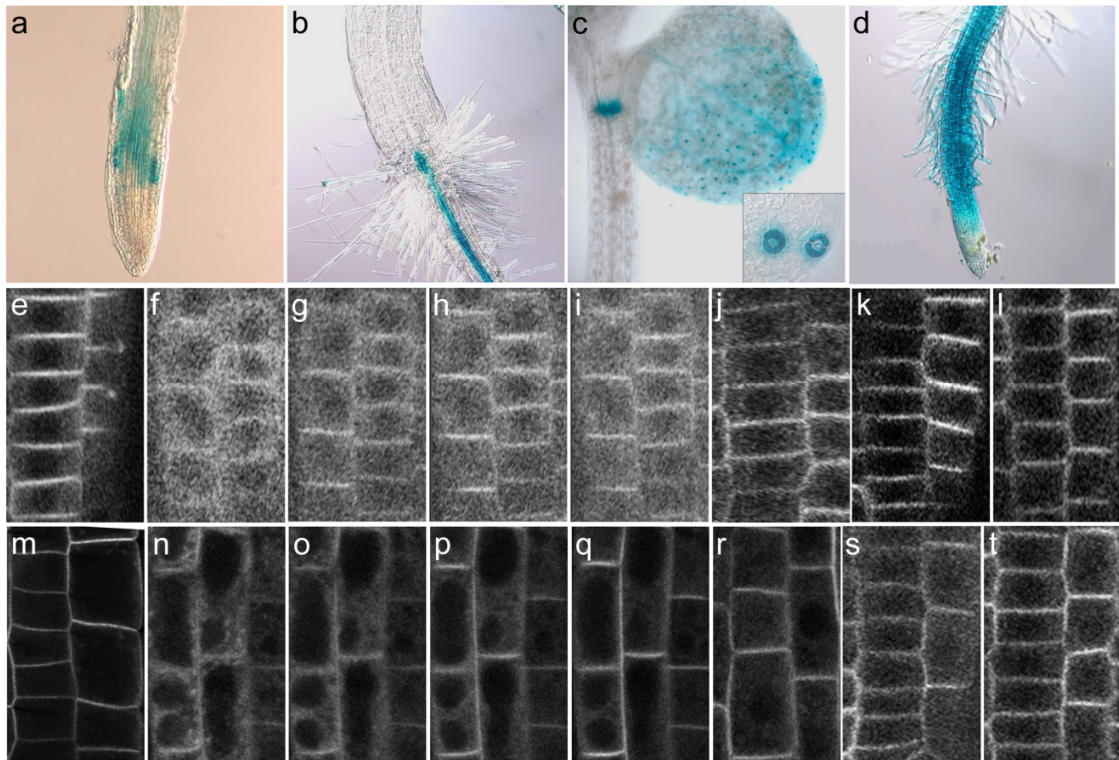


Figure 6. TCH3 and auxin cause PID to dissociate from the plasma membrane.

(a-d) Histochemical staining of *TCH3pro::TCH3:GUS* seedlings [33] showing that *TCH3* is expressed in epidermis cells of the elongation zone of the root tip (a), in vascular tissues at the root-hypocotyl junction (b), in the shoot apical meristem and in vascular tissues and stomata (inset) of the cotyledon (c). *TCH3* expression in roots is enhanced when grown on $0.1\mu\text{M}$ IAA (d).

(e) PID is membrane localized in *PIDpro::PID:VENUS* epidermal cells of seedling root tips.

(f-j) PID transiently dissociates from the plasma membrane 5 min after IAA treatment (f), but rapidly returns to the plasma membrane (10 min (g), 20min (h), 30 min (i) and 1 h (j) treatment).

(k-l, s-t) Pre-treatment with tetracain (30 min incubation, k-l), a CaM inhibitor, or Lanthanum (30 min incubation, s-t), a calcium channel inhibitor, does not influence PID localization (k, s) but blocks the auxin-induced dissociation of PID from the plasma membrane (5 min treatment with IAA and inhibitors, l, t).

(m-r) In seedling root tips of the *PIDpro::PID:VENUS/35Spro::TCH3-2* line PID shows normal plasma membrane localization (m) and IAA-induced transient dissociation from the plasma membrane (5min (n), 10min (o), 20 min (p), 30 min (q), 1h (r)).

CaMs. In view of our results in protoplasts, it is likely that the CaM-like protein TCH3 is involved in this process.

Together the results described here suggest that TCH3 acts as a calcium receptor in the PID signaling pathway that translates rapid peaks in cytosolic calcium into subtle changes in PIN polarity, by influencing the activity and by sequestering the kinase from the plasma membrane to the cytoplasm.

Discussion

Calcium is a common second messenger in signaling pathways, and has been found as one of the early signals in auxin responses. Experiments on plant cells showed that the cytosolic calcium concentration is increased within few minutes after auxin application [11-13]. Furthermore, PAT is suppressed by application of the calcium chelator EDTA, and restored after application of a calcium solution [26], indicating that calcium is also an important second messenger in the regulation of auxin transport.

PIN proteins are components of the cellular auxin efflux machinery. Their subcellular localization determines the direction of the auxin transport [22;41]. The protein serine/threonine kinase PINOID regulates PAT by establishing the proper apico-basal polarity of the PIN auxin efflux carriers [24]. The finding that two calcium binding proteins PBP1 and TCH3 interact with PID to regulate its kinase activity *in vitro*, provided a first molecular link between calcium and the regulation of PAT [32]. Here we investigated the *in vivo* role of TCH3 in the PID signaling pathway. First, we identified that TCH3 binds the catalytic domain of the PID kinase, and used *in vitro* kinase assays and genetic analysis to confirm the previous observations that TCH3 is a regulator of PID kinase activity [32]. Next, we showed the co-localization and the interaction between TCH3 and PID in *Arabidopsis* protoplasts. Finally, we could demonstrate that TCH3 is involved in PID subcellular localization dynamics, clarifying the molecular link between calcium signaling and auxin transport.

TCH3 competes with plasma membrane components for binding the catalytic domain of PID

Previously, we used *in vitro* pull down assays to show that TCH3 interacts with PID in a calcium-dependent manner [32]. Here, a similar assay was used in combination with PID deletion constructs to show that TCH3 interacts with the PID catalytic domain. Moreover, co-expression of TCH3 and PID in *Arabidopsis* protoplasts and subsequent FRET measurements demonstrated the *in vivo* interaction between the two proteins, and showed that TCH3 sequesters the normally plasma membrane-associated PID kinase to the cytoplasm. This suggests that interaction of TCH3 with the catalytic domain of PID provokes the release of the kinase from the plasma membrane. The cytoplasmic PID

sequestration is auxin-dependent, as auxin-starved protoplasts do not show internalization of PID. Most likely, auxin treatment of protoplasts results in elevated levels of cytosolic calcium, which in turn enhances the affinity of the TCH3 CaM-like protein for PID.

Recent data by Zegzouti and co-workers indicated that PID binds to phosphorylated inositides and phosphatidic acid, and that the amino acid insertion in the PID catalytic domain (insertion domain) is the key determinant in membrane association of the kinase [42]. We therefore hypothesize that PID co-localizes at the plasma membrane with its phosphorylation targets, the PIN auxin efflux carriers [25], through direct binding of membrane components to the insertion domain. An increase in cytosolic calcium, e.g. induced by auxin, facilitates binding of TCH3 to the catalytic domain of PID, thereby preventing the kinase-lipid interaction and resulting in sequestration of the kinase away from its phospho-targets to the cytoplasm (Figure 7). Based on this model, it would be interesting to test whether TCH3 and phosphoinositides are competing for the interaction with the PID catalytic domain.

PKC, one of the animal orthologs of the plant specific AGCVIII kinases to which PID belongs [43] directly binds calcium through a C2 domain. Calcium binding to this domain promotes a change in PKC subcellular localization from the cytosol to the plasma membrane and enhances the affinity of the C2 domain for phosphorylated inositides [44]. This plasma membrane translocation activates the PKC kinase. PID is also thought to be active at the plasma membrane. However in this case the (auxin-induced) increase in cytosolic calcium levels results in the opposite effect and removes the kinase from the plasma membrane. PID does not have the typical calcium binding domains, and instead the kinase has evolved to interact in a calcium-dependent manner with calcium receptors, such as TCH3. Changes in subcellular localization are a commonly used cellular mechanism to regulate protein activity by sequestering proteins away from their targets. To our knowledge, the calcium- and CaM-dependent release of the PID kinase is a new form of regulating the activity of a kinase that steers the polar subcellular targeting of transporter proteins.

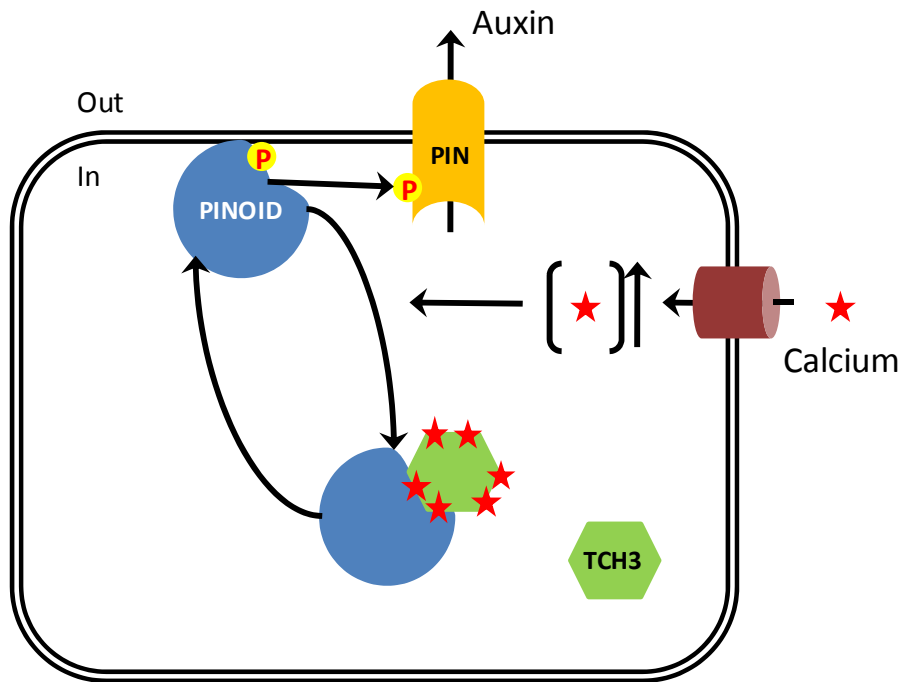


Figure 7. Model for auxin-induced sequestration of PID from the plasma membrane to the cytoplasm. High auxin levels increase the cytoplasmic calcium concentration, by activating plasma membrane-localized calcium channels. Enhanced binding of calcium to the CaM-like TCH3 enhances its affinity for PID, whereby TCH3 is able to compete for PID binding to plasma membrane components. This leads to sequestration of PID from the plasma membrane to the cytoplasm, away from its phosphorylation targets, the PIN proteins. At the same TCH3 binding to the PID catalytic domain inhibits kinase activity.

TCH3 is part of feedback loop of auxin on the direction of its own transport?

The proposed model in Figure 7 implies that a calcium release negatively and transiently regulates PID activity through its TCH3-induced dissociation from the plasma membrane, away from its phospho-targets, the PIN proteins. This TCH3-dependent inactivation of PID may be part of a regulatory loop that allows fast and possibly subtle alterations in PIN polarity in response to signals that lead to rapid changes in cytosolic calcium levels, such as auxin [11-13], unidirectional light or gravity [27;45-47]. Auxin is known to regulate its own transport, firstly by inhibiting PIN endocytosis [48], and secondly by regulating the subcellular PIN localization in *Arabidopsis* roots [49], probably in order to canalize and increase the auxin flow in response to increased cellular auxin concentrations. Sauer and co-workers concluded that PID is not required for auxin-dependent PIN lateralization in root cells, because they still observed PIN lateralization in auxin-treated *35Spro::PID* seedlings [49].

Auxin-induced PIN lateralization involves TIR1-dependent induction of auxin responsive gene expression, and does not occur as rapid as the auxin-induced dissociation of PID from the membrane that we report here. Our results suggest that elevated cellular auxin levels may transiently alter PID kinase activity by subcellular localization changes and inhibition of its kinase activity via TCH3 interaction. This may set the stage for the auxin-dependent PIN lateralization, or may only lead to a subtle modulation of PIN polar targeting. The fact that none of *TCH3* loss- and gain-of-function mutants display obvious phenotypes, and that we have not been able to detect changes in PIN polar targeting in roots of *35Spro::TCH3* and *tch3* mutant lines (M. Sauer, unpublished results) nor in *pid* knock-out roots (Chapter 5), may be explained by calcium dependency of the PID-TCH3 interaction (*35Spro::TCH3*) and by functional redundancy with other CaMs (*tch3*) or with the PID-related AGC3 kinases (*pid*).

Material and methods

Molecular cloning and constructs

Molecular cloning was performed following standard procedures [50]. Bacteria were grown on LC medium containing 100 µg/ml carbenicillin (Cb, all high copy plasmids), 50 µg/ml kanamycin (Km, pGreen) or 250 µg/ml spectinomycin (Spc, *pART27*) for *E. coli* strains DH5α or Rosetta (Novagen) or 20 µg/ml rifampicin (Rif) and 50 µg/ml Km, or 250 µg/ml Spc for *Agrobacterium* strain LBA1115. The constructs *pSDM6008* (*pET16H:TCH3*), *pSDM6004* (*pGEX:PID*) and *pSDM6005* (*pBluescript SK-PID*) were described previously [32]. Primers used in this study are listed in Table 1. To obtain a plasmid encoding the GST tagged first 100 amino acids of PID, the *SalI-SacI* (blunted) fragment from *pSDM6005* was cloned into the *XhoI* and *HindIII* (blunted) sites of *pGEX-KG* [51]. Fragments encoding the PID catalytic domain (aa 75-398) and the C-terminal part of PID (aa 339-438) were obtained by PCR amplification using the primer pairs PID PK CaD F - PID PK CaD R and PID PK CT F - PID PK CT R, respectively and cloned into *pGEX-KG* using *XhoI-HindIII* (blunted) and *EcoRI-HindIII* (blunted), respectively. To overexpress *TCH3* in *Arabidopsis thaliana*, its complete coding region was cloned from *pSDM6008* as a *BamHI* fragment into *pART7* and the expression cassette was

inserted as a *NotI* fragment into the *pART27* binary vector. To construct *35Spro::TCH3:YFP*, *35Spro::PID:YFP* and *35Spro::PID:CFP*, the coding regions were amplified by PCR from *pSDM6008* and *pSDM6004* with respectively primers TCH3 attB F1 and TCH3 attB R1, and PID attB F1 and PID attB R1 and the resulting PCR fragments were recombined into *pDONOR207* (BP reaction) and subsequently into *pART7*-derived destination vectors (LR reaction), containing either the *CFP* (PID) or the *YFP* (TCH3 and PID) coding region in frame with the Gateway cassette (Invitrogen). The *35Spro::PID:YFP* expression cassette was inserted as a *NotI* fragment into the pGreenII0179 binary vector.

Table 1. Primer list

PID PK CaD F	5'TTC- <i>XhoI</i> -TTTCGCCTCAT3'
PID PK CaD R	5'GCGCTCAGTTTAGACCTTTGA3'
PID PK CT F	5'TAATGACG- <i>EcoRI</i> -TCCGTAACAT3'
PID PK CT R	5'AAGCTCGTTCAAAAGTAATCGAAC3'
TCH3 attB F1	5'GGGGACAAGTTTGTACAAAAAAGCAGGCTTAATGGCGGATAAGCTCACT3'
TCH3 attB R1	5'GGGGACCACTTTGTACAAGAAAGCTGGGTAAGATAACAGCGCTTCAACA3'
PID attB F1	5'GGGGACAAGTTTGTACAAAAAAGCAGGCTTCAGCATGTTACGAGAATCAGACGGT3'
PID attB R1	5'GGGGACCACTTTGTACAAGAAAGCTGGGTCAAAAGTAATCGAACGCCGCTGG3'
PID exon1 F1	5'TCTCTCCGCCAGGTAAAAA3'
PID exon2 R1	5'CGCAAGACTCGTTGGAAAAG3'
TCH3pr F1	5'AAATGTCCACTCACCCATCC3'
TCH3pr R1	5'GGGAATTCTGAAGATCAGCTTTTGTGCG3'
LBaI	5'TGGTTCACGTAGTGGGCCATCG3'
AtROC5 F	5'CGGGAAGGATCGTGATGGA3'
AtROC5 R	5'CCAACCTTCTCGATGGCCT3'
α TUB F	5'CGGAATTCATGAGAGAGATCCTTCATATC3'
α TUB R	5'CCCTCGAGTTAAGTCTCGTACTCCTCTC3'

The attB recombination sites are underlined.

***In vitro* pull-down**

E. coli strain Rosetta (Novagen) was transformed with *pSDM6008*, *pSDM6004*, *pGEX-PIDaa2-103*, *pGEX-PIDaa75-398* and *pGEX-PIDaa339-438*. Single colonies were picked and grown overnight (o/n) at 37°C in 5 ml liquid LC medium containing Cb, 15 µg/ml Km and 34 µg/ml Chloramphenicol (Cam). The o/n culture was diluted 1/20 in 100 ml of fresh LC medium containing Cb and Cam and grown at 37°C until an OD₆₀₀ of 0.8. The cultures were induced with 1 mM IPTG for 4 h and bacteria were harvested by centrifugation and frozen. For GST-tagged PID, frozen bacterial pellets were resuspended

in 5 ml Extraction Buffer (EB: 20 mM Tris pH 7.5, 500 mM NaCl, 5 mM EDTA, 1 mM EGTA, 1 mM DTT, 0.2 % Triton X-100, 0.05 % Tween-20) supplemented with 0.1 mM Phenylmethanesulfonylfluoride (PMSF), 0.5 µg/ml Leupeptin and 5 µg/ml Trypsin Inhibitor and incubated on ice for 5 min. After sonication for 2 min, the mixtures were centrifuged at 10000 g for 15 min at 4°C. Supernatants were added to 500 µl of pre-equilibrated 50 % Glutathione sepharose 4B beads (Amersham-Pharmacia) and incubated for 1 h at 4°C. Beads were washed once with 10 ml EB, and twice with 10 ml Washing Buffer 1 (10 mM Tris pH 7.5, 150 mM NaCl, 5 mM EDTA, 1 mM EGTA, 1 mM DTT). Proteins were eluted by incubating beads at room temperature with 2 ml Elution Buffer 1 (50 mM Tris pH 8.0, 10 mM reduced glutathione). Eluates were passed through MicroSpin chromatography columns (BioRad) and concentrated using Vivaspin 6 device 10000 MWCO (Sartorius). For His-tagged TCH3, bacteria pellets were resuspended in Binding Buffer (BB: 20 mM Tris pH 7.5, 500 mM NaCl, 5 mM MgCl₂, 2 mM CaCl₂, 1 mM DTT, 0.2 % Triton X-100, 0.05 % Tween-20) supplemented with 0.1 mM PMSF, 0.5 µg/ml Leupeptin and 5 µg/ml Trypsin Inhibitor, incubated for 5 min on ice prior to lysis of cells by 2 min sonication. For *in vitro* pull down assays, 2 µg of purified GST-tagged protein was immobilized on Glutathione High Capacity Coated Plates (Sigma). After three washes with BB, 200 µl of total protein extract containing His-tagged TCH3 was added to each well and incubated for 1 h at 4°C, washed once with BB and twice with Washing Buffer 2 (10 mM Tris pH 7.5, 150 mM NaCl, 5 mM MgCl₂, 2 mM CaCl₂, 1 mM DTT). Protein complexes were eluted with 25 µl of 2x Laemmli sample buffer and boiled. Eluate samples were analyzed by SDS-PAGE (12 % gel). Proteins were blotted on a PDVF membrane (Millipore, USA) and detected using penta-his antibodies (Qiagen) according to the manufacturer's instructions.

Phosphorylation assays

His-tagged proteins were purified by immobilized-metal affinity chromatography. Bacterial pellets were resuspended in 2 ml of Lysis Buffer (LB: 25 mM Tris pH 8.0, 500 mM NaCl, 20 mM imidazole, 0.05 % Tween-20, 10 % glycerol) and incubated 5 min on ice. After sonication for 2 min, 100 µl of 20 % Triton X-100 was added and the mixture was incubated 5 min on ice, followed by centrifugation at 10000 g for 15 min at 4°C. The

soluble fraction was added with 400 μ l of pre-equilibrated 50 % NTA-agarose matrix (Qiagen) and mixed gently for 1.5 h at 4°C. Beads were washed three times with 2 ml of LB, 2 ml of Washing Buffer 3 (25 mM Tris pH 7.5, 500 mM NaCl, 40 mM imidazole, 0.01 % Tween-20, 10 % glycerol), and 2 ml of Wash Buffer 4 (25 mM Tris pH 7.0, 500 mM NaCl, 80 mM imidazole and 10 % glycerol). Elution was performed by incubating the beads on 600 μ l Elution Buffer 2 (25 mM Tris pH 7.0, 300 mM NaCl, 300 mM imidazole, 10 % glycerol) for 30 min at 4°C. Samples were analyzed by SDS-PAGE and quantified.

The Pepchip Kinase Slide A (Pepscan) was used for *in vitro* phosphorylation assays for PID in the presence of TCH3. Thirty ng of His:PID, His:TCH3 and His:PBP1 (Chapter 3, this thesis) were mixed with Kinase Mastermix (50 mM HEPES pH 7.4, 20 mM MgCl₂, 20 % v/v glycerol, 0.01 mg/ml BSA, 0.01 % v/v Brij-35, 2 mM CaCl₂), 10 μ M ATP and 300 μ Ci/ml γ -³³P-ATP (specific activity ~ 3000 Ci/mmol, Amersham). Fifty μ l of the reaction mix was incubated with the Pepchip Kinase Slide A for 4 h at 30°C in a humid chamber. Slides were washed twice with 2 M NaCl, twice with water and dried for 30 min. Slides were exposed to X-ray film FUJI Super RX for 12 and 24 h.

***Arabidopsis* lines, plant growth, transformation and protoplast transfections**

The *35Spro::PID-21*, *TCH3pro::TCH3:GUS* and *PIDpro::PID:VENUS* lines were described previously [23;25;33]. Loss-of-function alleles *pid-14* (SALK_049736), *tch3-1* (SALK_056345) and *tch3-2* (SALK_090554) were obtained from NASC [52].

Arabidopsis seeds were surfaced-sterilized by incubation for 15 min in 50 % commercial bleach solution and rinsed four times with sterile water. Seeds were vernalized for 2 to 4 days and germinated at 21°C, 16 h photoperiod and 3000 lux on solid MA medium [53] supplemented with antibiotics when required. Two- to three-week old plants were transferred to soil and grown in growth room at 21°C, 16 h photoperiod, 70 % relative humidity and 10000 lux.

To screen for the presence of the different T-DNA insertions, the T-DNA-specific LBA1 primer was combined in a PCR reaction with the gene-specific PCR primers PID exon1 F1 or PID exon2 R1 for *pid-14* and TCH3pr F1 or TCH3pr R1 for *tch3-1* and *tch3-*

2. Sequencing of the junction fragment and Northern blot analysis were used to confirm the insertion position and full knock-out of the loss-of-function alleles.

Arabidopsis thaliana ecotype Columbia wild type (for *35Spro::TCH3*) or the *35Spro::TCH3-2* line (for *35Spro::PID::YFP*) were transformed by a floral dip method as described [54] using *Agrobacterium* LBA1115 strain. The T1 transformants were selected on medium supplemented with 50 µg/ml Km for *35Spro::TCH3* or 20 µg/ml hygromycin (Hm) for *35Spro::PID* and with 100 µg/ml timentin to inhibit the *Agrobacterium* growth. For further analysis, single locus insertion lines were selected by germination on 25 µg/ml Km or 10 µg/ml Hm.

Protoplasts were obtained from *Arabidopsis thaliana* Columbia cell suspension cultures that were propagated as described [55]. Protoplast isolation and PEG-mediated transfections with 10 µg plasmid DNA were performed as initially indicated [56] and adapted by Schirawski and coworkers [55]. To obtain auxin-starved protoplasts, auxin (NAA) was removed from the media during protoplast isolation. Following transfection, the protoplasts were incubated for at least 16 h prior to observation.

Histochemical staining and microscopy

For the Histochemical detection of *GUS* expression, seedlings were fixed in 90 % acetone for 1 h at -20°C, subsequently washed three times in 10 mM EDTA, 100 mM sodium phosphate (pH 7.0), 2 mM $K_3Fe(CN)_6$ and stained for 2 h in 10 mM EDTA, 100 mM sodium phosphate (pH 7.0), 1 mM $K_3Fe(CN)_6$, 1 mM $K_4Fe(CN)_6$ containing 1 mg/ml 5-bromo-4-chloro-3-indolyl-β-D-glucuronic acid, cyclohexylammonium salt (Duchefa). Seedlings were post-fixed in ethanol-acetate (3:1), cleared in 70 % ethanol and stored in 100 mM sodium phosphate (pH 7.0). *GUS* expression patterns in cleared *Arabidopsis* seedlings were analyzed using a Zeiss Axioplan II microscope with DIC optics. Images were recorded by a ZEISS camera. *Arabidopsis* lines expressing YFP-fusion proteins were analyzed with a ZEISS Axioplan microscope equipped with a confocal laser scanning unit (MRC1024ES, BioRad, Hercules, CA), using a 40x oil objective. The YFP fluorescence was monitored with a 522-532 nm band pass emission filter (488 nm excitation). All images were recorded using a 3CCD Sony DKC5000 digital camera. For the protoplast experiments, a Leica DM IRBE confocal laser scanning microscope was

used with a 63x water objective, digital zoom and 51 % laser intensity. The fluorescence was visualized with an Argon laser for excitation at 514 nm (YFP) and 457 nm (CFP), with 522-532 nm (for the YFP) and 471-481 nm (for the CFP) emission filters. A transmitted light picture was taken for a reference. The images were processed by ImageJ (<http://rsb.info.nih.gov/ij/>) and assembled in Adobe Photoshop 7.0.

Fluorescence Resonance Energy Transfer (FRET)

Protoplasts were prepared and their fluorescence monitored using a Leica confocal microscope as described above. Lambda scanning was done by excitation at 457 nm (donor, CFP) and by measuring emission at 5 nm intervals from 460 to 585 nm using a RSP465 filter. Of every interval an image was obtained and the intensity of three fixed areas (regions of interest, ROIs) was quantified using the Leica confocal laser scanning software. The intensity of these three ROIs was averaged and normalized. Per sample lambda scanning was performed on three protoplasts and the obtained normalised intensity of all three protoplasts was averaged and used to calculate the standard deviation. The Student's t-test was used to test for significant differences in wavelength specific intensities between the test sample and the negative control. Significantly quenched donor emission wavelength intensity, combined with significantly increased acceptor emission wavelength intensity was considered indicative for protein-protein interaction-dependent FRET. Similar results were obtained for three independent transfections.

RNA extraction and Northern Blots

Total RNA was purified using the RNeasy Plant Mini kit (Qiagen). Subsequent RNA blot analysis was performed as described [57] using 10 µg of total RNA per sample. The following modifications were made: pre-hybridizations and hybridizations were conducted at 65°C using 10 % Dextran sulfate, 1 % SDS, 1 M NaCl, 50 µg/ml of single strand Herring sperm DNA as hybridization mix. The hybridized blots were washed for 20 min at 65°C in 2x SSPE 0.5 % SDS, and for 20 min at 42°C in respectively 0.2x SSPE 0.5 % SDS, 0.1x SSPE 0.5 % SDS and 0.1x SSPE. Blots were exposed to X-ray film FUJI Super RX. The probe for *TCH3* was isolated from *pSDM6008* as a *Bam*HI

fragment. The probes for *AtROC5*, for α *Tubulin* and *PID* were PCR amplified from Col genomic DNA and column purified (Qiagen). Probes were radioactively labeled using a Prime-a-gene kit (Promega).

Biological assays

For the root collapse assay, about 200 seedlings per line were grown in triplicate on vertical plates on MA medium, while the development of the seedling root was monitored and scored each day during 8 days for the collapse of the primary root meristem. For the phenotypic analysis of *pid-14+/35Spro::TCH3-1*, *pid-14+/35Spro::TCH3-3*, *pid-14+/35Spro::TCH3-4* and *pid-14/tch3-2* lines, about 300 seeds were plated in triplicate on MA medium and germinated for one week. The number of dicotyledon seedlings and of seedlings with specific cotyledon defects was counted and the penetrance of the specific phenotypes was calculated based on a 1:3 segregation ratio for *pid* homozygous seedlings. For GUS analysis, seeds of *TCH3pro::TCH3:GUS* were grown for 4 days on MA medium, supplemented with 5 μ M IAA when indicated. For the subcellular localization of PID in *Arabidopsis* roots, vertically grown 3 day-old *PIDpro:PID:VENUS* seedlings were treated with 5 μ M IAA (in MA medium) with 30 min pre-treatment with a calmodulin inhibitor (0.5 mM Tetracain, Sigma) or calcium channel blocker (1.25 mM Lanthanum, Sigma) when indicated. Analysis of the subcellular localization was done using the BioRad confocal microscope as described above.

Accession Numbers

The *Arabidopsis* Genome Initiative locus identifiers for the genes mentioned in this chapter are as follows: *PBPI* (At5g54490), *PID* (At2g34650), *TCH3* (At2g41100), *ROC* (At4g38740), α *Tubulin* (At5g44340).

Acknowledgments

The authors would like to thank M. Heisler and J. Braam for kindly providing us with the *PIDpro::PID:VENUS* line and the *TCH3pro::TCH3:GUS* line, respectively, J. Braam for sharing her unpublished data on the *tch3-3* allele, Michael Sauer for PIN localization on *TCH3* gain- and loss-of-function mutants, Arnoud van Marion for technical assistance,

and Gerda Lamers and Ward de Winter for their help with the microscopy and the tissue culture, respectively. This work was funded through grants from the Research Council for Earth and Life Sciences (ALW 813.06.004) and from the Netherlands Organisation for Health Research and Development (ZON 050-71-023), and with financial aid from the Dutch Organization of Scientific Research (NWO).

Reference list

1. Bouché N, Yellin A, Snedden WA, Fromm H (2005). **Plant-specific calmodulin-binding proteins**. *Ann. Rev. Plant Biol.* 56(1), 435-466.
2. Sanders D, Pelloux J, Brownlee C, Harper JF (2002). **Calcium at the crossroads of signaling**. *Plant Cell* 14 Suppl, S401-S417.
3. Luan S, Kudla J, Rodriguez-Concepcion M, Yalovsky S, Gruissem W (2002). **Calmodulins and calcineurin B-like proteins: calcium sensors for specific signal response coupling in plants**. *Plant Cell* 14 Suppl, S389-S400.
4. Strynadka NCJ, James MNG (1989). **Crystal structures of the helix-loop-helix calcium-binding proteins**. *Ann. Rev. Biochem.* 58(1), 951-999.
5. Travé G, Lacombe PJ, Pfuhl M, Saraste M, Pastore A (1995). **Molecular mechanism of the calcium-induced conformational change in the spectrin EF-hands**. *EMBO J.* 14(20), 4922-4931.
6. Snedden WA, Fromm H (2001). **Calmodulin as a versatile calcium signal transducer in plants**. *New Phytologist.* 151(1), 35-66.
7. Cheng SH, Willmann MR, Chen HC, Sheen J (2002). **Calcium signaling through protein kinases. The *Arabidopsis* calcium-dependent protein kinase gene family**. *Plant Physiol.* 129(2), 469-485.
8. Nakajima K, Benfey PN (2002). **Signaling in and out: Control of cell division and differentiation in the shoot and root**. *Plant Cell* 14, S265-S276.
9. Reinhardt D, Mandel T, Kuhlemeier C (2000). **Auxin regulates the initiation and radial position of plant lateral organs**. *Plant Cell* 12(4), 507-518.
10. Weijers D, Jurgens G (2005). **Auxin and embryo axis formation: the ends in sight?** *Curr. Opinion in Plant Biol.* 8(1), 32-37.
11. Shishova M, Lindberg S (2004). **Auxin induces an increase of Ca²⁺ concentration in the cytosol of wheat leaf protoplasts**. *J Plant Physiol.* 161(8), 937-945.
12. Gehring CA, Irving HR, Parish RW (1990). **Effects of auxin and abscisic acid on cytosolic calcium and pH in plant cells**. *Proc. Natl. Acad. Sci. USA.* 87(24), 9645-9649.
13. Felle H (1988). **Auxin causes oscillations of cytosolic free calcium and pH in *Zea mays* coleoptiles**. *Planta.* V174(4), 495-499.
14. Darwin C (1880). **The Power of Movement in Plants**. London: John Murray.

15. Muday GK, DeLong A (2001). **Polar auxin transport: controlling where and how much.** *Trends Plant Sci.* 6(11), 535-542.
16. Friml J, Wisniewska J, Benková E, Mendgen K, Palme K (2002). **Lateral relocation of auxin efflux regulator PIN3 mediates tropism in *Arabidopsis*.** *Nature.* 415(6873), 806-809.
17. Reinhardt D, Pesce ER, Stieger P, Mandel T, Baltensperger K, Bennett M, Traas J, Friml J, Kuhlemeier C (2003). **Regulation of phyllotaxis by polar auxin transport.** *Nature.* 426(6964), 255-260.
18. Sabatini S, Beis D, Wolkenfelt H, Murfett J, Guilfoyle T, Malamy J, Benfey P, Leyser O, Bechtold N, Weisbeek P, Scheres B (1999). **An auxin-dependent distal organizer of pattern and polarity in the *Arabidopsis* root.** *Cell.* 99(5), 463-472.
19. Friml J, Vieten A, Sauer M, Weijers D, Schwarz H, Hamann T, Offringa R, Jurgens G (2003). **Efflux-dependent auxin gradients establish the apical-basal axis of *Arabidopsis*.** *Nature.* 426(6963), 147-153.
20. Morris DA, Friml J, Zazimalova E. (2004) **The functioning of hormones in plant growth and development, the transport of auxins.** In *Plant hormones: Biosynthesis, signal transduction, action!* kluwer Academic Publishers, Dordrecht, NL;437-470.
21. Petrášek J, Mravec J, Bouchard R, Blakeslee JJ, Abas M, Seifertová D, Wisniewska J, Tadele Z, Kubes M, Covanová M, Dhonukshe P, Skupa P, Benková E, Perry L, Krecek P, Lee OR, Fink GR, Geisler M, Murphy AS, Luschnig C, Zazimalova E, Friml J (2006). **PIN Proteins Perform a Rate-Limiting Function in Cellular Auxin Efflux.** *Science.* 312(5775), 914-918.
22. Wisniewska J, Xu J, Seifertova D, Brewer PB, Ruzicka K, Blilou I, Rouquie D, Benkova E, Scheres B, Friml J (2006). **Polar PIN Localization Directs Auxin Flow in Plants.** *Science.* 312(5775), 883.
23. Benjamins R, Quint A, Weijers D, Hooykaas P, Offringa R (2001). **The PINOID protein kinase regulates organ development in *Arabidopsis* by enhancing polar auxin transport.** *Development.* 128(20), 4057-4067.
24. Friml J, Yang X, Michniewicz M, Weijers D, Quint A, Tietz O, Benjamins R, Ouwerkerk PBF, Ljung K, Sandberg G, Hooykaas PJJ, Palme K, Offringa R (2004). **A PINOID-dependent binary switch in apical-basal PIN polar targeting directs auxin efflux.** *Science.* 306(5697), 862-865.
25. Michniewicz M, Zago MK, Abas L, Weijers D, Schweighofer A, Meskiene I, Heisler MG, Ohno C, Huang F, Weigel D, Meyerowitz EM, Luschnig C, Offringa R, Friml J (2007). **Phosphatase 2A and PID kinase activities antagonistically**

- mediate PIN phosphorylation and apical/basal targeting in *Arabidopsis*.** *Cell*. 130(6), 1044-1056.
26. Dela Fuente RK, Leopold AC (1973). **A Role for Calcium in Auxin Transport.** *Plant Physiol.* 51(5), 845-847.
27. Lee JS, Evans ML (1985). **Polar transport of auxin across gravistimulated roots of maize and its enhancement by calcium.** *Plant Physiol.* 77, 824-827.
28. Baum G, Long JC, Jenkins GI, Trewavas AJ (1999). **Stimulation of the blue light phototropic receptor NPH1 causes a transient increase in cytosolic Ca²⁺.** *Proc.Natl.Acad.Sci.USA*. 96(23), 13554-13559.
29. Harada A, Sakai T, Okada K (2003). **Phot1 and phot2 mediate blue light-induced transient increases in cytosolic Ca²⁺ differently in *Arabidopsis* leaves.** *Proc.Natl.Acad.Sci.USA*. 100(14), 8583-8588.
30. Friml J, Wisniewska J, Benková E, Mendgen K, Palme K (2002). **Lateral relocation of auxin efflux regulator PIN3 mediates tropism in *Arabidopsis*.** *Nature*. 415(6873), 806-809.
31. Esmon CA, Tinsley AG, Ljung K, Sandberg G, Hearne LB, Liscum E (2006). **A gradient of auxin and auxin-dependent transcription precedes tropic growth responses.** *Proc.Natl.Acad.Sci.USA*. 103(1), 236-241.
32. Benjamins R, Galván-Ampudia CS, Hooykaas PJ, Offringa R (2003). **PINOID-mediated signaling involves calcium-binding proteins.** *Plant Physiol.* 132(3), 1623-1630.
33. Sistrunk ML, Antosiewicz DM, Purugganan MM, Braam J (1994). ***Arabidopsis* TCH3 encodes a novel Ca²⁺ binding protein and shows environmentally induced and tissue-specific regulation.** *Plant Cell*. 6(11), 1553-1565.
34. Braam J, Davis RW (1990). **Rain-, wind-, and touch-induced expression of calmodulin and calmodulin-related genes in *Arabidopsis*.** *Cell*. 60(3), 357-364.
35. McCormack E, Braam J (2003). **Calmodulins and related potential calcium sensors of *Arabidopsis*.** *New Phytologist*. 159(3), 585-598.
36. Bennett SRM, Alvarez J, Bossinger G, Smyth DR (1995). **Morphogenesis in Pinoid Mutants of *Arabidopsis thaliana*.** *Plant Journal*. 8(4), 505-520.
37. Christensen SK, Dagenais N, Chory J, Weigel D (2000). **Regulation of auxin response by the protein kinase PINOID.** *Cell*. 100(4), 469-478.
38. Lee SH, Cho HT (2006). **PINOID Positively Regulates Auxin Efflux in *Arabidopsis* Root Hair Cells and Tobacco Cells.** *Plant Cell*. 18(7), 1604-1616.

39. Siegel RM, Chan FK, Zacharias DA, Swofford R, Holmes KL, Tsien RY, Lenardo MJ (2000). **Measurement of molecular interactions in living cells by fluorescence resonance energy transfer between variants of the green fluorescent protein.** *Sci STKE*. 2000(38), L1.
40. Antosiewicz DM, Polisensky DH, Braam J (1995). **Cellular localization of the Ca²⁺ binding TCH3 protein of *Arabidopsis*.** *Plant J*. 8(5), 623-636.
41. Petrášek J, Mravec J, Bouchard R, Blakeslee JJ, Abas M, Seifertová D, Wisniewska J, Tadele Z, Kubes M, Covanová M, Dhonukshe P, Skupa P, Benková E, Perry L, Krecek P, Lee OR, Fink GR, Geisler M, Murphy AS, Luschnig C, Zazimalova E, Friml J (2006). **PIN Proteins Perform a Rate-Limiting Function in Cellular Auxin Efflux.** *Science*. 312(5775), 914-918.
42. Zegzouti H, Li W, Lorenz TC, Xie M, Payne CT, Smith K, Glenny S, Payne GS, Christensen SK (2006). **Structural and functional insights into the regulation of *Arabidopsis* AGC VIIIa kinases.** *J Biol. Chem*. 281(46), 35520-35530.
43. Galván-Ampudia CS, Offringa R (2007). **Plant evolution: AGC kinases tell the auxin tale.** *Trends Plant Sci*. 12, 541-547.
44. Corbálan-García S, Guerrero-Valero M, Marin-Vicente C, Gomez-Fernández JC (2007). **The C2 domains of classical/conventional PKCs are specific PtdIns(4,5)P(2)-sensing domains.** *Biochem. Soc. Trans*. 35(Pt 5), 1046-1048.
45. Baum G, Long JC, Jenkins GI, Trewavas AJ (1999). **Stimulation of the blue light phototropic receptor NPH1 causes a transient increase in cytosolic Ca²⁺.** *Proc.Natl.Acad.Sci.USA*. 96(23), 13554-13559.
46. Gehring CA, Williams DA, Cody SH, Parish RW (1990). **Phototropism and geotropism in maize coleoptiles are spatially correlated with increases in cytosolic free calcium.** *Nature*. 345(6275), 528-530.
47. Harada A, Sakai T, Okada K (2003). **Phot1 and phot2 mediate blue light-induced transient increases in cytosolic Ca²⁺ differently in *Arabidopsis* leaves.** *Proc.Natl.Acad.Sci.USA*. 100(14), 8583-8588.
48. Paciorek T, Zazimalová E, Ruthardt N, Petrášek J, Stierhof YD, Kleine-Vehn J, Morris DA, Emans N, Jürgens G, Geldner N, Friml J (2005). **Auxin inhibits endocytosis and promotes its own efflux from cells.** *Nature*. 435(7046), 1251-1256.
49. Sauer M, Balla J, Luschnig C, Wisniewska J, Reinohl V, Friml J, Benkova E (2006). **Canalization of auxin flow by Aux/IAA-ARF-dependent feedback regulation of PIN polarity.** *Genes and Development*. 20(20), 2902-2911.
50. Sambrook J, Fritsch F., Maniatis T. (1989) **Molecular cloning - A laboratory Manual.** Edited by C.Nolan. Cold Spring Harbor Laboratory press, NY, USA.

51. Guan KL, Dixon JE (1991). **Eukaryotic Proteins Expressed in Escherichia-Coli - An Improved Thrombin Cleavage and Purification Procedure of Fusion Proteins with Glutathione-S-Transferase.** *Analytical Biochemistry.* 192(2), 262-267.
52. Alonso JM, Stepanova AN, Leisse TJ, Kim CJ, Chen H, Shinn P, Stevenson DK, Zimmerman J, Barajas P, Cheuk R, Gadrinab C, Heller C, Jeske A, Koesema E, Meyers CC, Parker H, Prednis L, Ansari Y, Choy N, Deen H, Geralt M, Hazari N, Hom E, Karnes M, Mulholland C, Ndubaku R, Schmidt I, Guzman P, Aguilar-Henonin L, Schmid M, Weigel D, Carter DE, Marchand T, Risseeuw E, Brogden D, Zeko A, Crosby WL, Berry CC, Ecker JR (2003). **Genome-Wide Insertional Mutagenesis of *Arabidopsis thaliana*.** *Science.* 301(5633), 653-657.
53. Masson J, Paszkowski J (1992). **The Culture Response of *Arabidopsis thaliana* Protoplasts Is Determined by the Growth-Conditions of Donor Plants.** *Plant Journal.* 2(5), 829-833.
54. Clough SJ, Bent AF (1998). **Floral dip: a simplified method for Agrobacterium-mediated transformation of *Arabidopsis thaliana*.** *Plant Journal.* 16(6), 735-743.
55. Schirawski J, Planchais S, Haenni AL (2000). **An improved protocol for the preparation of protoplasts from an established *Arabidopsis thaliana* cell suspension culture and infection with RNA of turnip yellow mosaic tymovirus: a simple and reliable method.** *Journal of Virological Methods.* 86(1), 85-94.
56. Axelos M, Curie C, Mazzolini L, Bardet C, Lescure B (1992). **A Protocol for Transient Gene-Expression in *Arabidopsis thaliana* Protoplasts Isolated from Cell-Suspension Cultures.** *Plant Physiology and Biochemistry.* 30(1), 123-128.
57. Memelink J, Swords KMM, Staehelin LA, Hoge JHC. (1994) **Southern, Northern and Western blot analysis.** In *Plant Molecular Biology Manual.* Dordrecht, NL: Kluwer Academic Publishers.
58. Sorefan K, Girin T, Liljegren SJ, Ljung K, Robles P, Galván-Ampudia CS, Offringa R, Friml J, Yanofsky MF, Østergaard L. (2009). **A regulated auxin minimum is required for seed dispersal in *Arabidopsis*.** *Nature.* 28(459), 583-6.

CHAPTER 3

PINOID signaling regulated by small calcium-binding proteins

Carlos S. Galván-Ampudia ¹, Hélène Robert ¹, Yang Xiong, Karen A. Sap, Håvard
Hildeng Hauge, Jos Joore, Remko Offringa

¹ Both authors contributed equally to this work

Summary

The plant hormone auxin directs plant patterning and tropic growth responses through its unidirectional transport, which creates auxin maxima and minima that regulate basic cellular processes such as cell division, differentiation and elongation. The direction of this intercellular auxin transport is determined by the asymmetric localization of PIN auxin transporters, whose subcellular targeting is dependent on their phosphorylation by the plant specific PINOID (PID) protein serine/threonine kinase. Here we investigated the function of two small EF-hand proteins, PINOID BINDING PROTEIN1 (PBP1) and its close homolog PBP1H, which interact with PID in a calcium-enhanced manner. We show that PBP1 not only stimulates PID kinase activity, but also changes PID substrate preference *in vitro*. Genetic experiments with different loss- and gain-of-function lines indicate that PBP1 and PBP1H act redundantly to enhance PID activity during embryo development and that they suppress root growth, possibly through their stimulatory effect on PID. PBP1 overexpression partially inhibits the auxin-induced calcium-dependent sequestration of PID from the plasma membrane, indicating that apart from enhancing the activity of the PID kinase, PBP1 also stabilizes localization of PID at the plasma membrane, close to its phosphorylation targets, the PIN proteins. We propose that PBP1 and PBP1H fine-tune PID signaling, in a cell-type and tissue specific manner, thereby modulating the direction of PAT in response to changes in cytosolic calcium.

Introduction

Auxin plays important roles as signaling molecule in many cellular and developmental processes in plants. Intercellular polar auxin transport (PAT) generates auxin maxima and minima that are essential for tropic growth responses, embryogenesis, organ positioning and meristem maintenance. Auxin transport is mediated by three type of transport proteins [1;2], of which the PIN auxin efflux carriers are the rate limiting factors in auxin efflux that determine the direction of PAT through their asymmetric subcellular localization [3;4]. The plant specific protein serine/threonine kinase PINOID (PID) regulates PAT by controlling PIN localization, and thereby determining the direction of PAT [5;6]. Recent data indicate that PID is a plasma membrane-associated kinase that acts antagonistic to trimeric PP2A phosphatases, through direct phosphorylation of PINs [7;8].

Calcium is a common second messenger in signaling pathways. Early studies on sunflowers stem segments have shown that PAT is abolished in the presence of calcium chelators and restored by application of calcium, which suggests an important role for calcium in the regulation of PAT [9]. The first molecular evidence for a link between calcium and PAT was provided by the identification of the calcium-binding proteins PINOID BINDING PROTEIN1 (PBP1) and TOUCH3 (TCH3) as interacting proteins of PID [10]. The binding of PBP1 and TCH3 to PID, which is calcium-enhanced for PBP1 and completely dependent on calcium for TCH3, was found to respectively up-regulate and repress PID kinase activity *in vitro* [10]. In contrast to TCH3, which has six calcium-binding pockets, or EF-hands, PBP1 has a single one. PBP1 has also been named KRP2 (for KIC-related protein2), as it is part of a small protein family that includes the close PBP1 homolog PBP1H/KRP1 and KIC (KCBP-interacting Calcium binding protein) [11]. KIC is involved in the regulation of trichome development by a calcium-dependent interaction with the kinesin-like calmodulin-binding protein KCBP [11]. KCBP is a microtubule (MT) motor protein that determines trichome morphology by regulating branching and polar growth [12]. Calcium-dependent KIC-KCBP interaction inhibits binding of KCBP with the MT, thereby affecting trichome development [11]. Interestingly, this pathway also implicates KIPK, a KCBP-interacting protein kinase that belongs to the same AGCVIII kinase family as PID [13;14]. Here we present a functional

and genetic analysis of the PID-PBP1 interaction to elucidate the regulatory role of PBP1. *In vitro* experiments show that PID contains two major PBP1-binding sites and that PBP1 not only enhances PID kinase activity but also changes its substrate recognition signature. Furthermore, using *Arabidopsis thaliana* protoplasts we tested the effect of PBP1 on PID membrane localization. In order to elucidate the regulatory role of PBP1 *in planta* we characterized combinations of loss- and gain-of-function mutant lines of PBP1, PBP1H and PID. Our results indicate that PBP1 and PBP1H act redundantly to enhance PID kinase activity during embryo development, and that they partly suppress root growth, possibly through their stimulatory effect on PID. PBP1 overexpression partially inhibits auxin-induced calcium-dependent sequestration of PID from the plasma membrane, suggesting that apart from enhancing the activity of the PID kinase, PBP1 also influences PID subcellular localization. These data confirm previous *in vitro* data, indicating a role for PBP1 and PBP1H as positive regulators of PID kinase activity [10], and extend the function of these small EF-hand proteins to that of regulators of the specificity and subcellular localization the PID protein kinase.

Results

PBP1 interacts with PID in a calcium enhanced manner

Previously, PBP1/KRP2 was identified as an interactor of PINOID. Surprisingly, the same yeast two-hybrid screen did not identify the closest homolog of PBP1, PBP1H/KRP1 [10], which shares 78% mRNA sequence identity and 80% amino acid sequence identity (Figure 1a). In order to test the possible interaction between PBP1H and PID we performed *in vitro* pull-down experiments using bacteria expressed proteins. The results indicate that PBP1H also interacts with PID (Figure 1b), suggesting that PBP1 and PBP1H act redundantly *in planta*.

In order to map the PBP1 interaction sites in PID, we searched the amino acid sequence of this kinase for putative calmodulin (CaM) binding sites. A first search using the Eukaryotic Linear Motif (ELM) server [15] predicted a single IQ motif on PID (amino acids 255-273) within the insertion on the protein kinase catalytic domain (Figure 1c). IQ motifs occur in a wide range of calmodulin target proteins, which in some proteins mediate Ca²⁺-dependent interactions, however, this motif can also interact in a Ca²⁺-

independent manner [16;17]. A second search in the CaM target database [18] predicted three putative sites, one of which (amino acids 251-272) overlaps with the IQ motif previously predicted by the ELM server. The other two predicted sites (amino acids 59-78, and 376-393) are similar to a modified version of the IQ motif (Figure 1c) [17]. To confirm whether the predicted CaM binding sites are responsible for the interaction between PID and PBP1 we generated three deletions mutants of PID and performed *in vitro* pull-down assays for PBP1 (Figure 1c and d). Our results are consistent with the presence of two major PBP1 binding sites on PID (Figure 1d). PBP1 binds preferentially to the NT part of PID where Ca^{2+} considerably enhances the interaction (Figure 1d and e). The IQ motif within the protein kinase catalytic domain shows less affinity and calcium- independent binding, while the CT part seems to have no or only weak affinity for PBP1 (Figure 1d and e). In conclusion, our results suggest that PBP1 preferentially binds two sites of PID, an N-terminal one mediating a Ca^{2+} -enhanced interaction, and the central IQ motif that interacts with PBP1 in a Ca^{2+} -independent manner.

PBP1 enhances PID kinase activity

Previously we have shown that PBP1 enhances the autophosphorylation of PID *in vitro* [10], however, its effect on PID transphosphorylation remains unknown. Moreover, the recent discovery of PIN proteins as direct phosphorylation targets of PID [8] prompted us to investigate the effect of PBP1 on the PID-dependent transphosphorylation of the PIN2 central hydrophilic loop (PIN2HL). *In vitro* phosphorylation assays using *E. coli* produced proteins showed that PBP1 acts as a positive regulator of PID (Figure 2a). In contrast to PBP1, which increased PID activity by a 2-fold, PBP1H only had a very mild (1.2-fold) effect on PID dependent PIN2HL phosphorylation (Figure 2a). To investigate whether PBP1 also stimulated PID activity on other phospho-substrates, we used the Pepchip Kinomics Array (Pepscan) that contains 976 different peptides of known eukaryotic phosphorylated proteins spotted in triplicate on a glass slide [19;20]. The array was incubated with PID, or with PID and PBP1, both in the presence of calcium (Figure 2b). Each slide was scanned using the Biomex reader and analysed using the Biosplit software (Biomex AS). A comparison of the two arrays led to the identification of 39

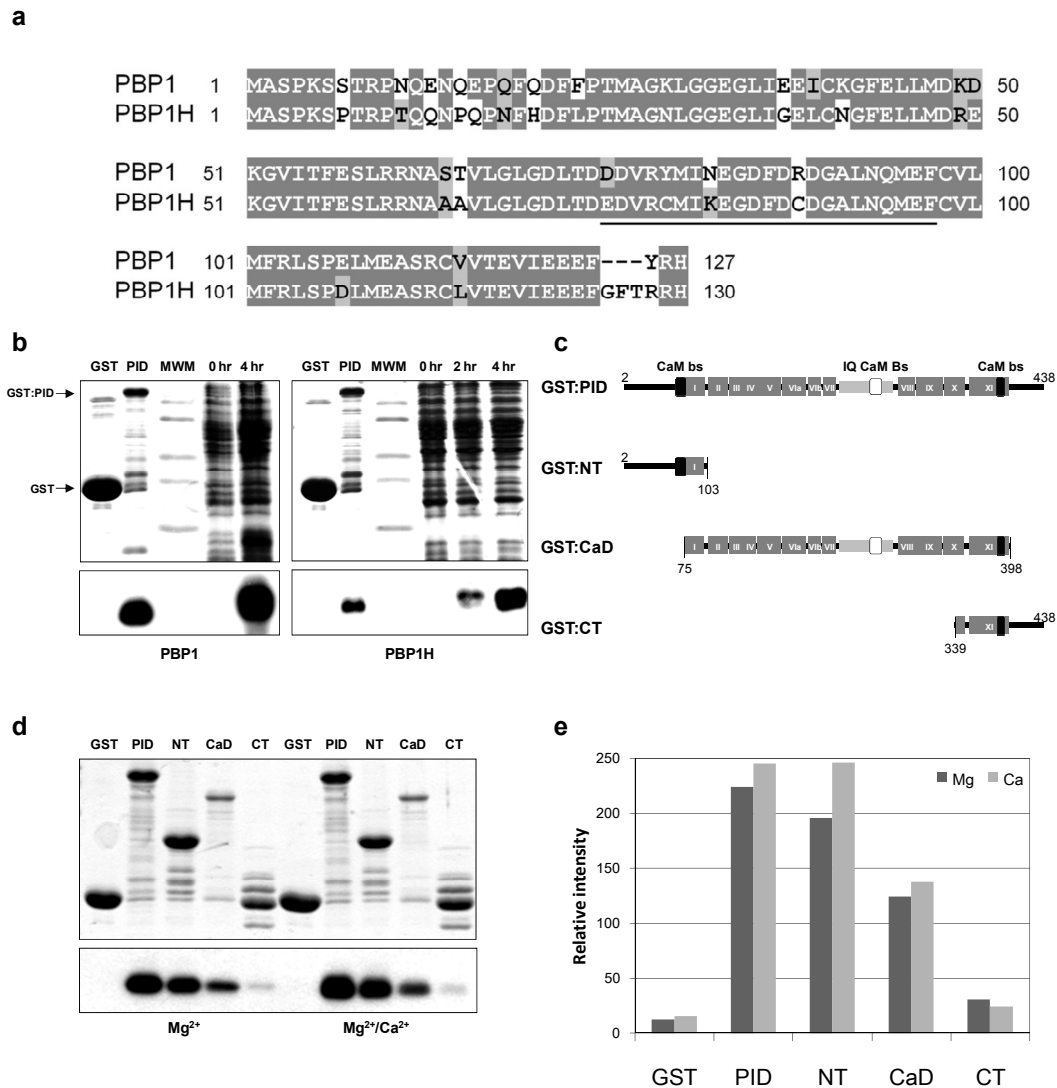


Figure 1. PBP1 and PBP1H interact with PID in a calcium enhanced manner.

(a) Alignment of the PBP1 and PBP1H proteins. The EF-hand domain is underlined.

(b) *In vitro* pull-down of His-PBP1 or His-PBP1H with GST-tagged PID from *E. coli* total protein extracts before (0 hr), or 2 and 4 hrs after induction of His-PBP1 or His-PBP1H expression by IPTG addition. The upper panel shows the Coomassie stained SDS-PAGE gel, the Western blot probed with anti-Penta His antibody is shown in the lower panel. GST: GST control; PID: GST-PID; MWM: molecular weight marker;

(c) Schematic representation of PID domains and the deletion mutants used for the pull downs assays in (d). The eleven conserved sub-domains of the protein kinase catalytic domain are represented by gray boxes and marked with Roman numbers. The insertion between sub-domain VII and VIII is represented as a light gray box. The predicted calmodulin binding sites are represented as white and black boxes for the IQ motif and its modified versions, respectively.

Figure 1 (*continued*)

(d) Mapping of the PBP1 binding sites in PID. The upper panel shows the Coomassie-stained SDS-PAGE gel, the Western blot with anti-Penta His antibody is shown in the lower panel. GST: GST control; PID: GST-PID²⁻⁴³⁸; NT: GST-PID²⁻¹⁰³; CaD: GST-PID⁷⁵⁻³⁹⁸; CT: GST-PID³³⁹⁻⁴³⁸.

(e) Densitometry analysis of the Western blot in (d). Exposed X-ray films and the corresponding Coomassie stained gels were scanned using a calibrated densitometer GS-800 (BioRad) and density measurements were performed using Gel Doc V4 software (BioRad). Western blot intensities were adjusted to the loading accordingly.

peptides that were significantly phosphorylated over background levels. In the presence of PBP1, PID dependent phosphorylation of the peptides was increased between 1.2- and 11.8-fold (Figure 2b, right panel), suggesting that PBP1 does not only act as a positive regulator, but also changes the substrate preference of PID. To obtain a better understanding of the effect of PBP1 on the substrate selectivity of PID we used the averaged phosphorylation intensities of the 40 substrates to generate a weighted phosphofingerprint by taking into account the frequency of each amino acid on positions -5 to +5 with respect to the phosphorylated residue and the efficiency of phosphorylation for each individual peptide (Figure 2c). Our results indicate that at least in these *in vitro* assays PID has a strong preference for lysine residues at position -4 from the phosphotarget (serine at position 0), for basic amino acids (Arg and Lys) at positions -5, -3, -2, 2 and 3 (Figure 2c, left panel), and no clear preference for positions -1 and 1. Interestingly, in the presence of PBP1 there is a clear shift towards the hydrophobic amino acids isoleucine and valine at positions -1 and 1, respectively, suggesting that PBP1 has an effect on PID substrate preference.

***PBP1* loss- and gain-of-function mutants are affected in root length**

As a first approach to analyze the function of PBP1 as a regulator of the PID kinase activity *in planta*, we isolated a *pbp1* knock-out mutant, and generated lines overexpressing the *PBP1* cDNA under control of the *35S* promoter. The *pbp1-1* allele (line GT6553 in Landsberg *erecta* (*Ler*) background) has a transposon inserted at 91bp after the ATG. RT-PCR analysis did not detect *PBP1* transcript in *pbp1-1* mutant seedlings, indicating that it is a complete loss-of-function allele (Figure 3a).

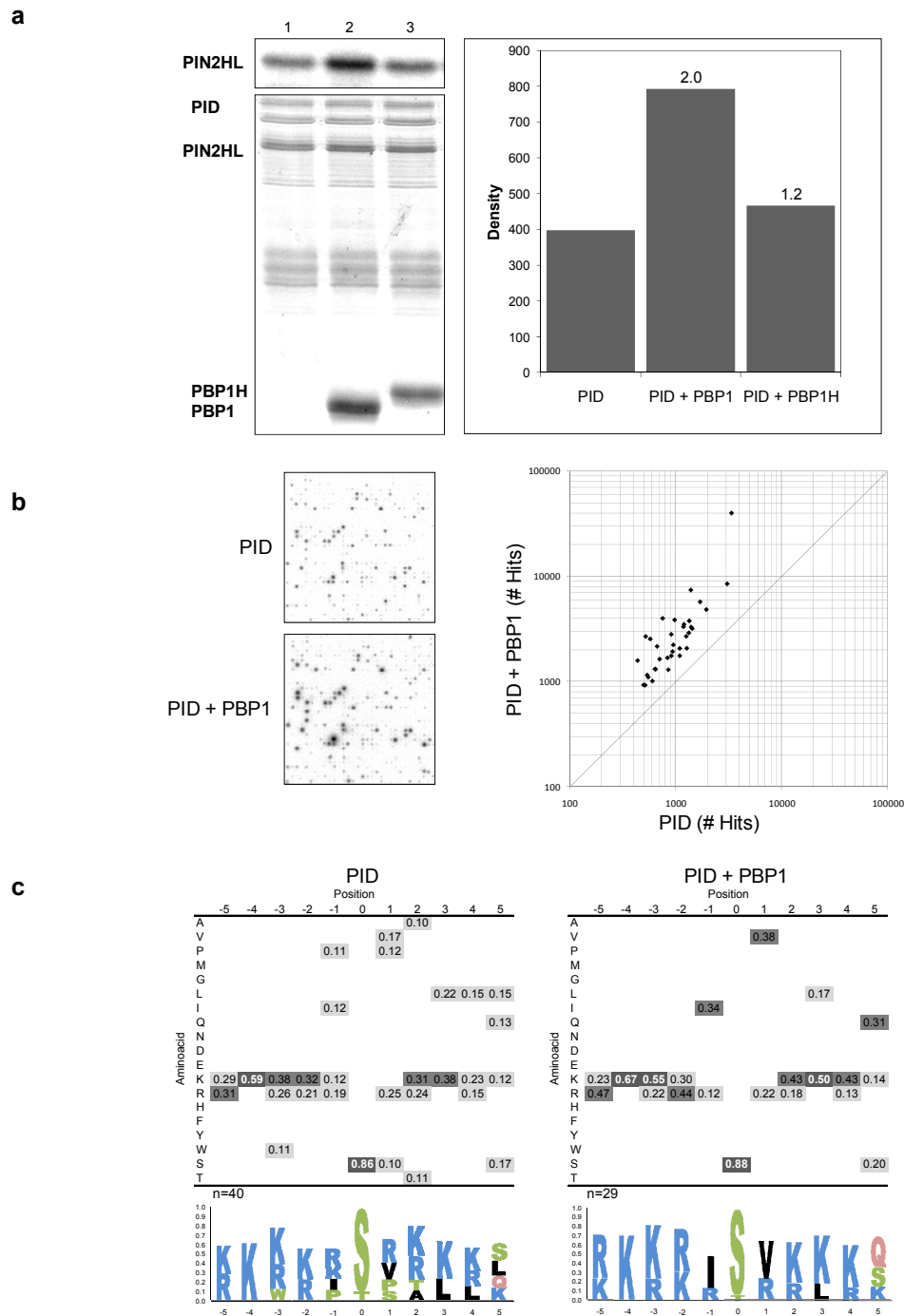


Figure 2. PBP1 enhances PID activity and changes its substrate preference.

(a) *In vitro* phosphorylation of the PIN2 central hydrophilic loop (PIN2HL) by PID. Autoradiogram (upper left panel) and Coomassie stained gel (lower left panel) showing PBP1 enhanced phosphorylation (lane 1: PID with PIN2HL, lane 2: PID and PBP1 with PIN2HL; lane 3: PID and PBP1H incubated with PIN2HL). The right panel represents the quantification of PID-dependent

Figure 2 (*continued*)

PIN2HL phosphorylation in the presence of PBP1 or PBP1H. The numbers above the bars indicate the fold increase compared to PID alone.

(b) Pepchip kinomics array incubated with PID (left upper panel) or PID in the presence of PBP1 (left lower panel) and comparison of the phosphorylation intensity of 39 peptides between the two arrays showing the differential positive effect of PBP1 on PID protein kinase activity (right panel).

(c) Phosphofingerprint of PID (left panel) or PID in the presence of PBP1 (right panel). The matrix representation (upper) shows the weighted frequency for each amino acid at the 11 positions of the peptides. Frequencies above 0.5 are depicted as dark gray boxes with white font, frequencies between 0.3-0.5 are shown as gray boxes and 0.1-0.3 as light gray boxes. The number of peptides used for each matrix is shown at the bottom (PID n=40 and PID+PBP1 n=29). In the fingerprint plot (lower) the size of the amino acids corresponds to the weighted frequency for each position. Only amino acids with a frequency above 0.1 are depicted. Positively charged amino acids are coloured in blue, hydrophobic in black, less hydrophobic in green and Asn or Gln in pink.

Detailed phenotypic analysis revealed that the primary roots of *pbp1-1* were longer than wild type roots (120% of the *Ler* root length, Student's t-test, $p < 0.02$, Figure 3c). Moreover, *pbp1-1* did not show any other phenotype, and since the expression of *PBP1H* was apparently not altered in *pbp1-1* (Figure 3a), this suggests that, except for a specific role for *PBP1* in root growth, *PBP1* and *PBP1H* act redundantly. From the multiple overexpression lines that were generated, two single locus lines were selected for further studies: one with a strong (*35Spro::PBP1-29*) and one with a medium (*35Spro::PBP1-53*) *PBP1* overexpression level (Figure 3b). The only observed phenotype in these lines was a slight but significant reduction of the root length. The root length of *35Spro::PBP1-29* and *35Spro::PBP1-53* seedlings was respectively 90% and 86% of that of wild-type seedlings (Student's t-test, $p < 0.02$, Figure 3c). The reduction in root length was still significant when seedlings of the *35Spro::PBP1* lines were germinated on medium containing 0.1 μM indole-3-acetic acid (IAA) or the auxin transport inhibitor naphthylphthalamic acid (NPA) (data not shown), suggesting that *PBP1* overexpression does not change the sensitivity to these compounds.

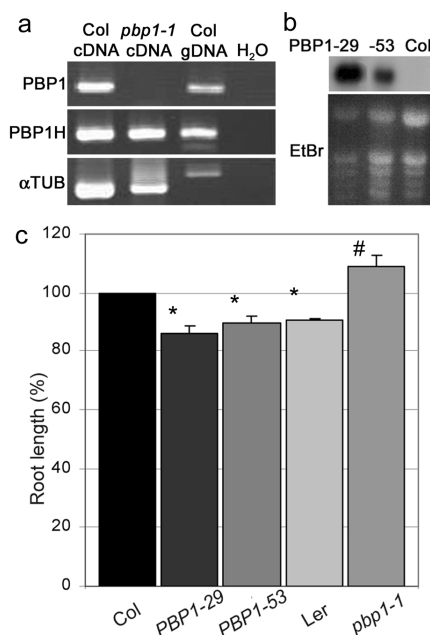


Figure 3. PBP1 controls root growth.

(a) RT-PCR on Col cDNA, *pbp1-1* cDNA and Col genomic DNA of one-week old seedlings indicates that *pbp1-1* is a null allele for *PBPI*, and that *PBPIH* expression is not affected by *pbp1* loss-of-function.

(b) Northern blot analysis showing the level of *PBPI* overexpression in seedlings of the *PBPI* overexpression lines *35Spro::PBPI-29* and *-53*, as compared to Col wild type. The ethidium bromide stained RNA gel is shown as loading control.

(c) Root length of eight day-old seedlings of *35Spro::PBPI-29* and *-53*, *pbp1-1* and *Ler*, indicated as a percentage of that of Col wild type. The mean of three experiments is shown, * significantly different from Col, # significantly different from *Ler* (Student's t-test, $p < 0.02$)

PBPI and PBP1H influence PID subcellular localization *in vivo*.

To confirm the interaction between PID and PBP1 or PBP1H, we transfected *Arabidopsis thaliana* derived cell suspension protoplasts with *35Spro::PID:CFP*, *35Spro::PBPI:YFP* or *35Spro::PBP1H:YFP*. Consistent with previous reports, PID showed a plasma membrane localization (Figure 4a) [7;8;13;21]. In contrast, PBP1 and PBP1H localized in the cytoplasm (Figure 4b and c). When we co-transfected *35Spro::PID:CFP* with *35Spro::PBPI:YFP* or *35Spro::PBP1H:YFP*, however, we observed that PID was sequestered from the plasma membrane to the cytoplasm (Figure 4d and e). To confirm that the observed internalization of PID is caused by a direct interaction between PID and PBP1 or PBP1H we measured fluorescence resonance energy transfer (FRET) by lambda

scanning [22]. Protoplasts co-transfected with *35Spro::CFP* and *35Spro::YFP* or transfected with *35Spro::YFP:CFP*, were used respectively as negative and positive control (Figure 4f and g). Protoplasts co-expressing PID:CFP and either PBP1:YFP or PBP1H:YFP were characterized by a quenching of the CFP signal (475nm, donor) and increased signal on YFP channel (527nm, acceptor) (Figure 4g), something that was also observed in protoplasts expressing the CFP:YFP fusion. Moreover, normalized emission intensities between the interacting and non interacting samples were significantly different (Student's t-test $p < 0.05$) (Figure 4g), suggesting that the sequestration of PID by PBP1 or PBP1H is caused by a direct interaction. To further analyze the effect of the PBP1-dependent regulation of PID in plants, we analyzed whether *PBPI* overexpression had any effect on *PID* expression and localization using the *PIDpro::PID:VENUS* line [8]. We focused our attention on epidermal cells in the distal elongation zone, as *PID* is expressed in this region [8], and we observed previously in these cells that auxin treatment induced rapid and transient sequestration of PID from the plasma membrane to the cytoplasm (Figure 4l and Chapter 2, this thesis). Moreover, *PBPI* overexpression resulted in a significant reduction in root length, suggesting that it acts in root epidermis cells. The auxin-dependent release of PID from the plasma membrane relies on an increase of the cytoplasmic calcium concentration through plasma membrane calcium channels, and on calmodulin-like activity, as it can be inhibited by pre-incubation with the plasma membrane calcium channel inhibitor Tetracain (Figure 4n), or with the calmodulin inhibitor Lanthanum (Figure 4o). *PBPI* overexpression did not result in a clear alteration of PID localization (Figure 4i), but it did partially inhibit the auxin-dependent transient sequestration of PID (Figure 4m). These results are contrasting with the protoplast data, where co-expression of PBP1 does lead to cytosolic localization of PID, and suggest that *in planta* PBP1 is not involved in the sequestration of PID, but that it stabilizes the membrane association of PID.

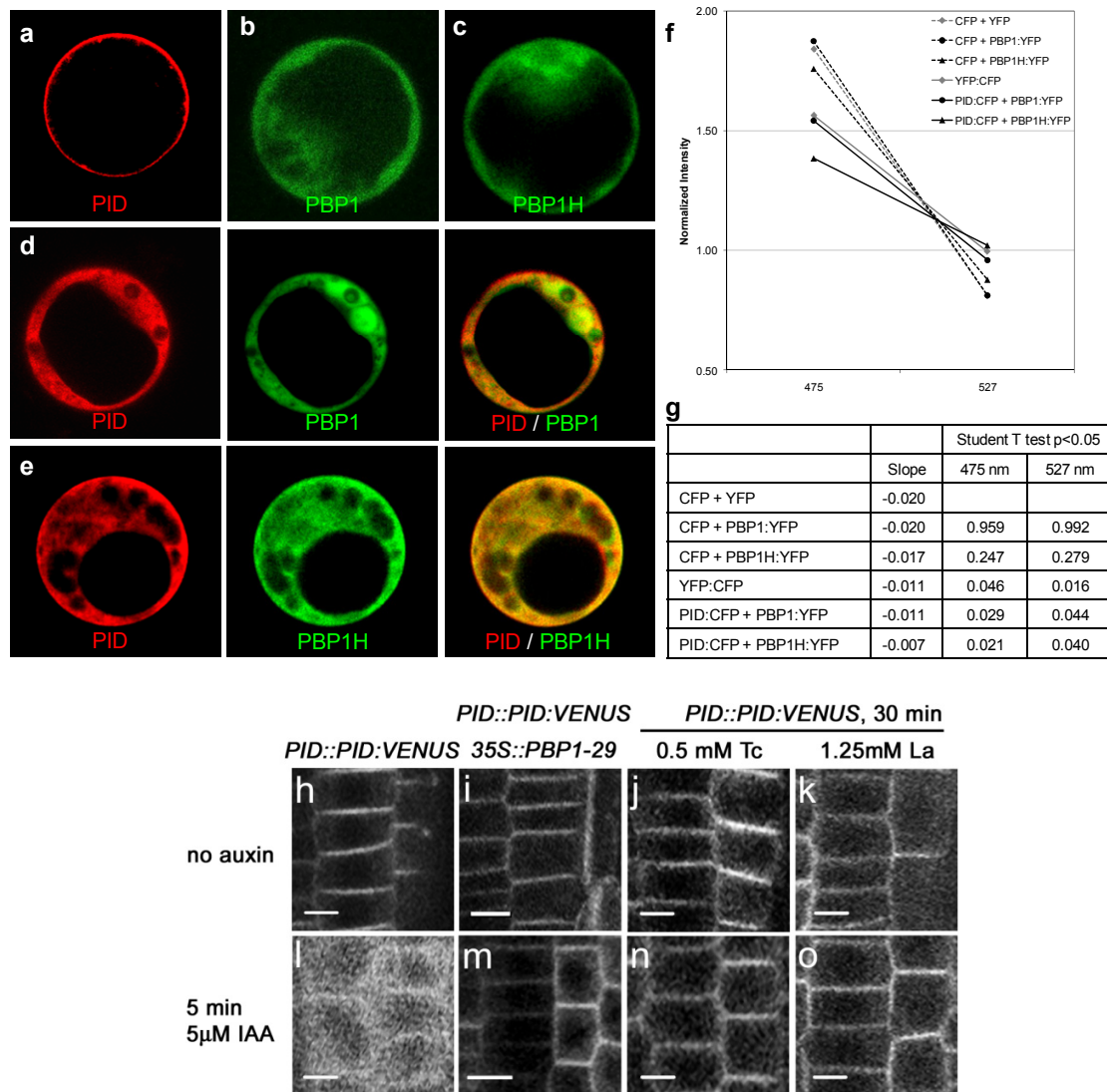


Figure 4. PBP1 interacts with PID in protoplasts, and its overexpression stabilizes the plasma membrane association of PID in root epidermis cells.

(a) Representative protoplast showing plasma membrane localization of PID
 (b, c) Cytoplasmic subcellular localization of PBP1:YFP (b) and PBP1H:YFP (c) in protoplast.
 (d, e) Protoplast co-transfected with PID and either PBP1 (d) or PBP1H (e). Both channels are shown independently (CFP in red and YFP in green) and its corresponding merged image.
 (f, g) Fluorescence resonance energy transfer (FRET) profiles of control protoplasts (co-expressing CFP and YFP, PBP1:YFP or PBP1H:YFP) and of protoplasts co-expressing PID and PBP1 or PBP1H (f).
 (h-o) Confocal sections showing the subcellular localization of PID:VENUS in epidermal cells of the elongation zone of seedling root tips of the lines *PIDpro::PID:VENUS* (h, j-l, n, o) and *PIDpro::PID:VENUS/35Spro::PBP1-29* (i, m). PID is membrane localized in control medium (h, i), but is transiently sequestered to

Figure 4 (continued)

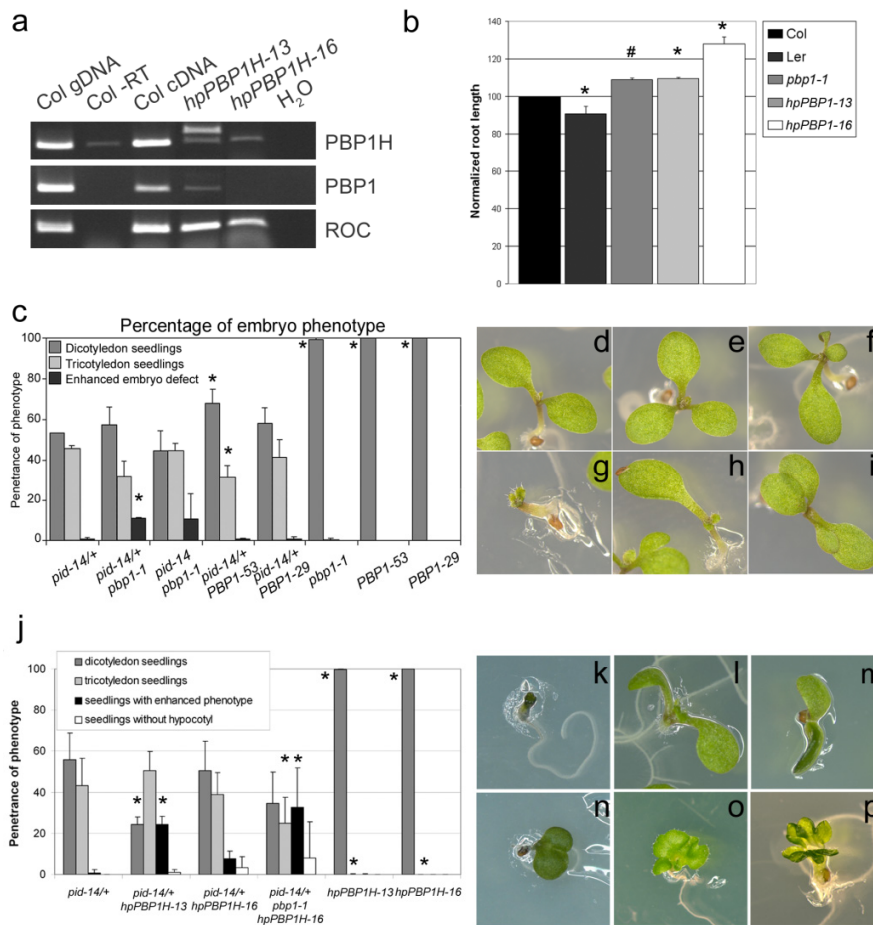
the cytoplasm after 5 min treatment with 5 μ M IAA (l), but less when *PBP1* is overexpressed (m). A 30 min pre-treatment with 0.5 mM Tetracain (j, n) or 1.25 mM Lanthanum (k, o) did not affect PID localization, but blocked the auxin-induced transient sequestration to the cytosol (n, o). Scale bars represent 10 μ m.

PBP1 and PBP1H act redundantly as positive regulators of PID activity

Since the loss-of-function allele *pbp1-1* did not give phenotypes other than the increased root length, and PBP1H was also shown to bind PID (Figure 1 and 3), we suspected that the two proteins were functionally redundant, and tried to identify *pbp1h* loss-of-function alleles. Unfortunately, in the two available T-DNA insertion lines (SALK_013868 and SALK_048098) with T-DNAs at positions -673 and -582 relative to the *PBP1H* ATG, respectively, *PBP1H* expression was found to be at wild-type levels (data not shown). Therefore, we attempted to knock-down both *PBP1* and *PBP1H* expression through RNA interference (RNAi), by overexpressing a hairpin RNA spanning the complete *PBP1H* coding region (*hpPBP1H*). Several lines were obtained containing a single locus insertion of the *hpPBP1H* construct, two of which (*hpPBP1H-13* and *hpPBP1H-16*) were studied in more detail. Expression analysis showed that *PBP1H* expression in both lines was significantly reduced (Figure 5a). The residual fragment amplified in both lines was also observed in the minus reverse transcriptase control, indicating that it was derived from contaminating DNA. In the *hpPBP1H-13* sample, a larger additional band was detected. Since Northern blot analysis indicated that line *hpPBP1H-13* shows the highest expression of the *hpPBP1H* RNA (data not shown), it is likely that this fragment represents the full length hairpin RNA amplified with the forward PCR primer. As anticipated based on the homology between the *PBP1* and *PBP1H* coding regions, *PBP1* expression was also suppressed in *hpPBP1H-13* and was even undetectable in *hpPBP1H-16* (Figure 5a). Overall, like for *pbp1-1* loss-of-function seedlings, the primary roots of *hpPBP1H-13* and *hpPBP1H-16* seedlings were longer compared to the wild type control (109% and 128%, respectively, Student's t-test, $p < 0.06$, Figure 5b). Interestingly, the increase in root length correlated with the *PBP1* knock-down level. Because of lack of further phenotypes we tested the effect of modified *PBP1* and *PBP1H*

expression on *pid* loss-of-function and *PID* overexpression phenotypes. Neither *PBP1* overexpression nor *pbp1* or *pbp1h* loss-of-function affected the strong seedling phenotypes caused by *PID* overexpression (results not shown). In contrast, *PBP1* overexpression slightly reduced the severity of the tricotyledon phenotype of the intermediately strong *pid-14* loss-of-function allele (47% for *pid-14* ($n = 1469$) 41% for *pid-14/35Spro::PBP1-29* ($n=1116$,Student's t-test, $p > 0.05$) and 31% for *pid-14/35Spro::PBP1-53* ($n = 1889$, Student's t-test, $p < 0.05$), Figure 5c) [5;23;24], although this reduction did not correlate with the level of *PBP1* overexpression.

In the *pid-14+/pbp1-1* double mutant the penetrance of cotyledon defects did not significantly differ from that in *pid-14+/+* (43%, $n = 1040$, Student's t-test, $p > 0.05$). However, seedlings with one cotyledon (5%, Figure 5h), four cotyledons (2%, Figures 5f and 5i) or even no cotyledons (4%, Figure 5g) were observed. We considered this a significant shift, as most of these phenotypes are never observed for the *pid-14* allele. Progeny of *pid-14+/hpPBP1H* double mutant plants contained a significantly higher number of seedlings with cotyledon defects (even up to 75% for *pid-14+/hpPBP1H-13*) compared to *pid-14+* and *pid-14+/pbp1-1* (Figures 5j and 5k-n). In both *pid-14+/hpPBP1H-13* and *pid-14+/hpPBP1H-16* the number of monocotyledon seedlings was increased (8% and 6%, respectively), whereas a significant number of seedlings without cotyledon could be observed in *pid-14+/hpPBP1H-13* (15%). Furthermore, several seedlings without hypocotyl (Figure 5l) or without hypocotyl and root (Figure 5m) were observed in *pid-14+/hpPBP1H-16* ($> 3\%$, Figure 5j). In progeny of the *pid-14+/pbp1-1/hpPBP1H-16* triple mutant lines the severity of the embryo/seedling phenotypes was even more enhanced, with 14% and 18% of the seedlings showing respectively one or no cotyledon (Figure 5k), and 8% of the seedlings lacking hypocotyl or hypocotyl and root (Figure 5l and 5m). Furthermore, seedlings without cotyledon had defects in the formation of the first leaves, which were fused at the blade (Figure 5o) or at the petiole (Figure 5p), indicating that *PID*, *PBP1*, *PBP1H* are involved in broader aspects of plant patterning than only cotyledon initiation and positioning. These data suggest that *PBP1* and *PBP1H* act redundantly in the *PID* pathway and have a positive effect on the kinase function. The observed defects in embryo patterning and phyllotaxis



in *pid-14/p**bp**1-1/hpPBP1H-16* confirm the proposed role of PID in regulation of organ boundaries [25].

Figure 5. PBP1 and PBP1H act redundantly on root growth, embryo patterning and phyllotaxis.

(a) RT-PCR reactions showing that both *PBP1* (middle) and *PBP1H* (top) expression are reduced in *hpPBP1H-13* whereas *PBP1* expression is absent in *hpPBP1H-16*. Controls are Col genomic DNA (gDNA), Col RNA in which the reverse transcriptase was omitted during the RT reaction (Col -RT), Col cDNA and water.

(b) The percentage of main root growth in *Ler* wild type, *p**bp**1-1*, *hpPBP1H-13* and *hpPBP1H-16* seedlings, normalized to Col wild type seedlings. The mean of three experiments is shown. Stars (*) and hash signs (#) indicate significant differences compared to Col and *Ler*, respectively (Student's t-test, $p < 0.06$).

(c) The percentage of cotyledon phenotypes in progeny of *pid-14+* ($n = 1469$), *pid-14+/p**bp**1-1* ($n = 1040$), *pid-14/p**bp**1-1* ($n = 291$), *pid-14+/35Spro::PBP1-29* ($n = 1116$), *pid-14+/35Spro::PBP1-53* ($n = 1889$),

Figure 5 (continued)

pbp1-1 ($n = 984$), *35Spro::PBP1-29* ($n = 595$), *35Spro::PBP1-53* ($n = 828$). *pid-14+* and *pid-14* indicate lines segregating or homozygous for the *pid-14* allele. Stars (*) indicated that the values are significantly different compared to *pid-14* (Student's t-test, $p < 0.05$).

(d-e) A segregating *pid-14+* population typically consist of 53% dicotyledonous seedlings (d) and 47% tricotyledonous seedlings (e).

(f-i) Seedlings with an aberrant number of cotyledons were observed in *pid-1/pbp1-1*: four cotyledon (f, i), no cotyledon (g) and one cotyledon (h) seedlings.

(j) The percentage of seedling phenotypes in *pid-14+*, *pid-14+/hpPBP1H-13*, *pid-14+/hpPBP1H-16*, *pid-14+/pbp1-1/hpPBP1H-16*, *hpPBP1H-13* and *hpPBP1H-16/pid-14+* and *pid-14* indicate lines segregating or homozygous for the *pid-14* allele, respectively. Stars (*) indicate significant differences compared to *pid-14* (Student's t-test, $p < 0.06$).

(k-n) Seedlings without cotyledon (k), without hypocotyl (l), without hypocotyl and root (m) and with fused cotyledons (n) as observed among progeny of the lines *pid-14/hpPBP1H-13*, *pid-14/hpPBP1H-16* and *pid-14/pbp1-1/hpPBP1H-16* (l).

(o-p) Seedlings without cotyledons in *pid-14/pbp1-1/hpPBP1H-16* show defects in the phyllotaxis of the first leaves, with either fused leaves (m) or fused petioles (n).

Discussion

Previous experiments have indicated that calcium is an important second messenger in auxin action. One of the earliest cellular responses to auxin is a rapid increase in cytosolic calcium [26-28], and calcium has been reported to play a crucial role in PAT [9]. Our finding that PID interacts in a calcium-dependent manner with the calmodulin-like protein TCH3 and the small calcium-binding protein PBP1, provided the first molecular evidence for the role of calcium as regulator of PAT [10]. In this chapter, we further investigated the role of PBP1 in plant development in relation to its interaction with PID.

Small calcium binding proteins stabilize plasma membrane localization of PINOID

PBP1 belongs to a small family of three single EF-hand calcium-binding proteins in *Arabidopsis*. Whereas the family member KIC has been shown to play a role in the regulation of trichome branching and polar growth by inhibiting the interaction between the kinesin-like calmodulin-binding protein (KCBP) to microtubuli [11;12], PBP1 and its close homolog PBP1H did not inhibit binding of KCBP to microtubule, suggesting that these two proteins have a different function [11]. Here we show that both PBP1 and

PBP1H bind to two different calmodulin binding sites in PID, for one of which the binding is enhanced in the presence of calcium. The second site, the IQ motif in the insertion of the protein kinase catalytic domain, shows a calcium independent interaction with PBP1 and PBP1H. As TCH3 was also found to bind the catalytic domain of PID (Chapter 2), it is tempting to speculate that PBP1/PBP1H and TCH3 compete for binding to the IQ site, and that at low cytosolic calcium levels this leads to PBP1/PBP1H-mediated activation of PID. In Chapter 2 we showed that TCH3-dependent inhibition can override the PBP1-dependent activation of PID *in vitro*, suggesting that at high calcium levels, TCH3 is able to outcompete PBP1/PBP1H for binding to the IQ site, and thereby to inhibit of PID activity.

In chapter 2, we also showed auxin-induced and calcium-dependent sequestration of PID in epidermis cells of the root elongation zone. Here we present *in planta* data that this occurs independent of PBP1, and that in fact *PBP1* overexpression even enhances the membrane-association of PID. These results corroborate our model that TCH3 is involved in PID sequestration, and indicate that PBP1 and PBP1H not only positively regulate PID action by enhancing its kinase activity, but also by retaining the kinase at the plasma membrane, in proximity of its phosphorylation targets, the PIN proteins. Curiously, our initial observations in protoplasts suggested that PBP1, like TCH3 is involved in sequestering PID from the plasma membrane to the cytosol, which is in contrast to our observations in root epidermis cells. It is likely however, that the observed effects in protoplasts are due to abnormally high levels of the PBP1:YFP fusion proteins. Normally PBP1 is a very unstable protein, but we have observed that the PBP1:YFP fusion is much more stable (F. Maraschin, J. Memelink and R. Offringa, unpublished data). The abundant PBP1:YFP protein seems to prohibit binding of the PID catalytic domain to plasma membrane components, whereas the labile PBP1 protein, which is present at a critical amount in the overexpression line, does have a stimulatory role on plasma membrane association of PID.

Small calcium binding proteins modulate PINOID substrate preference

Previously we have shown that PBP1 enhances the autophosphorylation activity of PID *in vitro*, however, its effect on the transphosphorylation activity was not investigated

[10]. Using the PIN2 hydrophilic loop as natural PID substrate, we could show now that PBP1 and PBP1H both enhance PID activity, and that PBP1 is most efficient as positive regulator of PID. Moreover, by using the Pepchip Kinomics array (Pepscan) we were able to demonstrate that PBP1 not only enhances PID protein kinase activity, but that it also moderates the substrate preference of PID. Possibly, PBP1 optimizes PID activity to recognize the phospho-substrates in the central hydrophilic loop of PIN proteins [8]. Several phospho-substrates have now been identified for PID, among which three serines in the hydrophilic loop of PIN proteins (M.K. Zago 2006, Thesis; Huang et al., submitted). It is worthwhile to mention that the PID substrate fingerprints derived from the Kinomics array have not been instrumental in identifying these phospho-targets in PIN proteins. The current fingerprints indicate that it is important to have positively charged residues both left and right of the phosphorylated residue, more resembling a PKC substrate consensus sequence, whereas the PID substrates that have been identified resemble more the PKA substrate consensus sequence. It is important to consider, that the phospho-peptides on the Kinomics array used for this experiment were predominantly based on animal kinase substrates, and that the PID fingerprint may be different on a phospho-peptide array with a less biased or even a plant-based content.

PBP1 and PBP1H are regulators of root growth and embryo patterning

Morphometric analysis of loss- and gain-of function mutants in *PBP1* and *PBP1H* indicated that these genes act partially redundant in repressing root growth, and although we could not find clear evidence for a change in sensitivity of the mutant lines to auxin, PAT inhibitors or *PID* overexpression, it is likely that PBP1 and PBP1H mediate their effect on root growth through their role as positive regulators of PID activity. Like *PID* overexpression, PBP1 enhanced PID activity may lead to increased basipetal auxin transport to the root elongation zone [5-7], which in turn inhibits root growth and thus explains the shorter root in *PBP1* overexpression lines. Consequently, the longer root in *pbp1(h)* loss-of-function lines may be the result of reduced basipetal PAT in the root tip as a result of reduced PID kinase activity. This positive regulatory function of PBP1(H) in the PID pathway is similarly observed during embryogenesis by the enhanced penetrance and/or severity of embryo/seedling phenotypes in *pid-14/pbp1-1*, *pid-*

14/hpPBP1H, *pid-14/pbp1-1/hpPBP1H-16* mutant lines as compared to *pid-14*. Upon germination, seedlings have a bilateral symmetry marked by the presence of two cotyledons separated by the shoot-root axis. This symmetric structure can be traced back to the embryogenesis, when the initiation of cotyledon primordia in the globular embryo marks the transition to the heart stage. Proper auxin distribution, based on the PAT activity, is primordial for the embryo patterning at crucial transition steps [30-32]. The auxin efflux carriers PIN1, PIN4 and PIN7 are involved in controlling the auxin gradients during embryogenesis [30]. At heart stage, the establishment of the cotyledons boundaries is based on the presence of an auxin maximum at the cotyledon tips. Treatment of embryos with exogenous auxin or PAT inhibitors gives rise to seedlings with abnormally positioned or fused cotyledons [25;30]. And mutations in *PIN1* and *PID* generate seedlings with an abnormal number of cotyledons. The *pin1 pid* double mutant seedlings have no cotyledons and fused leaves with an aberrant phyllotaxis. Both proteins, by controlling auxin distribution, are responsible for the establishment of a bilateral symmetry and the cotyledon outgrowth during embryogenesis [25]. We have observed that in the *pid-14* mutant background the absence of the PID positive regulators PBP1 and PBP1H perturbed embryogenesis even more, giving rise to seedlings with no to four cotyledons, whereas only tricotyledon seedlings were observed in *pid-14*. Such phenotypes have been described for strong alleles of *pid* or in the combination of *pid* with the *enhancer of pid* mutation, [23;33]. In fact, in Chapter 4 of this thesis we provide evidence that the related AGC3 kinase genes *WAG1* and *WAG2* act redundantly with PID in determining PIN polarity establishment, and that double and triple *pid/wag1/wag2* loss-of-function mutants show similar defects in cotyledon development. Together these results suggest that PBP1 and PBP1H are common positive regulators of these three AGC3 kinases during embryogenesis and seedling development.

In *pid-14/hpPBP1H-16* and *pid-14/pbp1-1/hpPBP1H-16*, also seedlings with strong patterning defects such as absence of hypocotyl or both hypocotyl and root were observed at low frequencies. Similar phenotypes have been reported for mutants impaired in auxin transport and signaling during embryogenesis like *pin1/pin3/pin4/pin7* quadruple mutant, *gnom*, *monopteros* and *bodenlos* [30]. In these mutants, miss-specification of the embryonic hypophysis leads to an absence of the root pole. This reveals the importance

of auxin transport and signaling for proper embryo patterning and the establishment of the shoot-root axis. It is therefore likely that PID is not only involved in cotyledon positioning, but also in the establishment/maintenance of the shoot-root axis by regulating the highly dynamic and regulated auxin transport during embryo development.

Material and methods

Molecular cloning and constructs

Molecular cloning was performed following standard procedures [34]. PCR primers used in this study are listed in Table 1. Bacteria were grown on LC medium containing 100 µg/ml carbenicillin (Cb) for *E. coli* strains DH5α or Rosetta (Novagen), 50 µg/ml kanamycin (Km) or 250 µg/ml spectinomycin for respectively binary vectors *pCAMBIA1300* and *pART27* in *E. coli* DH5α or *Agrobacterium tumefaciens* strain LBA1115. For the latter strain, 20 µg/ml rifampicin was included in the LC medium. The constructs *pSDM6004* (*pGEX-PID*), *pSDM6005* (*pBSK-PID*), *pSDM6007* (*pET16H:PBP1*) and *pGEX-PIN2HL* were described previously [10;35]. For the His-tagged PID vector, the full length DNA was obtained as *SalI* and *XmnI* fragment from *pSDM6005* and cloned into the *XhoI* and *BamHI* (blunted) sites of *pET-16H*. To obtain a plasmid encoding the GST tagged first 100 amino acids of PID, the *SalI-SacI* (blunted) fragment from *pSDM6005* was cloned into the *XhoI* and *HindIII* (blunted) sites of *pGEX-KG* [36]. The PID catalytic domain (aa 75-398) and PID C-terminal (aa 339-438) were PCR amplified using the primer pairs PID PK CaD F - PID PK CaD R and PID PK CT F - PID PK CT R, respectively, and cloned into *pGEX-KG* as respectively *XhoI-HindIII* (blunted) and *EcoRI-HindIII* (blunted) fragments. The coding region of *PBP1H* was PCR amplified from *Arabidopsis thaliana* Col-0 genomic DNA using primer set At4g27280 PBP1H F and At4g27280 PBP1H R, and the PCR product was ligated into *pET16H* as *SmaI* and *BamHI* fragment. *pART7-PID:CFP*, *pART7-PBP1:YFP*, *pART7-PBP1H:YFP*, and *pART7-YFP:CFP* fusions were constructed using the Gateway Technology (Invitrogen). Genes of interest were amplified by PCR with primers containing *attB* recombination sites (see table 1) from *pSDM6005*, *pET-16H PBP1*, *pET-16H PBP1H* and *pART7 YFP* destination vectors, respectively. BP reactions were performed in *pDONR207* according to manufacturer's protocol (Invitrogen). Recombinant plasmids

were isolated and sequenced. LR reactions were performed in *pART7* destination plasmids containing the YFP or CFP fluorescent markers in frame with the gateway recombinant cassette (Galvan-Ampudia, unpublished). The construct *pSDM6015* (*pBS-SK-PBP1*) was previously described [10]. For the *35Spro::PBP1* construct, the *PBP1* cDNA was excised as a *SalI-SpeI* fragment from *pSDM6015* and cloned into *pCambia1300int-35Snos*, giving rise to *pSDM6085*. To obtain the *PBP1H* RNAi construct *hpPBP1H*, a *PBP1H* fragment was PCR amplified from *pET-PBP1H* using the primers PBP1H RNAi F and PBP1H RNAi R, and ligated as anti-sense *EcoRI-KpnI* fragment into the *pHANNIBAL* vector [37]. The sense fragment was excised as a *ClaI-BamHI* fragment from *pET-PBP1H* and cloned into the corresponding restriction sites in *pHANNIBAL*. The resulting *hpPBP1H* expression cassette (*pSDM6043*) was transferred as a *NotI* fragment to the *pART27* binary vector (*pSDM6302*).

Table 1: Primer list

PID PK CaD F	5'TTCCTCGAGTTTCGCCTCAT3'
PID PK CaD R	5'GCGCTCAGTTTAGACCTTTGA3'
PID PK CT F	5'TAATGACGGAATTCTCCGTAACAT3'
PID PK CT R	5'AAGCTCGTTCAAAAAGTAATCGAAC3'
At4g27280 PBP1H F	5'TAATGGCGTCACCAAAGTCA3'
At4g27280 PBP1H R	5'GGAAGGGATCCCAAATCTCT3'
At2g46600 KIC F	5'TACTCGAGATGGAACCAACCGAGAAATCTATGTTAC3'
At2g46600 KIC R	5'ATGGTACCTCAAGGCATAGAAGAGAG3'
PBP1 attB F1	5'GGGGACAAGTTTGTACAAAAAAGCAGGCTTAATGGCATCTCCTAAATCCTCA3'
PBP1 attB R1	5'GGGGACCACTTTGTACAAGAAAGCTGGGTAATGCCGGTAAAACTCTTC3'
PBP1H attB F1	5'GGGGACAAGTTTGTACAAAAAAGCAGGCTTAATGGCGTCACCAAAGTCAC3'
PBP1H attB R1	5'GGGGACCACTTTGTACAAGAAAGCTGGGTAATGCCGGCGGTGAAGCC3'
KIC attB F1	5'GGGGACAAGTTTGTACAAAAAAGCAGGCTTAATGGAACCAACCGAGAAA3'
KIC attB R1	5'GGGGACCACTTTGTACAAGAAAGCTGGGTAAGGCATAGAAGAGAGATT3'
PID attB F1	5'GGGGACAAGTTTGTACAAAAAAGCAGGCTTCAGCATGTTACGAGAATCAGACGGT3'
PID attB R1	5'GGGGACCACTTTGTACAAGAAAGCTGGGTCAAAGTAATCGAACGCCGCTGG3'
PBP1H RNAi F	5'TCGAATTCATGGCGTCACCAAAGTCACC3'
PBP1H RNAi R	5'CAAATCTCTCCAGTGGGTACCATGC3'
PID screening F	5'TCTCTCCGCCAGGTA AAAA3'
PID reverse	5'CGCAAGACTCGTTGGAAAAAG3'
PBP1 F	5'TACCCTTACGTGAGCTTCAA3',
PBP1-R	5'TCACCTCCGTCACAACACAC3'
PBP1H-F	5'CATGCAATTAGAGAACGGGCA3'
PBP1H-R	5'AGGAACATCCATGGAAGCCA3'
LBal	5'TGGTTCACGTAGTGGGCCATCG3'
Ds3-2	5'CGATTACCGTATTTATCCCGTTC 3'
PBP1_RT	5'CCTCAACAAGACCAAACCAAG3'
PBP1H RT F	5'ATGGCGTCACCAAAGTCACC3'
PBP1H RT R	5'TGTTCAACACATCTGATCAAAGA3'

PID RT-F	5'AGGCACGTGACAACGTCTC3'
AtROC F	5'CGGGAAGGATCGTGATGGA3'
AtROC R	5'CCAACCTTCTCGATGGCCT3'
Alpha TUB F	5'CGGAATTCATGAGAGAGATCCTTCATATC3'
Alpha TUB R	5'CCCTCGAGTTAAGTCTCGTACTCCTCTTC3'

attB recombination sites are underlined

Protein purification and *in vitro* pull-down assays

E. coli strain Rosetta (Novagen) was transformed with the constructs encoding His-tagged PID, PBP1, PBP1H, KIC and GST-tagged PID, PID NT²⁻¹⁰³, PID CaD⁷⁵⁻³⁹⁸ and PID CT³³⁹⁻⁴³⁸. Single colonies were grown overnight at 37°C in liquid LC medium containing Carbenicillin (100 µg/ml) and Chloramphenicol (34 µg/ml), 5 ml preculture was diluted in 100 ml of fresh LC medium containing the same antibiotics and grown at 30°C until OD600 was 0.8. Following induction by 1 mM IPTG, the culture was grown at 30°C for 3 hr. Cultures were pellet by centrifugation at 4000 x g for 20 min at 4°C and stored at -20°C. For His-tagged proteins, bacterial pellets were resuspended in 2 ml of Lysis Buffer (25 mM Tris-HCl pH 8.0, 500 mM NaCl, 20 mM imidazole, 0,05% Tween 20 and 10% glycerol) and incubated 20 min on ice. After sonication for 2 min, 100 µl of 20% Triton X-100 was added and the mixture was incubated 5 min on ice, followed by centrifugation at 15,000 x g for 20 min at 4°C. Soluble fraction was added with 400 µl of pre-equilibrated 50% NTA-agarose matrix (QIAGEN) and mixed gently for 1.5 hr at 4°C. Beads were washed three times with 2 ml of Lysis Buffer, then with Wash Buffer 1 (25 mM Tris-HCl pH 7.5, 500 mM NaCl, 40 mM imidazole, 0,01% Tween 20 and 10% glycerol), and subsequently with Wash Buffer 2 (25 mM Tris-HCl pH7.0, 500 mM NaCl, 80 mM imidazole and 10% glycerol). Elution was performed by incubating the beads for 3 hr at 4°C in 600 µl Elution Buffer (25 mM Tris-HCl pH 7.0, 300 mM NaCl, 300 mM imidazole and 10% glycerol). For the GST-tagged proteins, frozen bacterial pellets were incubated for 10 min on ice, resuspended in 2 ml Extraction Buffer (150 mM NaCl, 2 mM KCl, 2 mM KH₂PO₄, 10 mM Na₂HPO₄, 2 mM EDTA, 2 mM EGTA, 10 mM DTT and 10% v/v B-PER (Pearce) and incubated on ice for 10 min. After sonication for 2 min, 100 µl of 20% Triton X-100 was added and the mixture was incubated for 5 min on ice, followed by centrifugation at 20,000 x g for 20 min at 4°C. Supernatants were added to

400 μ l of pre-equilibrated 50% Glutathione Sepharose 4B beads (Amersham-Pharmacia) and incubated for 1.5 hr. Beads were washed three times with 2 ml Extraction Buffer.

For *in vitro* pull-down assays, His-tagged bacterial pellets were resuspended in 2 ml of Binding Buffer (50 mM Tris-HCl pH 6.8, 100 mM NaCl, 10 mM CaCl₂ and 0.1% Tween-20), incubated for 20 min on ice, followed by sonication for 2 min. Then 100 μ l of 20% Triton X-100 was added and the mixture was incubated for 5 min on ice, followed by centrifugation at 20,000 x g for 20 min at 4°C. Supernatant was added (0.4 ml) to 50 μ l of pre-equilibrated 50% Glutathione Sepharose 4B beads (Amersham-Pharmacia biotech) bound with GST-tagged proteins. After incubation for 1.5 hr, beads were washed three times with 2 ml of Binding Buffer. Beads were resuspended in 25 μ l 2X SDS loading buffer (0.125 M Tris-HCl pH 6.8, 4% SDS, 20% glycerol, 3 M β -mercaptoethanol and 0.05% bromophenol blue) and boiled. Samples were analyzed by SDS-PAGE. Proteins were blotted on a PDVF membrane (Millipore, USA) and immunodetected using penta-His antibodies (QIAGEN) according as the manufacturer's instructions.

***In vitro* protein kinase assays.**

His- or GST-tagged proteins were purified as described above. *In vitro* kinase assays were performed in a final volume of 15 μ l with 1X kinase buffer (25 mM Tris-HCl pH 7.5, 5 mM MgCl₂, 2 mM CaCl₂ and 1 mM DTT), 2 μ g purified GST-tagged kinase, 2 μ g purified His-tagged PBP1 or PBP1H, 2 μ g GST-PIN2 HL, 100 μ M ATP and 1 μ Ci [γ -³²P] ATP (3000 Ci/mM) (GE Amersham). Reactions were incubated at 30°C for 30 min and stopped by adding 4 μ l of 5X SDS loading buffer (0.3125 M Tris-HCl pH 6.8, 10% SDS, 50% glycerol, 7.5 M β -mercaptoethanol and 0.125% bromophenol blue) and boiled for 5 min. Samples were separated by SDS-PAGE. After electrophoresis, gels were washed 3 times with 5% TCA 1% Na₂H₂P₄O₇, Coomassie stained, dried and exposed to a PhosphoImager screen (Molecular Dynamics).

PepChip Kinomics array

Pepchip Kinomics arrays (Pepscan) were incubated with 50 μ l of the reaction mix for 4 hr at 30°C in a humid chamber. Slides were washed once with TBS (10 mM Tris pH 7.5,

NaCl 150 mM), once with 1 M urea and 2 M NaCl in TBS, two times with 2 M NaCl, two times with dH₂O and dried for 30 min. The reaction mix consisted of the Kinase Mastermix (25 mM Tris pH 7.4, 5 mM MgCl₂, 1 mM DTT, 10% v/v glycerol, 0.02 mg/ml BSA, 0.005% v/v Brij-35), 100 μM ATP and 300 μCi/ml [γ -³³P] ATP (3000 Ci/mM) (GE Amersham), supplemented with 1 mM CaCl₂ final concentration. to which either 5 μg of purified GST-PID or 5 μg of purified GST-PID and His-PBP1 was added. Slides were scanned using the Biomex reader and analysed using the Biosplit software (Biomex AS). For each peptide the results of the three identical sectors present on one slide were averaged and the standard deviation (SD) was calculated. Inconsistencies between sectors was filtered out by using $SD\% \leq 50$ from the mean as a criterium. All values below the sum of the average value for all peptides on the array and the average SD were considered as background levels.

Protoplast transfection

Protoplasts were isolated from *Arabidopsis thaliana* Col-0 cell suspension cultures and 10 μg plasmid DNA was introduced by PEG-mediated transfection as described originally by Axelos and co-workers [38] and adapted by Schirawski and co-workers [39]. Following transfection, the protoplasts were incubated for at least 16h. Images were obtained by confocal microscopy.

Confocal microscopy

For the protoplast experiments, a Leica DM IRBE confocal laser scanning microscope was used with a 63X water objective, digital zoom and 51% laser intensity. The fluorescence was visualized with an Argon laser for excitation at 514 nm (YFP) and 457 nm (CFP) with 522-532 nm and 471-481 nm emission filters, respectively. *Arabidopsis PIDpro::PID:VENUS* roots were observed using a 40X oil objective with a ZEISS Axioplan microscope equipped with a confocal laser scanning unit (MRC1024ES, BioRad, Hercules, CA). The YFP fluorescence was monitored with a 522-532 nm band pass emission filter (488 nm excitation). All images were recorded using a 3CCD Sony DKC5000 digital camera. The images were processed by ImageJ (<http://rsb.info.nih.gov/ij/>) and assembled in Adobe Photoshop 7.0.

Fluorescence Resonance Energy Transfer (FRET)

Protoplasts were prepared and the fluorescence monitored using the Leica confocal microscope as described above. Lambda scanning was done at 457 nm excitation and emission was measured at intervals of 5 nm at the spectrum from 460 to 585 nm using a RSP465 filter. An image was obtained of every interval and the intensity of three fixed areas (ROIs) was quantified using Leica confocal laser scanning software. The intensity of these three ROIs was averaged and normalized. Of each sample three protoplasts were measured and the obtained normalised intensity of all three protoplasts was averaged and the standard deviation was calculated. Student's t-test was used to test for a significant reduction in intensity at 475 nm (CFP emission) and a significant enhancement in intensity at 527 nm (YFP emission) in the FRET sample as compared to a negative control (e.g. protoplasts co-expressing CFP and YFP).

***Arabidopsis* lines, plant growth and transformation**

The *35Spro::PID-21* and the *PIDpro::PID:VENUS* lines were described previously [5;8]. The *pid-14* (SALK_049736), *pbp1-1* (Ds transposon line GT6553) and *pbp1h-1* and *-2* alleles (SALK_013868 and SALK_048098) were obtained from NASC for the SALK lines and from the Cold Spring Harbor Laboratory for the transposon insertion line [40;41]. For the detection of the insertions, we used gene-specific primers and the insertion-specific primers LBA1 and Ds3-2 for respectively the SALK lines and the transposon line. The flanking region of each insertion was sequenced to confirm the insertion position, and RT-PCR analysis was performed to determine if the insertion resulted in a complete loss-of-function allele.

Arabidopsis seeds were surfaced-sterilized by incubation for 15 min in 50% commercial bleach solution and rinsed four times with sterile water. Seeds were vernalized for 2 to 4 days at 4°C and germinated (21°C, 16 h-photoperiod and 42 $\mu\text{mol}/\text{m}^2/\text{s}$) on solid MA medium supplemented with antibiotics when required [42]. Two- to three-week old plants were transferred to soil and grown at 21°C and 70% relative humidity with a 16 hr photoperiod (140 $\mu\text{mol}/\text{m}^2/\text{s}$).

Arabidopsis thaliana ecotype Columbia (Col) was transformed by the floral dip method as described [43]. Primary transformants were selected on medium supplemented with 20 µg/ml hygromycin (Hm) for *pSDM6085* or 70 µg/ml Km for *pSDM6302* and 100 µg/ml timentin to inhibit the *Agrobacterium* growth. For further analysis, single locus insertion lines were selected by germination on 10 µg/ml hygromycin or 25 µg/ml kanamycin and checked for transgene expression by Northern blot or RT-PCR analysis.

Northern blot and RT-PCR analysis

Total RNA was purified using the RNeasy Plant (Qiagen) and Invisorb Spin Plant RNA (Invitex) Mini kits. Subsequent RNA blot analysis was performed as described [44] using 10 µg of total RNA per sample. The following modifications were made: pre-hybridizations and hybridizations were conducted at 65°C using 10% Dextran sulfate, 1% SDS, 1 M NaCl, 50 µg/ml of single strand Herring sperm DNA as hybridization mix. The hybridized blots were washed for 20 min at 65°C in 2X SSPE 0.5% SDS, and for 20 min at 42°C in respectively 0.2X SSPE 0.5% SDS, 0.1X SSPE 0.5% SDS and 0.1X SSPE. Blots were exposed to X-ray film FUJI Super RX. Probes were PCR amplified and column purified (Qiagen): with PBP1-F and -R for *PBP1* from *pSDM6007*; PBP1H-F and -R for *PBP1H* from *pET-16H PBP1H*, RT-F and exon2-R for *PID* from *pSDM6004*, *AtROC*-F and -R for *AtROC*, alpha TUB-F and -R for *αTubulin* from Col-0 genomic DNA. Probes were radioactively labelled using α-³²P-ATP (Amersham) and the Prime-a-gene kit (Promega).

RT-PCRs were performed as described in [45] using 10 µg of total RNA from one-week old seedlings for the RT reaction. The PCR reactions were performed with one tenth of the RT volume with the same gene specific primers used for the probe amplification in the Northern blot analysis. An RT reaction from Col seedlings RNA in which the reverse-transcriptase was omitted served as a negative control.

Biological assays

For the root meristem collapse assay, about 100 seedlings per line were grown in triplicate on vertical plates containing solid MA medium. The development of the seedling root was monitored and scored each day during eight days for the collapse of the

primary root meristem. For the phenotypic analysis of the crosses with *pid-14*, about 300 seeds (100 seeds for *pid-14/pbp1-1* and controls) were plated in triplicate, germinated and grown for one week on solid MA medium. The number of dicotyledon seedlings and of seedlings with cotyledon defects was counted and the penetrance of the phenotypes was calculated based on a 1:3 segregation ratio for homozygous *pid* seedlings. For root length measurements, at least 50 seedlings for each genotype were grown in triplicate on vertical plate for eight days and roots were scanned. Root lengths were measured using ImageJ. To observe the auxin-induced changes in the subcellular localization of PID in *Arabidopsis* roots, vertically grown three day-old *PIDpro::PID:VENUS* and *PIDpro::PID:VENUS/35Spro::PBP1-29* seedlings were treated with 5 μ M IAA (in MA medium) following 30 min pre-treatment with a calmodulin inhibitor (0.5 mM Tetracain, Sigma) or a calcium channel blocker (1.25 mM Lanthanum, Sigma) when indicated.

Accession Numbers

The *Arabidopsis* Genome Initiative locus identifiers for the genes mentioned in this chapter are as follows: *PBP1/KRP2* (At5g54490), *PBP1H/KRP1* (At4g27280), *KIC* (At2g46600), *PID* (At2g34650), *TCH3* (At2g41100), *KCBP* (At5g65930), *KIPK* (At3g52890), *ROC* (At4g38740), *α Tubulin* (At5g44340), *PIN2* (At5g57090).

Acknowledgments

The authors thank Marcus Heisler and Pieter Ouwkerk for kindly providing the *PIDpro::PID:VENUS* line and *pCambia1300int-35Snos*, respectively, and Gerda Lamers and Ward de Winter for their help with respectively microscopy and tissue culture. This work was funded through grants from the Research Council for Earth and Life Sciences (ALW 813.06.004) and from the Netherlands Organisation for Health Research and Development (ZON 050-71-023), and with financial aid from the Dutch Organization of Scientific Research (NWO).

Reference list

1. Muday GK, DeLong A (2001). **Polar auxin transport: controlling where and how much.** *Trends Plant Sci.* 6(11), 535-542.
2. Tanaka H, Dhonukshe P, Brewer PB, Friml J (2006). **Spatiotemporal asymmetric auxin distribution: a means to coordinate plant development.** *Cell Mol. Life Sci.* 63(23), 2738-2754.
3. Wisniewska J, Xu J, Seifertová D, Brewer PB, Ruzicka K, Blilou I, Rouquié D, Benková E, Scheres B, Friml J (2006). **Polar PIN localization directs auxin flow in plants.** *Science.* 312(5775), 883.
4. Petrášek J, Mravec J, Bouchard R, Blakeslee JJ, Abas M, Seifertová D, Wisniewska J, Tadele Z, Kubes M, Covanová M, Dhonukshe P, Skupa P, Benková E, Perry L, Krecek P, Lee OR, Fink GR, Geisler M, Murphy AS, Luschnig C, Zazimalova E, Friml J (2006). **PIN Proteins Perform a Rate-Limiting Function in Cellular Auxin Efflux.** *Science.* 312, 914-918.
5. Benjamins R, Quint A, Weijers D, Hooykaas P, Offringa R (2001). **The PINOID protein kinase regulates organ development in *Arabidopsis* by enhancing polar auxin transport.** *Development.* 128(20), 4057-4067.
6. Friml J, Yang X, Michniewicz M, Weijers D, Quint A, Tietz O, Benjamins R, Ouwerkerk PBF, Ljung K, Sandberg G, Hooykaas PJJ, Palme K, Offringa R (2004). **A PINOID-dependent binary switch in apical-basal PIN polar targeting directs auxin efflux.** *Science.* 306(5697), 862-865.
7. Lee SH, Cho HT (2006). **PINOID Positively Regulates Auxin Efflux in *Arabidopsis* Root Hair Cells and Tobacco Cells.** *Plant Cell.* 18(7), 1604-1616.
8. Michniewicz M, Zago MK, Abas L, Weijers D, Schweighofer A, Meskiene I, Heisler MG, Ohno C, Huang F, Weigel D, Meyerowitz EM, Luschnig C, Offringa R, Friml J (2007). **Phosphatase 2A and PID kinase activities antagonistically mediate PIN phosphorylation and apical/basal targeting in *Arabidopsis*.** *Cell.* 130(6), 1044-1056.
9. Dela Fuente RK, Leopold AC (1973). **A Role for Calcium in Auxin Transport.** *Plant Physiol.* 51(5), 845-847.
10. Benjamins R, Galván-Ampudia CS, Hooykaas PJ, Offringa R (2003). **PINOID-mediated signaling involves calcium-binding proteins.** *Plant Physiol.* 132(3), 1623-1630.
11. Reddy VS, Day IS, Thomas T, Reddy AS (2004). **KIC, a novel Ca²⁺ binding protein with one EF-hand motif, interacts with a microtubule motor protein and regulates trichome morphogenesis.** *Plant Cell.* 16(1), 185-200.

12. Reddy AS, Day IS (2000). **The role of the cytoskeleton and a molecular motor in trichome morphogenesis.** *Trends Plant Sci.* 5(12), 503-505.
13. Galvan-Ampudia CS, Offringa R (2007). **Plant evolution: AGC kinases tell the auxin tale.** *Trends Plant Sci.* 12(12), 541-547.
14. Day IS, Miller C, Golovkin M, Reddy AS (2000). **Interaction of a kinesin-like calmodulin-binding protein with a protein kinase.** *J. Biol. Chem.* 275(18), 13737-13745.
15. Puntervoll P, Linding R, Gemund C, Chabanis-Davidson S, Mattingsdal M, Cameron S, Martin DM, Ausiello G, Brannetti B, Costantini A, Ferre F, Maselli V, Via A, Cesareni G, Diella F, Superti-Furga G, Wyrwicz L, Ramu C, McGuigan C, Gudavalli R, Letunic I, Bork P, Rychlewski L, Kuster B, Helmer-Citterich M, Hunter WN, Aasland R, Gibson TJ (2003). **ELM server: A new resource for investigating short functional sites in modular eukaryotic proteins.** *Nucleic Acids Res.* 31(13), 3625-3630.
16. Bahler M, Rhoads A (2002). **Calmodulin signaling via the IQ motif.** *FEBS Lett.* 20;513(1), 107-113.
17. Rhoads AR, Friedberg F (1997). **Sequence motifs for calmodulin recognition.** *FASEB J.* 11(5), 331-340.
18. Yap KL, Kim J, Truong K, Sherman M, Yuan T, Ikura M (2000). **Calmodulin target database.** *J. Struct. Funct. Genomics.* 1(1), 8-14.
19. Ritsema T, Joore J, van Workum W, Pieterse CM (2007). **Kinome profiling of *Arabidopsis* using arrays of kinase consensus substrates.** *Plant Methods.* 3:3., 3.
20. Stulemeijer IJ, Stratmann JW, Joosten MH (2007). **Tomato mitogen-activated protein kinases LeMPK1, LeMPK2, and LeMPK3 are activated during the Cf-4/Avr4-induced hypersensitive response and have distinct phosphorylation specificities.** *Plant Physiol.* 144(3), 1481-1494.
21. Zegzouti H, Li W, Lorenz TC, Xie M, Payne CT, Smith K, Glenney S, Payne GS, Christensen SK (2006). **Structural and functional insights into the regulation of *Arabidopsis* AGC VIIIa kinases.** *J. Biol. Chem.* 281(46), 35520-35530.
22. Siegel RM, Chan FK, Zacharias DA, Swofford R, Holmes KL, Tsien RY, Lenardo MJ (2000). **Measurement of molecular interactions in living cells by fluorescence resonance energy transfer between variants of the green fluorescent protein.** *Sci. STKE.* 2000(38), L1.
23. Bennett SRM, Alvarez J, Bossinger G, Smyth DR (1995). **Morphogenesis in Pinoid Mutants of *Arabidopsis thaliana*.** *Plant Journal.* 8(4), 505-520.

24. Christensen SK, Dagenais N, Chory J, Weigel D (2000). **Regulation of auxin response by the protein kinase PINOID.** *Cell.* 100(4), 469-478.
25. Furutani M, Vernoux T, Traas J, Kato T, Tasaka M, Aida M (2004). **PIN-FORMED1 and PINOID regulate boundary formation and cotyledon development in *Arabidopsis* embryogenesis.** *Development.* 131(20), 5021-5030.
26. Felle H (1988). **Auxin causes oscillations of cytosolic free calcium and pH in *Zea mays* coleoptiles.** *Planta.* V174(4), 495-499.
27. Gehring CA, Irving HR, Parish RW (1990). **Effects of auxin and abscisic acid on cytosolic calcium and pH in plant cells.** *Proc. Natl. Acad. Sci. USA.* 87(24), 9645-9649.
28. Shishova M, Lindberg S (2004). **Auxin induces an increase of Ca²⁺ concentration in the cytosol of wheat leaf protoplasts.** *J Plant Physiol.* 161(8), 937-945.
29. Baens M, Noels H, Broeckx V, Hagens S, Fevery S, Billiau AD, Vankelecom H, Marynen P (2006). **The dark side of EGFP: defective polyubiquitination.** *PLoS ONE.* 20;1:e54., e54.
30. Friml J, Vieten A, Sauer M, Weijers D, Schwarz H, Hamann T, Offringa R, Jurgens G (2003). **Efflux-dependent auxin gradients establish the apical-basal axis of *Arabidopsis*.** *Nature.* 426(6963), 147-153.
31. Weijers D, Sauer M, Meurette O, Friml J, Ljung K, Sandberg G, Hooykaas P, Offringa R (2005). **Maintenance of embryonic auxin distribution for apical-basal patterning by PIN-FORMED-dependent auxin transport in *Arabidopsis*.** *Plant Cell.* 17(9), 2517-2526.
32. Weijers D, Jürgens G (2005). **Auxin and embryo axis formation: the ends in sight?** *Curr. Opin. Plant Biol.* 8(1), 32-37.
33. Treml BS, Winderl S, Radykewicz R, Herz M, Schweizer G, Hutzler P, Glawischnig E, Ruiz RAT (2005). **The gene ENHANCER OF PINOID controls cotyledon development in the *Arabidopsis* embryo.** *Development.* 132(18), 4063-4074.
34. Sambrook J, Fritsch F., Maniatis T. (1989) **Molecular cloning - A laboratory Manual.** Edited by C.Nolan. Cold Spring Harbor Laboratory press, NY, USA.
35. Abas L, Benjamins R, Malenica N, Paciorek T, Wisniewska J, Moulinier-Anzola JC, Sieberer T, Friml J, Luschnig C (2006). **Intracellular trafficking and proteolysis of the *Arabidopsis* auxin-efflux facilitator PIN2 are involved in root gravitropism.** *Nat. Cell Biol.* 8(3), 249-256.

36. Guan KL, Dixon JE (1991). **Eukaryotic proteins expressed in *Escherichia coli*: an improved thrombin cleavage and purification procedure of fusion proteins with glutathione S-transferase.** *Anal. Biochem.* 192(2), 262-267.
37. Wesley SV, Helliwell CA, Smith NA, Wang M, Rouse DT, Liu Q, Gooding PS, Singh SP, Abbott D, Stoutjesdijk PA, Robinson SP, Gleave AP, Green AG, Waterhouse PM (2001). **Construct design for efficient, effective and high-throughput gene silencing in plants.** *Plant Journal.* 27(6), 581-590.
38. Axelos M, Curie C, Mazzolini L, Bardet C, Lescure B (1992). **A Protocol for Transient Gene-Expression in *Arabidopsis thaliana* Protoplasts Isolated from Cell-Suspension Cultures.** *Plant Physiology and Biochemistry.* 30(1), 123-128.
39. Schirawski J, Planchais S, Haenni AL (2000). **An improved protocol for the preparation of protoplasts from an established *Arabidopsis thaliana* cell suspension culture and infection with RNA of turnip yellow mosaic tymovirus: a simple and reliable method.** *Journal of Virological Methods.* 86(1), 85-94.
40. Alonso JM, Stepanova AN, Leisse TJ, Kim CJ, Chen H, Shinn P, Stevenson DK, Zimmerman J, Barajas P, Cheuk R, Gadrinab C, Heller C, Jeske A, Koesema E, Meyers CC, Parker H, Prednis L, Ansari Y, Choy N, Deen H, Geralt M, Hazari N, Hom E, Karnes M, Mulholland C, Ndubaku R, Schmidt I, Guzman P, Aguilar-Henonin L, Schmid M, Weigel D, Carter DE, Marchand T, Risseeuw E, Brogden D, Zeko A, Crosby WL, Berry CC, Ecker JR (2003). **Genome-Wide Insertional Mutagenesis of *Arabidopsis thaliana*.** *Science.* 301(5633), 653-657.
41. Sundaresan V, Springer P, Volpe T, Haward S, Jones JD, Dean C, Ma H, MARTIENSSEN R (1995). **Patterns of gene action in plant development revealed by enhancer trap and gene trap transposable elements.** *Genes and Development.* 9(14), 1797-1810.
42. Masson J, Paszkowski J (1992). **The Culture Response of *Arabidopsis thaliana* Protoplasts Is Determined by the Growth-Conditions of Donor Plants.** *Plant Journal.* 2(5), 829-833.
43. Clough SJ, Bent AF (1998). **Floral dip: a simplified method for *Agrobacterium*-mediated transformation of *Arabidopsis thaliana*.** *Plant Journal.* 16(6), 735-743.
44. Memelink J, Swords KMM, Staehelin LA, Hoge JHC. (1994) **Southern, Northern and Western blot analysis.** In *Plant Molecular Biology Manuel.* Dordrecht, NL: Kluwer Academic Publishers.
45. Weijers D, Franke-van Dijk M, Vencken RJ, Quint A, Hooykaas P, Offringa R (2001). **An *Arabidopsis* Minute-like phenotype caused by a semi-dominant mutation in a RIBOSOMAL PROTEIN S5 gene.** *Development.* 128(21), 4289-4299.

CHAPTER 4

Fine tuning PINOID action by PDK1-mediated phosphorylation

Carlos S. Galván-Ampudia, Christa Testerink and Remko Offringa

Summary

The PINOID protein kinase (PID) is the only identified determinant of apical polar targeting of PIN proteins. Previous reports have shown that PID not only co-localizes at the plasma membrane (PM), but that it also phosphorylates PIN proteins. How exactly this phosphorylation affects the polar subcellular localization of PIN proteins and which factors determine localization and activity of PID is still unknown. Until now, only a few PID interacting proteins have been described. Among them, 3-phosphoinositide-dependent kinase 1 (PDK1) was shown to phosphorylate the activation loop of PID and to enhance its kinase activity *in vitro*. To further elucidate the effect of PDK1 on PID, we have used *Arabidopsis thaliana* cell suspension derived protoplasts. We show that PDK1 induces a switch in PID subcellular localization from the plasma membrane to endomembrane compartments and microtubules (MT). We demonstrate that the phosphorylation status of PID determines its subcellular localization. By specifically removing the phosphorylation targets sites of PDK1, PID was unable to be recruited to MT. In accordance, by mimicking PDK1-phosphorylation PID localized to the MT in the absence of PDK1. Moreover, osmotic shock treatment, which is known to induce PDK1 activity, resulted in relocation of PID to MT-like structures in *Arabidopsis thaliana* root epidermal cells. We propose a model of the molecular mechanism of PID-dependent polar targeting as a combined action of PDK1 and phospholipids.

Introduction

As sessile organisms, plants have developed mechanisms to constantly monitor their surroundings in order to be able to adapt to changes in their environment. Following the initial observations by Darwin more than a century ago, it is well established now that abiotic environmental signals such as light and gravity modulate plant growth and architecture by causing changes in the distribution of the signalling molecule auxin (indole-3-acetic acid) [1]. However, the involvement of auxin distribution in directing growth responses to abiotic stresses, such as high salinity or osmotic stress is only just emerging [2].

The distribution of auxin is determined by its polar cell-to-cell transport that is controlled by three types of plasma membrane (PM) proteins, the AUX1/LAX auxin influx carriers, the P glycoprotein (PGP) type ABC transporters, and the PIN auxin efflux carriers [3]. The PIN proteins are considered the primary drivers of transport that determine the direction of auxin flow through their asymmetric subcellular distribution [4]. In *Arabidopsis*, the *PIN* family is composed of 8 genes which are expressed at different stages of plant development to regulate auxin-mediated processes such as embryogenesis [5], root meristem maintenance and growth [6;7], phyllotaxis [8], formation of new organs [9], and tropic growth [10;11]. The PIN members can be classified in two groups: i) five PIN1-type PINs that have a large central hydrophilic loop (PINHL) and direct polar auxin transport (PAT) through their asymmetric localisation at the PM, and ii) three PIN5-type PINs that have a smaller or no central hydrophilic loop, localize to the ER and seem to be involved in controlling subcellular auxin levels [12].

The PIN1-type PINs cycle via actin-mediated vesicle transport between PM and endosomal compartments, and this cyclic vesicle transport is essential for polarity establishment [13;14]. Although the exact mechanism of PIN polarity establishment is still elusive, the first identified component in this pathway is the plant AGC protein ser/thr kinase *PINOID* (PID). PID instructs apical (shoot meristem facing) PIN polarity, and acts antagonistically with protein phosphatase 2A (PP2A) in determining the phosphorylation status of the PINHL [15;16].

As a PIN polarity determinant, PID is an excellent target for the regulation of the direction of transport by external stimuli through upstream regulators, such as 3-

phosphoinositide-dependent kinase 1 (PDK1). PDK1-dependent phosphorylation is a conserved eukaryotic mechanism for the regulation of many signal transduction pathways downstream of AGC protein kinases. PDK1 was shown to phosphorylate PID on two well-conserved residues of the activation loop (Ser 288 and Ser 290), resulting in enhanced kinase activity towards a generic substrate *in vitro* [17]. *PDK1* is a conserved gene among eukaryotes that regulates and activates other kinases by phosphorylation [18;19]. In *Arabidopsis*, two *PDK1* genes are present, (*PDK1-1* and *PDK1-2*), which both encode proteins with an N-terminal protein ser/thr kinase domain and a plekstrin homology (PH) domain at the C-terminus [20]. The PH domain binds many phospholipids, but only phosphatidic acid (PA) and phosphatidylinositol-(4,5)-bisphosphate (PIP2) have been shown to stimulate PDK1 kinase activity [20;21]. As in mammals and yeast, plant PDK1 activates and phosphorylates the activation loop of different AGC protein kinases (named after protein kinase A (PKA), cyclic GMP-dependent protein kinase (PKG) and protein kinase C (PKC)) [17;21-24].

Here we investigated the effect of PDK1-dependent phosphorylation of PID at the cellular level, and show that PDK1 causes a change in the subcellular localization of PID from PM to endomembrane structures and microtubules (MT) in *Arabidopsis* cell suspension derived protoplasts. PDK1-mediated phosphorylation of PID was required for this relocalization. Furthermore, osmotic stress treatment, which is known to induce the PDK1 pathway [23], leads to recruitment of PID to MT-like structures in *Arabidopsis* root epidermis cells. Our results indicate that stress responses initiate a lipid signaling cascade that leads to PDK1-dependent activation and relocalisation of PID, and reveal PDK1 as a direct molecular link between stress responses and auxin- mediated plant development and growth.

Results

PDK1 regulates PID subcellular localization

To investigate the effect of PDK1-dependent PID phosphorylation at the cellular level, we expressed translational fusions of these proteins to respectively cyan and yellow

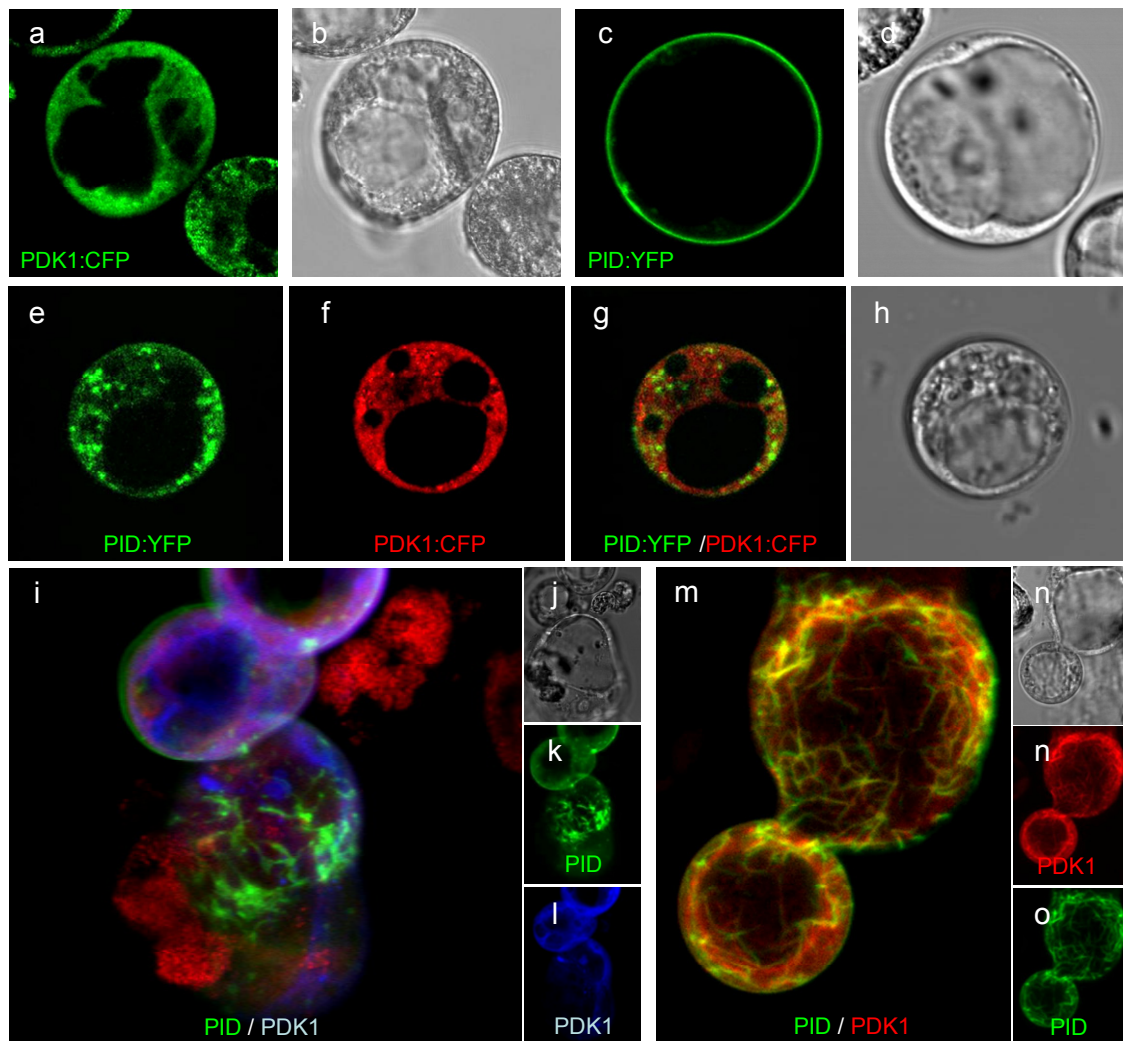


Figure 1. Subcellular localization of PDK1 and PID in protoplasts.

(a-d) *Arabidopsis* cell suspension derived protoplast transfected with *35Spro::PDK1:CFP* (a and b) or *35Spro::PID:YFP* (c and d). Confocal image (a and c) and transmitted light image (b and d).

(e-o) Representative pictures of protoplast co-transfected with *35Spro::PDK1:CFP* and *35Spro::PID:YFP*. (e-h) PID (e, YFP channel, green) is recruited into endomembrane compartments when co-expressed with PDK1 (f, CFP channel, red). The merged image (g) shows that PID is recruited into different endomembrane-like compartments than PDK1. Transmitted light image (h).

(i-l) PDK1 recruits PID to cytoskeleton like structures. Confocal projection of a protoplast where PID localize in filaments (k, YFP channel, green) and PDK1 localizes in the cytosol (l, CFP channel, blue). Merged image (i) with red signal representing autofluorescence of dead cells. Transmitted light image (j).

(m-o) PDK1 and PID co-localize in filaments-like structures. Confocal projections of protoplasts co-expressing PDK1:CFP (n, red) and PID:YFP (o, green). Merged projection (m) where the yellow signal is indicative for co-localization of the two proteins. Transmitted light image (n).

fluorescent protein (CFP and YFP) in *Arabidopsis thaliana* cell suspension protoplasts. As previously reported, PID:YFP was localized at the PM of these cells (Figure 1c and d) [25]. Protoplasts expressing only PDK1:CFP showed labelling of endomembrane-like structures throughout the cytoplasm (Figure 1a and b). Co-expression of PDK1:CFP and PID:YFP strikingly led to PID relocation from the PM to endomembrane-like structures (Figure 1e-h). In a subpopulation of protoplasts, PID was found in filamentous cytoskeleton-like structures, while PDK1 subcellular localization was unchanged (Figure 1i-l). Co-localization of PID:YFP and PDK1:CFP at the cytoskeleton-like structures was observed occasionally (Figure 1m-o). Thus, PDK1 induces recruitment of PID from the PM into endomembrane- and cytoskeleton-like structures in *Arabidopsis* protoplasts.

PDK1 recruits PID to microtubules

Previous studies in cowpea mesophyll protoplasts made use of the microtubule plus-end binding protein Cytoplasmic Linker Protein170 (CLIP170) as a MT marker [26]. Protoplasts transfected with CLIP170¹⁻¹²⁴⁰ showed similar MT localization (Figure 2). Co-transfection with PID:CFP, PDK1:mRFP and YFP:CLIP170¹⁻¹²⁴⁰ corroborated that PID is recruited to the MT network, as we found clear co-localization of PID and CLIP170¹⁻¹²⁴⁰ (Figure 2). Interestingly, PID was localized not only in cortical MT (Figure 2a-e) but also in transcytoplasmic MT (Figure 2f-j). Moreover, PDK1 was found to remain in endomembrane like structures (Figure 2c and h). No co-localization of the three proteins was observed, probably because of the low efficiency of transfection of all constructs. Furthermore, our results show that PID MT localization is dependent on the presence of PDK1 as we could not find co-localization between CLIP170¹⁻¹²⁴⁰ and PID when no PDK1 was transfected (Figure 2k-l). Our findings suggest that PDK1 acts as a switch to regulate PID subcellular translocation from the PM to the MT network.

PDK1-dependent phosphorylation regulates PID subcellular translocation

Previously, the PID kinase was shown to be activated by PDK1 phosphorylation at one or two serines (S288 and S290) in the activation loop of PID (Figure 3A) [17]. In order to test whether this phosphorylation by PDK1 is important for the subcellular translocation of PID, we mutated the *35Spro::PID:CFP* construct so that in the encoded protein both

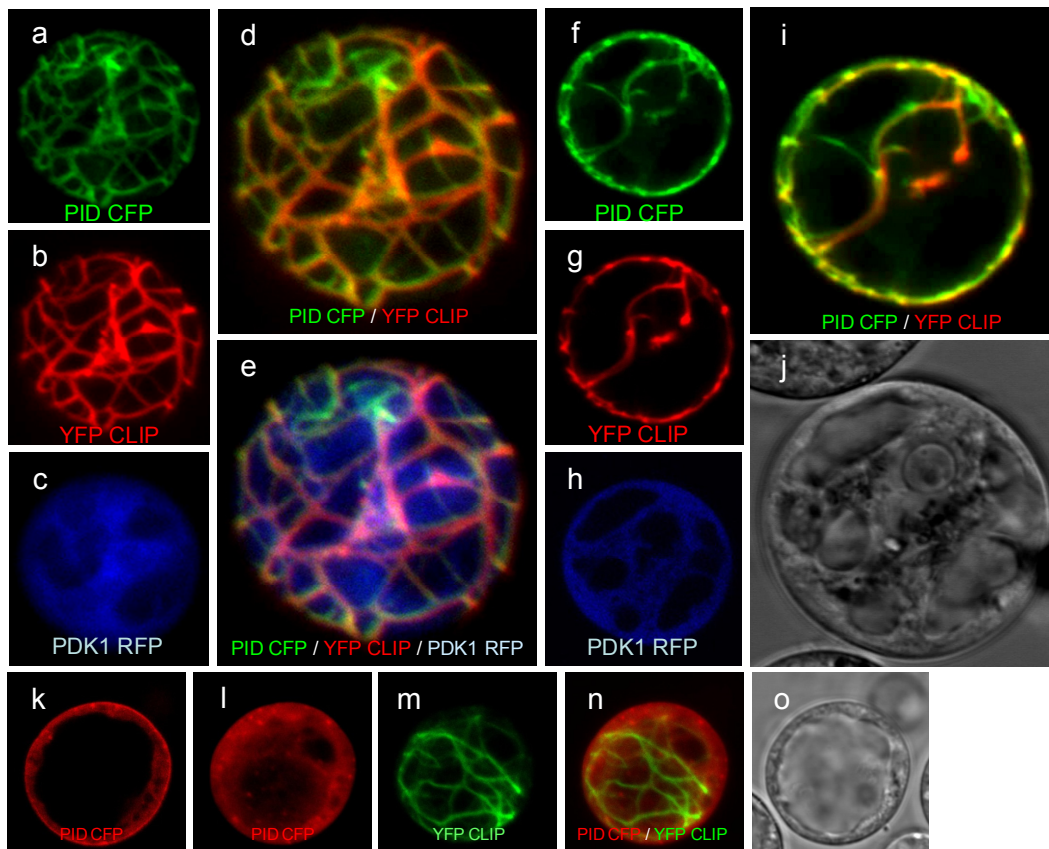


Figure 2. PDK1-dependent microtubule localization of PID in protoplasts.

(a-j) Representative protoplast co-expressing PID:CFP (a and f, green), YFP:CLIP170¹⁻¹²⁴⁰ (b and g, red) and PDK1:mRFP1 (c-e, blue). Confocal projection (a-e) and single middle confocal image (f-j) of a protoplast labelled with the cortical or transcytoplasmic microtubules, respectively. Merged projection of two (d and i, green and red) or three (e, green, red and blue) channels as indicated.

(k-o) Protoplast co-expressing PID:CFP and YFP:CLIP170¹⁻¹²⁴⁰. Confocal section of the protoplast showing plasma membrane and cytoplasmic localization of PID:CFP (k, red). Confocal projection of the same protoplast showing PID:CFP (l, red) and YFP:CLIP170¹⁻¹²⁴⁰ microtubule (m, green) localisation. The merged image (n) shows that PID does not localize to the microtubules. Transmitted light image (o).

serines were substituted by alanine (PID^{SA}:CFP) or by glutamic acid (PID^{SE}:CFP) to prevent or mimic phosphorylation by PDK1, respectively. The wild type and mutant *PID:CFP* constructs were transfected either alone or together with *PDK1:YFP*. Remarkably, in these experiments PID:CFP either localized at the plasma membrane, at endomembranes or at MT (Figure 3d), and mixed localisation patterns were not observed. This allowed to quantify the data by categorizing the localisation for at least 40 individual

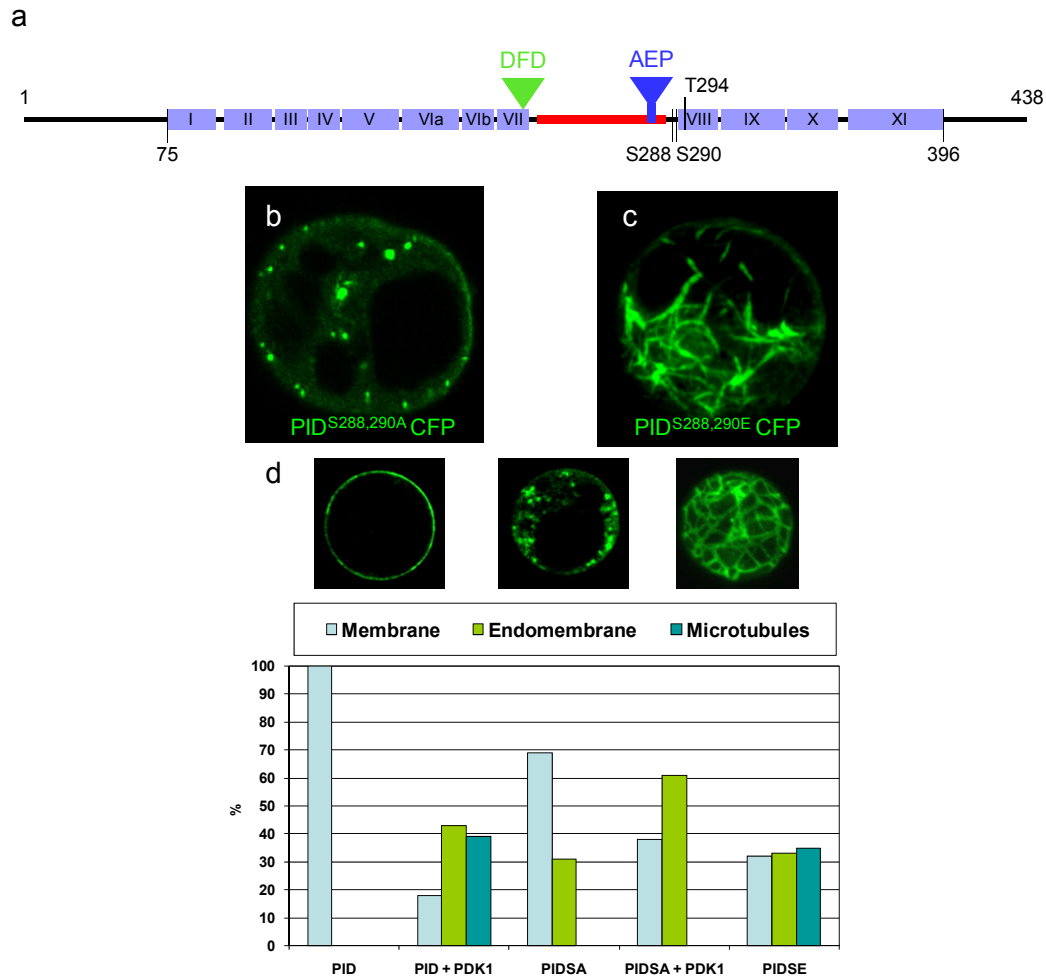


Figure 3. Subcellular localization of PID is dependent on its PDK1-dependent phosphorylation state.

(a) Schematic representation of PID domain organization. The eleven conserved subdomains of the serine/threonine protein kinase domain (75-396 aa) are depicted with purple boxes. The insertion in the activation loop typical for the plant specific AGCVIII kinases is shown in red. The conserved Asp-Phe-Asp (DFD) and Ala-Glu-Pro (AEP) motif in the activation loop are depicted in green and blue, respectively. The positions of the putative PDK1 phosphorylation sites in the activation loop of PID are indicated (S288, S290 and T294).

(b) Endomembrane internalization of the loss-of-phosphorylation PID^{S288, S290A}:CFP (PID^{SA}) version.

(c) PDK1-independent microtubule localization of the phosphomimic PID^{S288, S290E}:CFP (PID^{SE}) version.

(d) Quantitative analysis of PDK1-dependent PID translocation. Transfected protoplast were counted and categorized according to the subcellular localization of PID:CFP: protoplast with membrane localization (upper left panel), endomembrane localization (upper middle panel) or microtubule localization (upper right panel). Percentage of the transfected protoplast with the indicated constructs (lower panel). Number of protoplasts scored: PID ($n=83$), PID+PDK1 ($n=142$), PIDSA ($n=173$), PIDSA+PDK1 ($n=97$) and PIDSE ($n=40$).

protoplasts (Figure 3d). PID:CFP expressed alone only showed plasma membrane localisation, and co-transfection with *PDK1:YFP* resulted in endomembrane and MT localisation in 43 % and 39 % of the protoplasts, respectively (Figure 3d). In a similar way, the phosphomimick PID^{SE}:CFP version localized to both microtubules and endomembranes (33% and 35%, respectively), even when no PDK1 was co-transfected (Figure 3c), suggesting that the PID phosphorylation status itself affects subcellular translocation. Interestingly, when the non-phosphorylatable PID^{SA}:CFP fusion protein was expressed alone, we only observed internalization to endomembrane-like structures (31% of the expressing protoplasts, Figure 3b and d) and this percentage was enhanced up to 61% when PDK1 was cotransfected (Figure 3d). These results show that phosphorylation of PID by PDK1 acts as a trigger not only to activate but also to translocate PID to different subcellular compartments. Phosphorylation of S288 and S290 seems to be essential for MT localisation of PID, but is not required for the PDK1-induced PID localisation at endomembrane structures.

Osmotic shock triggers PID translocation in *Arabidopsis* roots

Our observations suggest that PDK1 might play an important role in the regulation of PID action through regulation of its subcellular location. However, in other expression systems, PID has mostly been found to localize to the PM, raising the question whether our observations are an artifact of the protoplast system. Therefore, we closely investigated PID subcellular location in a plant line expressing a PID:VENUS fusion under control of its endogenous promoter (*PIDpro::PID:VENUS*). Previous analysis of this line has shown that PID is expressed in epidermis cells of the root meristem, and that in these cells, under control conditions PID:VENUS mainly localized at the PM, but that some cytoplasmic signal can be observed [16]. (Figure 4a, upper and lower panel) [16;27]. Since PDK1 is known to be activated by PA and PIP₂, we decided to study PID subcellular localization in response to a stress condition that induces *de novo* synthesis of these lipids [20;28;29]. In particular, osmotic shock has been shown to greatly induce the production of both PA and PIP₂ in *Arabidopsis* [30;31]. When plants were transferred to medium containing 350mM NaCl to induce an osmotic shock, cells lost turgor and plasmolyzed (Figure 4b and c). Interestingly, under these conditions PID:VENUS was

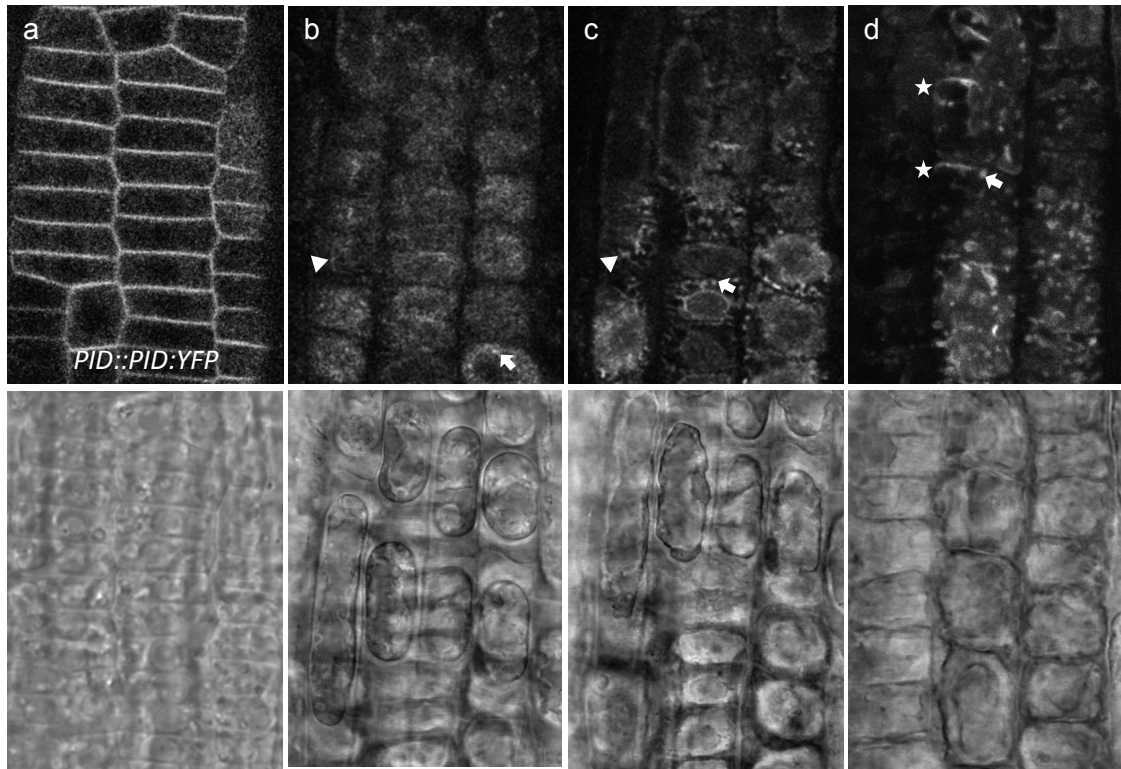


Figure 4. PID localization dynamics during osmotic shock in roots.

(a-d) Confocal projections showing the subcellular localization of *PIDpro::PID:VENUS* in the epidermal cell layer at the transition zone. Confocal projection (upper panels) and respective transmitted light sections (lower panels).

(a) *PID:VENUS* localizes in the PM in MS control conditions.

(b) Immediately after 5 min of osmotic shock (350 mM NaCl in MS) cells plasmolyse (lower panel) and *PID:VENUS* is recruited to filament-like structures (arrowheads) and endomembrane compartments (arrows). (c) Confocal projections after 20 min of osmotic shock. Filament-like structures (arrowheads) and endomembrane compartments (arrows) are indicated.

(d) After 120 min epidermal cells recover their turgor and *PID:VENUS* start to appear at the apical PM (stars).

completely released from the PM and was recruited to endomembrane structures (Figure 4b and c, arrows) and filamentous structures that resemble the cytoskeleton (Figure 4b and c, arrow heads), similar to our observations in protoplasts (Figure 1e-o). Approximately two to three hours after the start of the treatment, the root cells recover turgor, and *PID:VENUS* was slowly recruited back to the apical side of the PM (Figure 4d, stars). Importantly, root growth was re-initiated after this time (data not shown), indicating that the osmotic shock was not lethal to the roots. Thus, PID translocation to

internal cellular structures is not limited to the protoplast system, but also occurs in *Arabidopsis* roots. Moreover, these results point towards a possible biological relevance for the PDK1-dependent regulation of PID, in which osmotic stress might activate PDK1, possibly via synthesis of lipid second messengers, which in turn recruit PID into endomembrane compartments and MT in order to re-establish cell polarity and redirect root growth.

Discussion

The capability of plants to adapt to their changing environment by modulating their growth has fascinated scientists for decades. The phenomenon implies that growth and certain developmental programmes are subjected to the regulation of different signal transduction pathways that constantly monitor biotic and abiotic stimuli. On the one hand, polar auxin transport regulates plant growth and development by generating maxima and minima at different parts of the plant body. This cell-to-cell transport requires a coordinated establishment of polarity within the neighbouring cells necessary for the maintenance of directionality of auxin flow. On the other hand, it is well known that biotic and abiotic stimuli direct plant growth, of which the best known examples are light (phototropism, shade avoidance) and gravity (gravitropism) (reviewed in [1;32-36]). The combination of multiple signal transduction pathways triggered by environmental stimuli cause local changes in auxin distribution necessary for the reorientation or reprogramming of developmental and growth processes. How do these complex signal transduction cascades interconnect? And how do different combinations of stimuli affect auxin distribution through the modulation of polar auxin transport? It is likely that stress responses act upstream of essential components of auxin-mediated growth, such as PID. Here we investigated the effect of an upstream regulator of PID, PDK1, which phosphorylates and regulates PID kinase activity. Our results show that PDK1 regulates PID subcellular localization through differential phosphorylation. We propose a model for the PDK1-dependent regulation of PID, in which phospholipid signalling and protein phosphorylation plays a central role in regulating activity and place of action of PID.

New insights into PDK1-dependent regulation of AGC kinases

Regulation of protein kinases by phosphorylation is a common and evolutionary conserved mechanism in many organisms. In eukaryotes, PDK1 signalling plays a central role in the regulation of diverse metabolic processes, apoptosis, cell division, protein synthesis, and stress responses [19;29]. PDK1 is upstream of many AGC kinases, and regulates their activity by phosphorylation of a conserved ser/thr at the activation loop, also known as the T-loop [19;29]. In plants, the AGCVIII subfamily represents orthologs of the animal PKA/PKC/PKB, and despite the difference in regulatory accessory domains, the way of regulation by PDK1 activation is similar [17;21;24;29]. In fact, the majority of the *Arabidopsis* AGVIII kinases are activated by PDK1 phosphorylation [17;21;24]. Based on what was known from PDK1 phosphorylation of the activation loop in animal kinases and *in vitro* data, PDK1 phosphorylation likely occurs at S288 and/or S290. Replacement of these residues by the phosphomimic glutamic acid resulted in enhanced PID autophosphorylation [17;51]. In addition, T294 has been implicated as putative PDK1 phosphorylation sites in PID, however replacement of this threonine by glutamic acid abolished autophosphorylation, suggesting that this threonine might also be the site of auto-phosphorylation [51]. Of the three putative PDK1 targets (S288, S290 and T294, Figure 3) only S290 and T294 are present in all plant AGC kinases, including the AGCVI subfamily represented by the *p70 ribosomal S6 kinase (S6K)*, AGCVII which are homologues of the *nuclear Dbf2-related kinase (NDR)*, and the AGC Other subfamily that comprises the *incomplete root hair elongation kinases (IRE)* [29]. Interestingly, only S6 and AGCVIII kinases, for which PDK1-dependent activation has been demonstrated, contain a third putative phosphorylation site (S288) [17;23;24;29]. Whether all three sites are phosphorylated by PDK1 and required for PID activation and translocation needs further investigation. For now our data indicate clearly that PDK1 phosphorylation of S288 and/or S290 is crucial for MT localisation, and not for endomembrane-localisation of PID. However, the fact that PID localisation in protoplasts can be clearly categorized into three distinct classes, and that PID^{SE}:CFP still shows PM localisation in 30% of the protoplasts suggests that PID phosphorylation by PDK1 is not the only determinant, and that PID localisation is also dependent on other cell-type specific components.

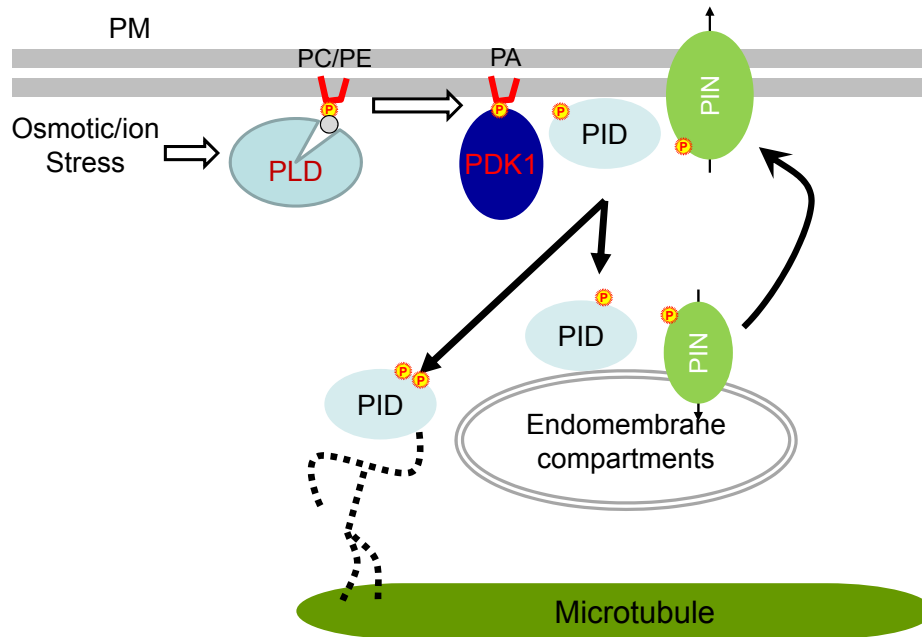


Figure 5. Proposed model for PDK1-dependent regulation of PID. Osmotic stress treatment induced activation of PLD leads to the formation of phosphatidic acid, which in turn leads to the recruitment and activation of PDK1 at the plasma membrane. Here, PDK1 phosphorylates PID, which is then recruited to endomembrane compartments or microtubules (MT), depending on the phosphorylation status. Possibly a protein complex composed of scaffold proteins and microtubule motors are involved in localization of PID at the MT (dashed lines).

Moreover, the enhanced endomembrane localisation of PID^{SA}:CFP in the presence of PDK1 suggests that this process is triggered by phosphorylation of one or more other residues (possibly T294) by PDK1. Our data provide an important extension of the existing paradigm that PDK1 phosphorylation only leads to activation of the plant AGCVIII kinases [17;21;24].

The PDK1-dependent recruitment of PID into endomembrane compartments and microtubules (Figure 1 and 2), suggests that upon activation by phosphorylation, PID is re-directed in subcellular locations where phosphorylation is required. Possibly, PID phosphorylates PIN proteins at the endomembrane compartments to target them for apical endocytic sorting (Figure 5). Whether the observed PID-labelled endomembrane compartments correspond with PIN loaded vesicles still needs to be determined. Furthermore, PID might also regulate the machinery that sort and transport PIN loaded

cargos through the microtubule network. Although there is controversial data on the involvement of microtubules in the transport of PIN endocytic cargos, there is evidence that point towards MTs being necessary for intracellular trafficking of PIN proteins and the establishment of cell polarity [37;38].

Several of the plant AGCVIII kinases are membrane localized [25;27;39], and at least for PID it has been shown that it binds phospholipids. Possibly, phosphorylation of the activation loop might change the affinity towards these phospholipids, and thus allow PID to be released from the membrane, or to be recruited to endosomal membrane compartments. Another possibility is that phosphorylation changes the binding affinity for other regulatory protein necessary for the relocation of PID (Figure 5). This implies that the MT localization of PID might be regulated by a protein complex. Interestingly PID interacts with a plant specific scaffold protein BT1 (BTB AND TAZ DOMAIN), which belongs to the BT protein family. Other members of this includes NPH3-like proteins (NON-PHOTOTROPIC HYPOCOTYL3) implicated in the regulation of phototropism and polar auxin transport and organogenesis [40-44]. Moreover, BT1 interacts with a kinesin related protein establishing a possible link of PINOID signalling and MT network (Figure 5) [45]. Further research is necessary to answer these hypotheses. In conclusion, PDK1 plays a central role in regulating PID action, where phosphorylation acts as a trigger to activate and translocate PID to different subcellular compartments.

Lipid signalling and polar auxin transport

Our results in *Arabidopsis* roots provide a model for the study of cell polarity and a possible biological relevance for the PDK1-dependent regulation of PID (Figure 4). Osmotic stress induces the activation different signalling pathways that rely in the production of secondary messengers that activate and control the action of different proteins [46]. In particular, the production of PA controlled by phospholipase D (PLD) [30], could be necessary for the activation and recruitment of PDK1 at the PM (Figure 5) [20;28]. Interestingly, recently PLD ζ 2 has been implicated in the regulation of cycling of PIN2. A *pld ζ 2 loss-of-function* mutant was found to be more resistant to the vesicle trafficking inhibitor brefeldin A (BFA), suggesting that PLD ζ 2 is required for

endocytosis of PIN proteins. On the other hand, PLD-regulated PA levels might have an effect in the activity or subcellular localization of key components of PAT, such as PID or RCN1, both which bind PA [24;47]. Surprisingly, PID:VENUS seems to be recruited primarily to the apical side of the PM at the epidermal cell layer (Figure 4d, stars), suggesting that after the loss of polarity due the plasmolysis there is a still unknown signal that predetermines PID subcellular localization. In conclusion, our results show that PDK1-dependent regulation plays a central role in regulating activity and place of action of PID.

Material and methods

Molecular cloning and constructs

Molecular cloning was performed following standard procedures [48]. PCR primers used in this study are listed in Table 1. Bacteria were grown on LC medium containing 100 µg/ml carbenicillin (Cb) for *E. coli* strains DH5α or DB3.1. The construct *pSK YFP:CLIP170* were described previously [26]. *pAS PDK1* was kindly provided by Dr. Lazlo Bögre. *pART7-PID:CFP*, *pART7-PID:YFP*, *pART7-PDK1:CFP*, *pART7-PDK1:mRFP*, and *pART7-YFP:CLIP170¹⁻¹²⁴⁰* fusions were constructed using the Gateway Technology (Invitrogen). Destination vectors used in this study were constructed by introducing the Gateway recombination cassette (Invitrogen) frame with YFP, CFP or mRFP1 between the *CaMV 35S* promoter and the *CaMV 35S* terminator of the *pART7* vector. Genes of interest were amplified by PCR with primers containing *attB* recombination sites (see table 1) from *Arabidopsis thaliana* ecotype Columbia (Col-0) cDNA from siliques using primer set PID attB1 F - PID attB2 R for *PID*, from *pAS PDK1* using the primer set PDK1 attB1F - PDK1 attB2 R for *PDK1*, and from *pSK YFP:CLIP170* using the primer set YFP attB1 F - CLIP170¹⁻¹²⁴⁰ attB2 R for the N terminal region of CLIP170 (1-1240 aminoacids). BP reactions were performed in *pDONR207* according to manufacturer's protocol (Invitrogen). Recombinant plasmids were isolated and sequenced. LR reactions were performed in the *pART7*-derived destination plasmids described above. Specific base pair substitutions were introduced using the QuikChange XL Site-directed Mutagenesis kit (Stratagene). Reactions were

performed using *pDONR PID* as a template and the primer sets PID SS288,290AA F - PID SS288,290AA R and PID SS288,290EE F - PID SS288,290EE R, respectively, according to manufacturer's protocol.

Table 1: Primer list

PID attB1 F	5'GGGG <u>ACAAGTTTGTACAAAAAAGCAGGCTT</u> CAGCATGTTACGAGAATCAGACGGT3'
PID attB2 R	5'GGGG <u>ACCACTTTGTACAAGAAAGCTGGGTCAAAGTAATCGAACGCCGCTGG</u> 3'
PDK1 attB1 F	5'GGGG <u>ACAAGTTTGTACAAAAAAGCAGGCTTA</u> ATGTTGGCAATGGAGAAAGAA3'
PDK1 attB2 R	5'GGGG <u>ACCACTTTGTACAAGAAAGCTGGGTAG</u> CGGTTCTGAAGAGTCTCGAT3'
YFP attB1 F	5'GGGG <u>ACAAGTTTGTACAAAAAAGCAGGCTTA</u> ATGGTGAGCAAGGGCGAGGAG3'
CLIP170 ¹⁻¹²⁴⁰ attB2 R	5'GGGG <u>ACCACTTTGTACAAGAAAGCTGGGTACTT</u> GAGCTCGAGCTTCACCTTATCA3'
PID SS288,290AA F	5'GGTACTGCCCCGGGCTGGTGCCTTCGTTGGTACGC3'
PID SS288,290AA R	5'GCGTACCAACGAACGCACCAGCCCCGGGCAGTAACC3'
PID SS288,290EE F	5'GGTACTGCCCCGGAAGGTGAGTTCGTTGGTACGC3'
PID SS288,290EE R	5'GCGTACCAACGAACCTACCTTCCCCGGGCAGTAACC3'

attB recombination sites are underlined

Protoplast transfection

Protoplasts were isolated from *Arabidopsis thaliana* Col-0 cell suspension cultures and 10 µg plasmid DNA was introduced by PEG-mediated transfection as described originally by Axelos and co-workers [49] and adapted by Schirawski and co-workers [50]. Following transfection, the protoplasts were incubated for at least 16h. Images were obtained by confocal microscopy.

***Arabidopsis* growth and biological assays**

The *PIDpro::PID:VENUS* line was described previously [16]. *Arabidopsis* seeds were surfaced-sterilized by incubation for 10 min in 50% commercial bleach solution and rinsed five times with sterile water. Seeds were vernalized for 3 days at 4°C and germinated (21°C, 16 h-photoperiod and 42 µmol/m²/s) on solid Murashige and Skoog (MS) medium. Vertically grown five day-old *PIDpro::PID:VENUS* seedlings were treated with 350 mM NaCl in liquid MS medium and visualized under the confocal microscope.

Confocal microscopy

For the protoplast experiments, a Leica DM IRBE confocal laser scanning microscope was used with a 63X water objective, digital zoom and 51% laser intensity. The fluorescence was visualized with an Argon-Krypton lasers for excitation at 457 nm (CFP), 514 nm (YFP) and 568 nm (mRFP) with 475-495 nm, 520-545 nm and 600-640 nm emission filters, respectively. *Arabidopsis PIDpro::PID:VENUS* roots were observed using a 40X oil objective with a Nikon Eclipse confocal microscope. The YFP fluorescence was monitored with a 522-532 nm band pass emission filter (514 nm excitation). The images were processed by ImageJ (<http://rsb.info.nih.gov/ij/>) and assembled in MS PowerPoint.

Accession Numbers

The *Arabidopsis* Genome Initiative locus identifiers for the genes mentioned in this chapter are as follows: *PID* (At2g34650), *PDK1* (At5g04510).

Acknowledgments

The authors thank Marcus Heisler for kindly providing the *PIDpro::PID:VENUS* line and Gerda Lamers and Ward de Winter for their help with respectively microscopy and tissue culture. We thank Pankaj Dhonukshe for the *pSK YFP:CLIP170* clone, and Erik Manders and Ronald Breedijk from the Center for Advance Microscopy (SILS, University of Amsterdam) for their assistance with confocal microscopy. This work received financial aid from the Dutch Organization of Scientific Research (NWO), through grants from the Research Council for Earth and Life Sciences (ALW 813.06.004), NWO-Chemical Sciences (VIDI grant 700.56.429) and from the Netherlands Organisation for Health Research and Development (ZON 050-71-023).

Reference list

1. Muday GK (2001). **Auxins and tropisms**. *J. Plant Growth Regul.* 20(3), 226-243.
2. Sun F, Zhang W, Hu H, Li B, Wang Y, Zhao Y, Li K, Liu M, Li X (2008). **Salt modulates gravity signaling pathway to regulate growth direction of primary roots in *Arabidopsis***. *Plant Physiol.* 146(1), 178-188.
3. Tanaka H, Dhonukshe P, Brewer PB, Friml J (2006). **Spatiotemporal asymmetric auxin distribution: a means to coordinate plant development**. *Cell Mol. Life Sci.* 63(23), 2738-2754.
4. Wisniewska J, Xu J, Seifertová D, Brewer PB, Ruzicka K, Blilou I, Rouquié D, Benková E, Scheres B, Friml J (2006). **Polar PIN localization directs auxin flow in plants**. *Science*. 312(5775), 883.
5. Friml J, Vieten A, Sauer M, Weijers D, Schwarz H, Hamann T, Offringa R, Jurgens G (2003). **Efflux-dependent auxin gradients establish the apical-basal axis of *Arabidopsis***. *Nature*. 426(6963), 147-153.
6. Blilou I, Xu J, Wildwater M, Willemsen V, Paponov I, Friml J, Heidstra R, Aida M, Palme K, Scheres B (2005). **The PIN auxin efflux facilitator network controls growth and patterning in *Arabidopsis* roots**. *Nature*. 433(7021), 39-44.
7. Friml J, Benkova E, Blilou I, Wisniewska J, Hamann T, Ljung K, Woody S, Sandberg G, Scheres B, Jurgens G, Palme K (2002). **AtPIN4 mediates sink-driven auxin gradients and root patterning in *Arabidopsis***. *Cell*. 108(5), 661-673.
8. Reinhardt D, Pesce ER, Stieger P, Mandel T, Baltensperger K, Bennett M, Traas J, Friml J, Kuhlemeier C (2003). **Regulation of phyllotaxis by polar auxin transport**. *Nature*. 426(6964), 255-260.
9. Benková E, Michniewicz M, Sauer M, Teichmann T, Seifertová D, Jürgens G, Friml J (2003). **Local, efflux-dependent auxin gradients as a common module for plant organ formation**. *Cell*. 115(5), 591-602.
10. Friml J, Wisniewska J, Benková E, Mendgen K, Palme K (2002). **Lateral relocation of auxin efflux regulator PIN3 mediates tropism in *Arabidopsis***. *Nature*. 415(6873), 806-809.
11. Muller A, Guan C, Galweiler L, Tanzler P, Huijser P, Marchant A, Parry G, Bennett M, Wisman E, Palme K (1998). **AtPIN2 defines a locus of *Arabidopsis* for root gravitropism control**. *EMBO J.* 17(23), 6903-6911.
12. Mravec J, Skupa P, Bailly A, Hoyerova K, Krecek P, Bielach A, Petrasek J, Zhang J, Gaykova V, Stierhof YD, Dobrev PI, Schwarzerova K, Rolcik J, Seifertova D, Luschnig C, Benkova E, Zazimalova E, Geisler M, Friml J (2009). **Subcellular**

- homeostasis of phytohormone auxin is mediated by the ER-localized PIN5 transporter.** *Nature.* 459(7250), 1136-1140.
13. Dhonukshe P, Tanaka H, Goh T, Ebine K, Mahonen AP, Prasad K, Blilou I, Geldner N, Xu J, Uemura T, Chory J, Ueda T, Nakano A, Scheres B, Friml J (2008). **Generation of cell polarity in plants links endocytosis, auxin distribution and cell fate decisions.** *Nature.* 456(7224), 962-966.
 14. Geldner N, Friml J, Stierhof YD, Jurgens G, Palme K (2001). **Auxin transport inhibitors block PIN1 cycling and vesicle trafficking.** *Nature.* 413(6854), 425-428.
 15. Friml J, Yang X, Michniewicz M, Weijers D, Quint A, Tietz O, Benjamins R, Ouwerkerk PBF, Ljung K, Sandberg G, Hooykaas PJJ, Palme K, Offringa R (2004). **A PINOID-dependent binary switch in apical-basal PIN polar targeting directs auxin efflux.** *Science.* 306(5697), 862-865.
 16. Michniewicz M, Zago MK, Abas L, Weijers D, Schweighofer A, Meskiene I, Heisler MG, Ohno C, Huang F, Weigel D, Meyerowitz EM, Luschnig C, Offringa R, Friml J (2007). **Phosphatase 2A and PID kinase activities antagonistically mediate PIN phosphorylation and apical/basal targeting in *Arabidopsis*.** *Cell.* 130(6), 1044-1056.
 17. Zegzouti H, Anthony RG, Jahchan N, Bogre L, Christensen SK (2006). **Phosphorylation and activation of PINOID by the phospholipid signaling kinase 3-phosphoinositide-dependent protein kinase 1 (PKD1) in *Arabidopsis*.** *Proc. Natl. Acad. Sci. USA.* 103(16), 6404-6409.
 18. Alessi DR, James SR, Downes CP, Holmes AB, Gaffney PR, Reese CB, Cohen P (1997). **Characterization of a 3-phosphoinositide-dependent protein kinase which phosphorylates and activates protein kinase B α .** *Curr. Biol.* 7(4), 261-269.
 19. Mora A, Komander D, van Aalten DM, Alessi DR (2004). **PKD1, the master regulator of AGC kinase signal transduction.** *Semin. Cell Dev. Biol.* 15(2), 161-170.
 20. Deak M, Casamayor A, Currie RA, Downes CP, Alessi DR (1999). **Characterisation of a plant 3-phosphoinositide-dependent protein kinase-1 homologue which contains a pleckstrin homology domain.** *FEBS Lett.* 451(3), 220-226.
 21. Anthony RG, Henriques R, Helfer A, Meszaros T, Rios G, Testerink C, Munnik T, Deak M, Koncz C, Bogre L (2004). **A protein kinase target of a PKD1 signalling pathway is involved in root hair growth in *Arabidopsis*.** *EMBO J.* 23(3), 572-581.

22. Tang Y, McLeod M (2004). **In vivo activation of protein kinase A in *Schizosaccharomyces pombe* requires threonine phosphorylation at its activation loop and is dependent on PDK1.** *Genetics*. 168(4), 1843-1853.
23. Mahfouz MM, Kim S, Delauney AJ, Verma DP (2006). ***Arabidopsis* TARGET OF RAPAMYCIN interacts with RAPTOR, which regulates the activity of S6 kinase in response to osmotic stress signals.** *Plant Cell*. 18(2), 477-490.
24. Zegzouti H, Li W, Lorenz TC, Xie M, Payne CT, Smith K, Glenny S, Payne GS, Christensen SK (2006). **Structural and functional insights into the regulation of *Arabidopsis* AGC VIIIa kinases.** *J. Biol. Chem.* 281(46), 35520-35530.
25. Galvan-Ampudia CS, Offringa R (2007). **Plant evolution: AGC kinases tell the auxin tale.** *Trends Plant Sci.* 12(12), 541-547.
26. Dhonukshe P, Gadella TWJ (2003). **Alteration of Microtubule Dynamic Instability during Preprophase Band Formation Revealed by Yellow Fluorescent Protein-CLIP170 Microtubule Plus-End Labeling.** *Plant Cell*. 15(3), 597-611.
27. Lee SH, Cho HT (2006). **PINOID Positively Regulates Auxin Efflux in *Arabidopsis* Root Hair Cells and Tobacco Cells.** *Plant Cell*. 18(7), 1604-1616.
28. Anthony RG, Khan S, Costa J, Pais MS, Bogre L (2006). **The *Arabidopsis* protein kinase PTI1-2 is activated by convergent phosphatidic acid and oxidative stress signaling pathways downstream of PDK1 and OXI1.** *J. Biol. Chem.* 281(49), 37536-37546.
29. Bogre L, Okresz L, Henriques R, Anthony RG (2003). **Growth signalling pathways in *Arabidopsis* and the AGC protein kinases.** *Trends Plant Sci.* 8(9), 424-431.
30. Bargmann BO, Laxalt AM, ter RB, van SB, Merquiol E, Testerink C, Haring MA, Bartels D, Munnik T (2009). **Multiple PLDs required for high salinity and water deficit tolerance in plants.** *Plant Cell Physiol.* 50(1), 78-89.
31. Testerink C, Munnik T (2005). **Phosphatidic acid: a multifunctional stress signaling lipid in plants.** *Trends Plant Sci.* 10(8), 368-375.
32. Alabadi D, Blazquez MA (2009). **Molecular interactions between light and hormone signaling to control plant growth.** *Plant Mol. Biol.* 69(4), 409-417.
33. Chehab EW, Eich E, Braam J (2009). **Thigmomorphogenesis: a complex plant response to mechano-stimulation.** *J. Exp. Bot.* 60(1), 43-56.
34. Christie JM (2007). **Phototropin blue-light receptors.** *Annu. Rev. Plant Biol.* 58:21-45., 21-45.

35. Gilroy S (2008). **Plant tropisms.** *Curr. Biol.* 18(7), R275-R277.
36. Takahashi H, Miyazawa Y, Fujii N (2009). **Hormonal interactions during root tropic growth: hydrotropism versus gravitropism.** *Plant Mol. Biol.* 69(4), 489-502.
37. Boutte Y, Crosnier MT, Carraro N, Traas J, Satiat-Jeunemaitre B (2006). **The plasma membrane recycling pathway and cell polarity in plants: studies on PIN proteins.** *J. Cell Sci.* 119(Pt 7), 1255-1265.
38. Kleine-Vehn J, Langowski L, Wisniewska J, Dhonukshe P, Brewer PB, Friml J (2008). **Cellular and Molecular Requirements for Polar PIN Targeting and Transcytosis in Plants.** *Molecular Plant.* 1(6), 1056-1066.
39. Zourelidou M, Muller I, Willige BC, Nill C, Jikumaru Y, Li H, Schwechheimer C (2009). **The polarly localized D6 PROTEIN KINASE is required for efficient auxin transport in *Arabidopsis thaliana*.** *Development.* 136(4), 627-636.
40. Cheng Y, Qin G, Dai X, Zhao Y (2007). **NPY1, a BTB-NPH3-like protein, plays a critical role in auxin-regulated organogenesis in *Arabidopsis*.** *Proc. Natl. Acad. Sci. USA.* 20;104(47), 18825-18829.
41. Furutani M, Kajiwarra T, Kato T, Trembl BS, Stockum C, Torres-Ruiz RA, Tasaka M (2007). **The gene *MACCHI-BOU 4/ENHANCER OF PINOID* encodes a NPH3-like protein and reveals similarities between organogenesis and phototropism at the molecular level.** *Development.* 134(21), 3849-3859.
42. Robert HS (2008). **Calcium- and BTB domain protein-modulated PINOID kinase directs polar auxin transport.** Institute of Biology, Leiden University, The Netherlands.
43. Robert HS, Quint A, Brand D, Vivian-Smith A, Offringa R (2008). **BTB AND TAZ DOMAIN scaffold proteins perform a crucial function in *Arabidopsis* development.** *Plant J.*
44. Motchoulski A, Liscum E (1999). ***Arabidopsis* NPH3: A NPH1 photoreceptor-interacting protein essential for phototropism.** *Science.* 286(5441), 961-964.
45. Zago MK (2006). **Components and targets of the PINOID signaling complex in *Arabidopsis thaliana*.** Leiden University. 2006.
46. Mahajan S, Pandey GK, Tuteja N (2008). **Calcium- and salt-stress signaling in plants: shedding light on SOS pathway.** *Arch. Biochem. Biophys.* 471(2), 146-158.
47. Testerink C, Dekker HL, Lim ZY, Johns MK, Holmes AB, Koster CG, Ktistakis NT, Munnik T (2004). **Isolation and identification of phosphatidic acid targets from plants.** *Plant J.* 39(4), 527-536.

48. Sambrook J, Fritsch F., Maniatis T. (1989) **Molecular cloning - A laboratory Manual**. Edited by C.Nolan. Cold Spring Harbor Laboratory press, NY, USA.
49. Axelos M, Curie C, Mazzolini L, Bardet C, Lescure B (1992). **A Protocol for Transient Gene-Expression in *Arabidopsis thaliana* Protoplasts Isolated from Cell-Suspension Cultures**. *Plant Physiology and Biochemistry*. 30(1), 123-128.
50. Schirawski J, Planchais S, Haenni AL (2000). **An improved protocol for the preparation of protoplasts from an established *Arabidopsis thaliana* cell suspension culture and infection with RNA of turnip yellow mosaic tymovirus: a simple and reliable method**. *Journal of Virological Methods*. 86(1), 85-94.
51. Christensen SK, Dagenais N, Chory J, Weigel D (2000). **Regulation of auxin response by the protein kinase PINOID**. *Cell*. 100(4), 469-478.

CHAPTER 5

AGC3 kinases orient plant development by directing PIN polar targeting

Carlos S. Galván-Ampudia, Jürgen Kleine-Vehn, Fang Huang, Ab Quint, Arnoud van Marion, Michiel Dam, Jiri Friml and Remko Offringa

Summary

The PINOID (*PID*) protein serine/threonine kinase has been identified as a key component in the regulation of plant development. It directs polar transport of the plant hormone auxin by instructing apical polar targeting of PIN auxin efflux carriers through phosphorylation of the large central PIN hydrophilic loop. Nonetheless, *pid* loss of function only triggers a clear apical-to-basal polarity shift of PIN1 in the epidermis of the inflorescences meristem, leading to needle shaped inflorescences that are still capable of organ formation. Also the three cotyledon phenotype that is typical for *pid* mutants is only partially penetrant, even in the strong alleles, suggesting that other redundantly acting kinases may compensate for the loss of *PID* function. *PID* belongs to the plant specific family of AGCVIII kinases, where it groups into the AGC3 clade with three other kinases, named *WAG1*, *WAG2* and *AGC3-4*. Here we investigated the possible role of these other AGC3 kinases in determining PIN polarity. We show that all AGC3 kinases are membrane-associated proteins that phosphorylate the hydrophilic loop of PIN proteins. Double loss-of-function *pid/wag* mutants show stronger pleiotropic defects during embryo and inflorescence development than the *pid* mutant, whereas the triple loss-of-function *pid/wag1/wag2* mutant develops embryos without cotyledons, agravitropic roots, hypocotyls with reduced phototropic response, and strong defects in leaf morphology and a single pin-like inflorescence. Moreover, overexpression of *WAG1* and *WAG2*, like that of *PID*, induces agravitropic growth of young seedlings and collapse of the primary root meristem. The developmental defects of the loss- and gain-of-function mutants correlate with defects in apical PIN polarity, indicating that *WAG1* and *WAG2* function redundantly with *PID* in instructing apical targeting of PIN proteins. A promoter-swap complementation experiment shows, however, that the AGC3 protein kinases are not completely functionally redundant, and that depending on the tissue they act together or in parallel to orient plant development by instructing PIN polarity.

Introduction

Plants growth and development is directed and regulated by many different signaling molecules, and of all these compounds, auxin - or indole-3-acetic acid (IAA) is known to play the most central role. It directs cell division, -growth and -differentiation through polar auxin transport (PAT) generated auxin maxima and minima [1-7]. PAT is mediated in part through the action of the PIN-FORMED (PIN) transmembrane auxin efflux transporters, that determine the direction of transport through their asymmetric subcellular localisation [7-10] Wisniewska. In *Arabidopsis*, the *PIN* gene family is composed of eight members that act both independently and coordinately to regulate a plethora of developmental programs. PIN1 is necessary during embryo patterning and development, and the initiation and development of lateral organs [1;2;5;11]. PIN2 is expressed in the root at the epidermis and cortex cell layers and controls root growth and gravitropism [12;13]. PIN3 is involved in the regulation of gravi- and phototropism [14], while PIN4 and PIN7 are essential for embryo patterning [15;16]. The differential, partially overlapping expression patterns of the *PIN* gene family members and their subcellular polar localization are essential to generate the dynamic auxin maxima and minima that are necessary for plant tissue patterning and growth [7].

The subcellular distribution of PIN efflux carriers is dependent on their primary amino acid sequence and on the presence of cellular components that direct their (polar) targeting to the plasma membrane [10]. Previously, we have identified the PINOID (PID) protein serine/threonine kinase as a regulator of PAT [17], and more recently we have shown that PID is a membrane-associated kinase that directs targeting of PIN proteins to the apical (shoot facing) side of the plasma membrane by phosphorylating these PIN proteins in their large central hydrophilic loop (HL) [18;19].

The phenotypes of the *pid* loss-of-function mutants correlate with the tissues where *PID* is expressed, and where PIN proteins show apical localisation [17;18]. However, pin-like inflorescences of the *pid* mutant are not completely defective in organ initiation, even though PIN1 shows basal localisation. Moreover, even in strong *pid* alleles the three cotyledon phenotype is not fully penetrant, and roots are only weakly agravitropic, correlating with the fact that no clear changes in PIN polarity can be detected in these tissues [18;20;21]. In view of the key role for PID in PIN polar

targeting, these observations strongly suggests that there are other protein kinases that act redundantly with PID in establishing PIN polarity.

PID belongs to the plant-specific family of ACGVIII kinases, where it groups together with three other kinases in the AGC3 subfamily (see Chapter 1). *WAG1* and *WAG2* have been initially found through transcripts induced by auxin application and repressed upon exposure to light in etiolated seedlings [22;23]. Moreover, *WAG1* is expressed very weakly in petioles of the first true leaves, and abundantly in root tips and lateral root primordia [23]. *WAG2* is more abundantly expressed in the same tissues as *WAG1* [23]. *Arabidopsis* loss-of-function single mutants result in weak root waving phenotype, but double mutants show a constitutive root waving in vertically grown seedlings, and root curling is more resistant to the PAT inhibitor 1-naphthylphthalamic acid (NPA), indicating that WAG protein kinases act redundantly in the regulation of root waving [23]. Root growth is a highly complex mechanism which is the result of the interaction between gravitropism, thigmotropism and circumnutation [24-26]. Interestingly, *wag* mutants respond normally to gravity stimulation, indicating that they are involved in root growth, possibly through the regulation of PAT [23;27]. Recently, Cheng and coworkers have reported that all four AGC3 kinases are expressed in *Arabidopsis* embryos, and that accordingly *pid/wag1/wag2/agc3-4* quadruple loss-of-function mutants show failure in cotyledon initiation and development during embryogenesis [28].

In this chapter we addressed the question whether the other three AGC3 kinases are involved in PIN polar targeting, and whether they act redundantly or differently to PID. We show that all four AGC3 kinases are plasma membrane associated proteins and are able to phosphorylate the hydrophilic loop of PIN proteins. Furthermore, we show that multiple combinations of double and triple loss-of-function mutants have strong and different pleiotropic defects in plant development. Most important, such developmental defects correlate with changes in PIN polarity in different stages of development. Gene complementation experiments show that AGC3 kinases have partial overlapping functions during plant development, however we also present evidence that *WAG2* and *AGC3-4* act in parallel pathways PID and *WAG1*. Consistently, we show that *WAGs* control the early events of phototropism, probably through the regulation of PAT. Our

results provide compelling data that AGC3 kinases are partially redundant in regulating PIN polarity through direct phosphorylation and that are essential in the regulation of PAT through plant development and growth.

Results

AGC3 kinases are membrane associated and phosphorylate PIN proteins *in vitro*

PID is a membrane-associated protein kinase that shows an overlapping subcellular localization with its PIN phosphorylation targets [19]. To obtain a first indication whether the other three AGC3 kinases would be involved in regulating PIN polarity, we tested their subcellular localization, and checked whether they were able to phosphorylate the PINHL *in vitro*.

Transformation of *Arabidopsis* protoplasts with *35Spro::kinase:CFP* constructs showed that all four AGC3 kinases are membrane-associated (Figure 1 a-d). In addition, WAG1, WAG2 and AGC3-4 also localized to the nucleus, where AGC3-4:CFP showed a very specific (spotty) localisation. (Figure 1 b-d). Furthermore, in *in vitro* phosphorylation assays using bacterial expressed proteins all four AGC3 kinases were able to phosphorylate the PIN2HL. Interestingly, WAG2 showed a higher autophosphorylation and PIN2HL phosphorylation activity compared to the other three kinases (Figure 1e). These results make it more likely that all four AGC3 kinases are involved in regulating PIN polarity through direct phosphorylation of the PINHL. However, recent analysis of the D6PK clade of the AGC1 subfamily of kinases (AGC1-1/PK64, AGC1-2, PK5 and PK7) has shown that these kinases are also membrane localized and that they phosphorylate the PIN1HL *in vitro* and *in vivo*. Although analysis of loss- and gain-of-function mutant lines provided evidence for a role of these kinases in regulating PAT, no indications were obtained that these kinases direct PIN polar targeting [29]. We therefore set out to analyse loss- and gain-of function lines, and since we were not able to obtain a homozygous loss-of-function line or an overexpression line for AGC3-4, this analysis focused on the WAG1 and WAG2 kinases.

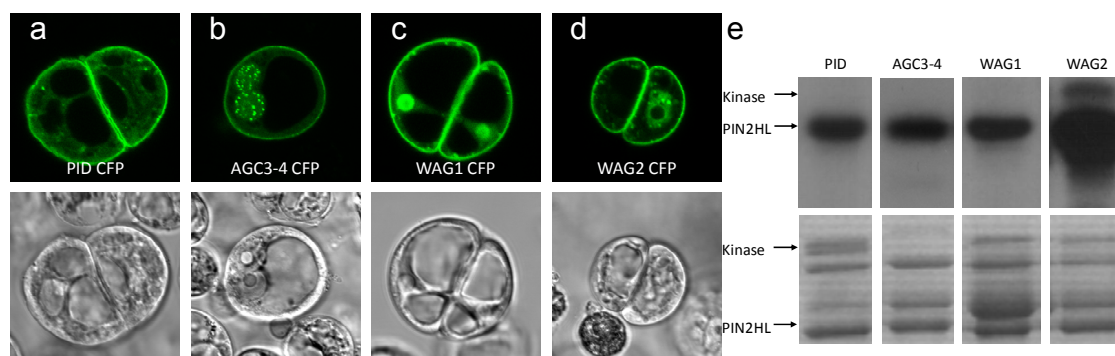


Figure 1 AGC3 kinases are membrane-associated and phosphorylate the PIN2HL *in vitro*.

(a-d) Cells suspension derived protoplast expressing translational fusions of the AGC kinases with CFP.

(e) *In vitro* phosphorylation of the PIN2HL by the AGC3 kinases. Autoradiogram (upper panel) and coomassie stained gel (lower panel).

***PID* and *WAG* protein kinases act redundantly throughout plant development**

As shown previously by Santner and Watson [23], single or double *wag1* and *wag2* T-DNA insertion mutants (SALK) showed no effect on embryo development (Figure 1e), whereas 47% of the seedlings homozygous for the *pid-14* allele that was used in our studies developed three cotyledons, consistent with previous observations for other strong *pid* alleles (Figure 2a and e)[18;30-32]. In the *pid-14/wag1* or *pid-14/wag2* double mutant background, the penetrance of cotyledon defects remained about 50%, but a significant number of seedlings developed only one cotyledon or even lacked cotyledons (Figure 2b-e). Interestingly, *pid-14/wag2* had a stronger effect on embryo development with respectively 14% and 23% mono- and no-cotyledon seedlings, versus respectively 1% and 4% for *pid-14/wag1* (Figure 2b and e). Among progeny of a *pid-14+/wag1/wag2* plants all of the genotyped *pid-14/wag1/wag2* triple mutant seedlings completely lacked cotyledons (Figure 2c-e), whereas the *pid-14+/wag1/wag2* or *wag1/wag2* seedlings developed two cotyledons (data not shown). The complete lack of cotyledons is a phenotypic characteristic of *pid/pin1* double loss-of-function mutants [32]. Our results indicate that the *PID* and *WAG* genes act redundantly, and that their action is essential for proper initiation and development of cotyledons during embryogenesis.

The overlapping expression patterns of the *PID* and *WAG* genes in the root tip [17;19;23] suggest that the three genes might also act redundantly in regulating root growth and development. We established transgenic lines expressing *WAG* genes fused to

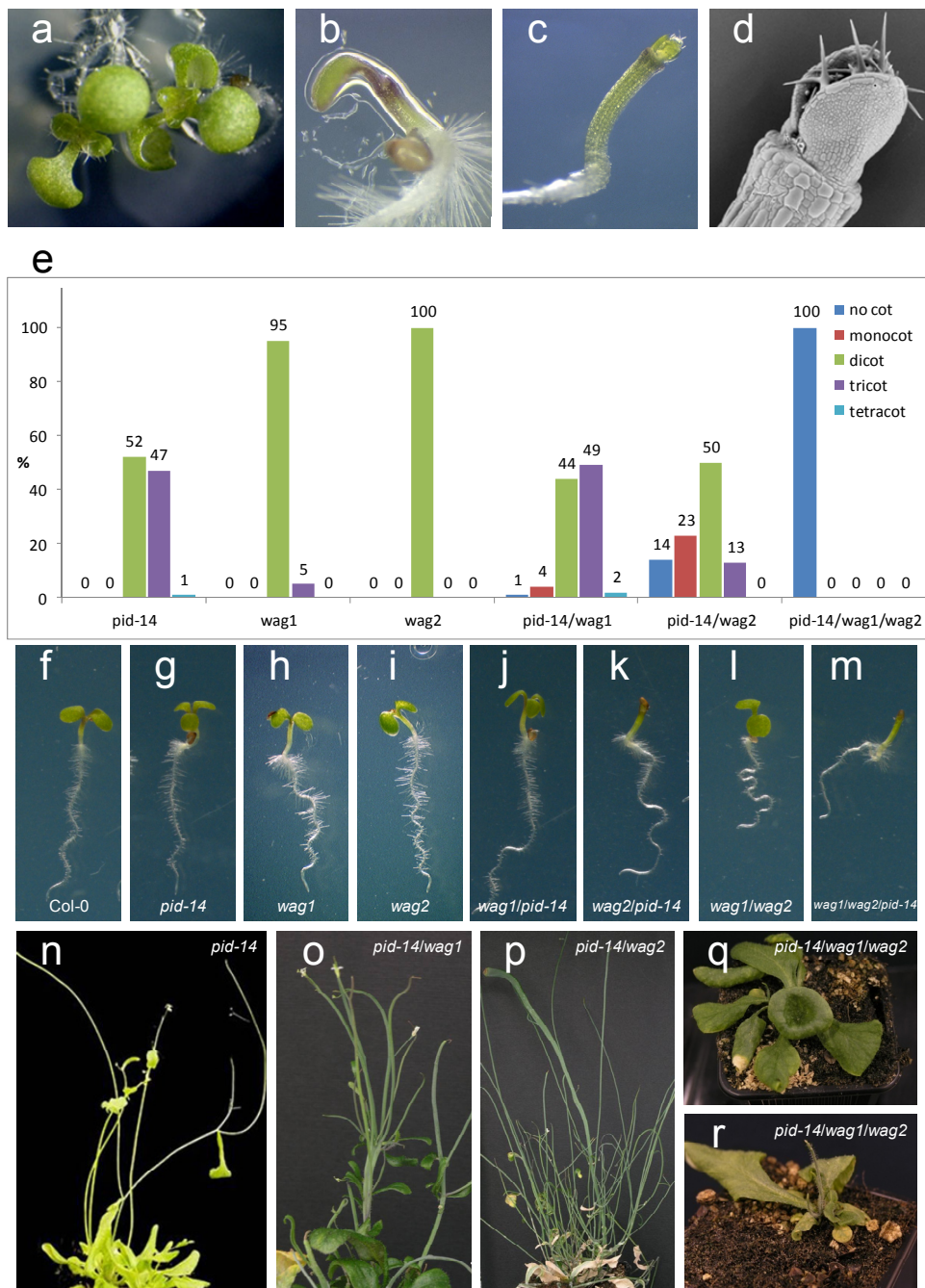


Figure 2 PID and WAG protein kinases act redundantly, and are essential for cotyledon development, gravitropic root growth, and leaf and inflorescence development.

(a-d) Cotyledon phenotypes. (a) a di- and tricotyledon seedling in a *pid-14/+* segregating population. (b) monocot *wag2/pid-14* seedling, (c) *wag1/wag2/pid-14* seedling without cotyledons, (d) scanning electromicroscopy detail of the apex of a no-cot seedling. (e) Frequency of cotyledon defects observed in different mutant combinations. (f-m) Root phenotypes of indicated single, double and triple mutants. (n-r) Adult plant phenotypes of the indicated double and triple mutants.

the YFP reporter in the *wag1/wag2* mutant background. Selected lines homozygous for a single *WAG1pro::WAG1:YFP* or *WAG2pro::WAG2:YFP* locus showed a waving pattern comparable to that of respectively the *wag2* or the *wag1* single mutant, showing that our constructs are complementing and that the fusion proteins are functional (Supplemental figure 1a-c). Despite the observed rescue, we could not visualize the expression of the WAG:YFP fusion proteins using confocal microscopy, suggesting that the proteins are subjected to a rapid turnover. Both genes were expressed in the root tip according to previous reported promoter GUS lines (Supplemental figure 1d-g)[23]. When grown on 45° inclined 1.5% agar plates *pid-14* seedlings displayed wild type root growth (Figure 2f and g), whereas *wag1* or *wag2* seedling roots were slightly more wavy (Figure 2h and i), *pid-14/wag1* or *pid-14/wag2* double mutant roots showed a similar waving phenotype as roots of the corresponding single *wag* mutant, and *wag1/wag2* double mutant roots showed an enhanced waving (Figure 2j-l). Interestingly, *pid-14/wag1/wag2* triple mutant seedlings roots were shorter and were partially agravitropic (Figure 2m), indicating that the *PID* and *WAG* genes also act redundantly in root growth and are essential for gravitropism. Moreover, we observed that the short roots of the *pid-14/wag1/wag2* triple mutant seedlings did not develop lateral roots. Analysis of *pid-14/wag2* double mutant seedlings showed, however, that the lack of lateral roots was a secondary effect of the absence of cotyledons, as monocot *pid-14/wag2* seedlings did show lateral root development, and the nocot seedlings did make lateral roots when the first leaves appeared. This observation is consistent with previous observations showing that early [33].

Single *wag1* or *wag2* or double mutant plants did not show clear defects in vegetative and inflorescence development [23]. In contrast, *pid-14/wag1* and *pid-14/wag2* double mutants showed inflorescence phenotypes that are also observed for strong *pin1* alleles or *pin1pid* double mutants [3], such as fasciated pin-like structures, leaf curling, and loss of apical dominance (Figure 2n-p). Moreover, *pid-14/wag1/wag2* triple mutant plants formed a reduced number of rosette leaves, which were curled and occasionally fused or cup shaped, and eventually developed few short pin-like inflorescences (Figure 2q and r). Interestingly, a single copy of wild type *PID* is sufficient to restore inflorescence development, indicating that *PID* function is dominant,

but the enhanced phenotypes in the double and triple mutants show that the WAG kinases act partially redundant during inflorescence development.

PID and WAG-dependent PIN localization

To investigate whether the observed phenotypes in the triple mutant were the result of changes in subcellular localization of PIN proteins, we performed whole mount immunolocalization on progeny of a *pid-14+/wag1/wag2* plant. Immunolocalisation of PIN1 in embryos showed that the apical PIN1 localization observed in the epidermis of cotyledon primordia of wild type embryos (Figure 3a and b) was lost in the apical dome of triple mutant embryos (Figure 3c and d). Furthermore, immunodetection of PIN1 and PIN2 in 5 days old seedling roots showed that single or double mutants of *pid-14*, *wag1* and *wag2* did not affect PIN1 or PIN2 subcellular localization (Figure 3e-h, Supplemental figure 1h-i). However, the partially agravitropic *pid-14/wag1/wag2* triple mutants showed a loss of PIN2 membrane localization in lateral root cap cells, and a switch in subcellular localization to the basal (root tip facing) side of epidermis cells close to the meristem (Figure 3i). A single copy of the *PID* gene is sufficient to reestablish PIN2 apical localization and to restore gravitropic root growth (Figure 3j). Interestingly, epidermis cells more distal to the meristem still showed apical (shoot tip facing) localization (Figure 3i), suggesting that PIN2 polar targeting in these cells is controlled by a PID/WAG-independent pathway. Our data indicate that the WAG kinases act redundantly with PID to regulate PIN polarity during embryogenesis, root gravitropism and aerial organ development.

WAG1 and AGC3-4 but not WAG2 partially complement *pid* developmental defects

The above conclusion implies that all four kinases direct apical PIN polar targeting in different tissues in the plant, however, polar PIN localization can be apical, lateral or basal, and many cell types show apico-lateral, baso-lateral, or even apolar localization [1;2;14;18;34]. A crucial question thus is whether phosphorylation by these four kinases labels PINs for the same or for different recycling routes? To address this question we placed the *kinase:YFP* fusion genes under control of the *PID* promoter and transformed *pid-14+/wag1/wag2* plants with the resulting constructs. Primary transformants (T1)

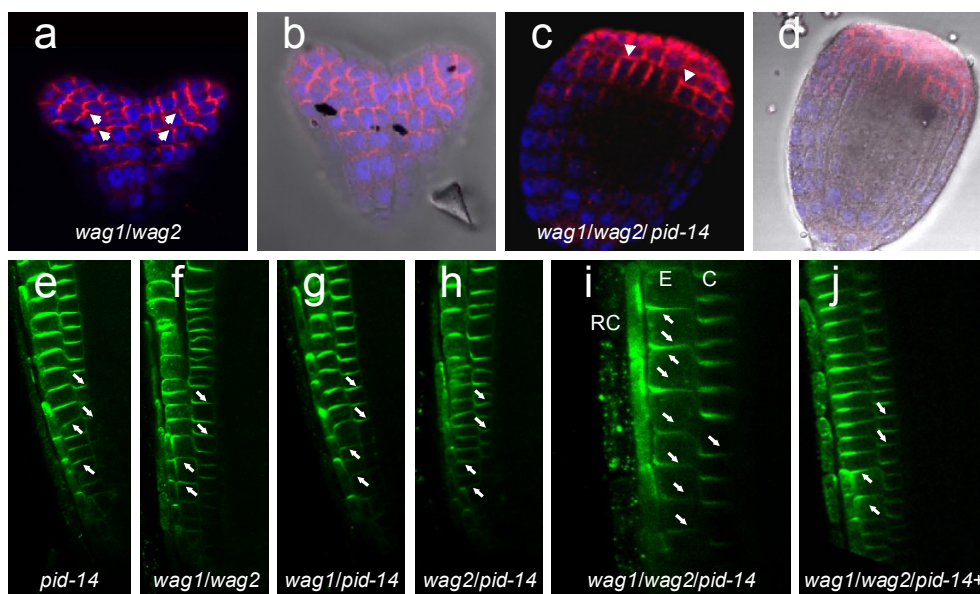


Figure 3 PID and the WAG kinases are required for proper apical localization of PIN proteins during embryo development and gravitropic root growth.

(a-b) Whole mount immunolocalisation of PIN1 in *wag1/wag2* (a, b) or *wag1/wag2/pid-14* (c,d) embryos.

(e-j) Whole mount immunolocalisation of PIN2 in roots of 5 days old seedlings of the indicated single, double and triple mutants. The PIN polarity is indicated by white arrows. RC: lateral root cap; E: epidermis; C: cortex.

genotyped homozygous for the *pid-14* mutation were grown and scored for complementation of the triple mutant inflorescence phenotypes (Table 1). Respectively 64% and 61% of the *PIDpro::PID:YFP* and *PIDpro::WAG1:YFP* containing triple mutant T1 plants developed normal inflorescences (Table 1, Figure 4a,b), indicating that PID and WAG1 do act in a similar way on PIN polarity. The complementation by *PIDpro::WAG1:YFP* was weak, since for most of the complementing lines T2 plants showed *pid* phenotypes (Figure 4c-e), whereas this was not the case for the complementation by *PIDpro::PID:YFP*. In contrast, none of the *PIDpro::WAG2:YFP* and *PIDpro::AGC3-4:YFP* containing triple mutant plants were fertile and all showed pin-like inflorescences (Table 1, Figure 4f and g), indicating that WAG2 and AGC3-4 cannot functionally replace PID. The inflorescences, however, were significantly longer than those of the *pid-14/wag1/wag2* triple mutant, suggesting that *PIDpro::WAG2:YFP* and *PIDpro::AGC3-4:YFP* do alleviate some aspects of the triple mutant phenotype (Figure 4f,g). In addition, *PIDpro::AGC3-4:YFP* transgenic lines occasionally showed

fasciation at the inflorescence apex, suggesting that there is differentiation between WAG2 and AGC3-4 function. To corroborate that the pin-like structures on the lines were caused by mislocalization of PIN1 on the L1 layer of the shoot apical meristem (SAM), we have crossed all lines with *pid⁺/wag1/wag2/PIN1pro::PIN1:GFP* and looked at the F1 generation. Triple loss-of-function of *PID* and *WAGs* complemented with *PIDpro::WAG2:YFP* showed apolar localization of PIN1:GFP in the L1 layer (Figure 4i). Interestingly, *PIDpro::WAG1:YFP* which showed partial complementation of the inflorescence could restored apical localization of PIN1:GFP in certain cells (Figure 4h), suggesting that *PID* and *WAG1* might have similar functions in organ initiation and inflorescence development.

Table 1. Testing AGC3 kinase complementation of the *pid-14/wag1/wag2* mutant by promoter swap analysis

Construct	<i>wag1/wag2/pid-14</i> Hm ^r	Inflorescence	
		WT	<i>pid</i>
<i>PIDpro::PID:YFP</i>	17	64%	36%
<i>PIDpro::WAG1:YFP</i>	18	61%	39%
<i>PIDpro::WAG2:YFP</i>	30	0%	100%
<i>PIDpro::AGC3-4:YFP</i>	15	0%	100%

Column 3 indicates the percentages of the hygromycin resistant primary transformants with the *wag1/wag2/pid-14* genotype (Column 2) that show either wild type of *pid* inflorescence development.

Next, we investigated whether AGC kinases can restore the initiation of cotyledons during embryogenesis in the *pid-14/wag1/wag2* mutant background. Transgenic lines expressing *PIDpro::PID:YFP* restored the initiation of cotyledons. However, 24% of the seedlings showed three cotyledons (Supplemental table 1). Transformants lines containing *PIDpro::WAG1:YFP* and *PIDpro::AGC3-4:YFP* showed a partial restoration reflected in the decrease number of seedlings lacking cotyledons, from 21% to respectively 7% and 15% (Supplemental table 1). Moreover *PIDpro::WAG2:YFP* showed no complementation as the percentage of seedlings lacking cotyledons were similar to the observed in the *pid-14/wag1/wag2* mutant. Our results

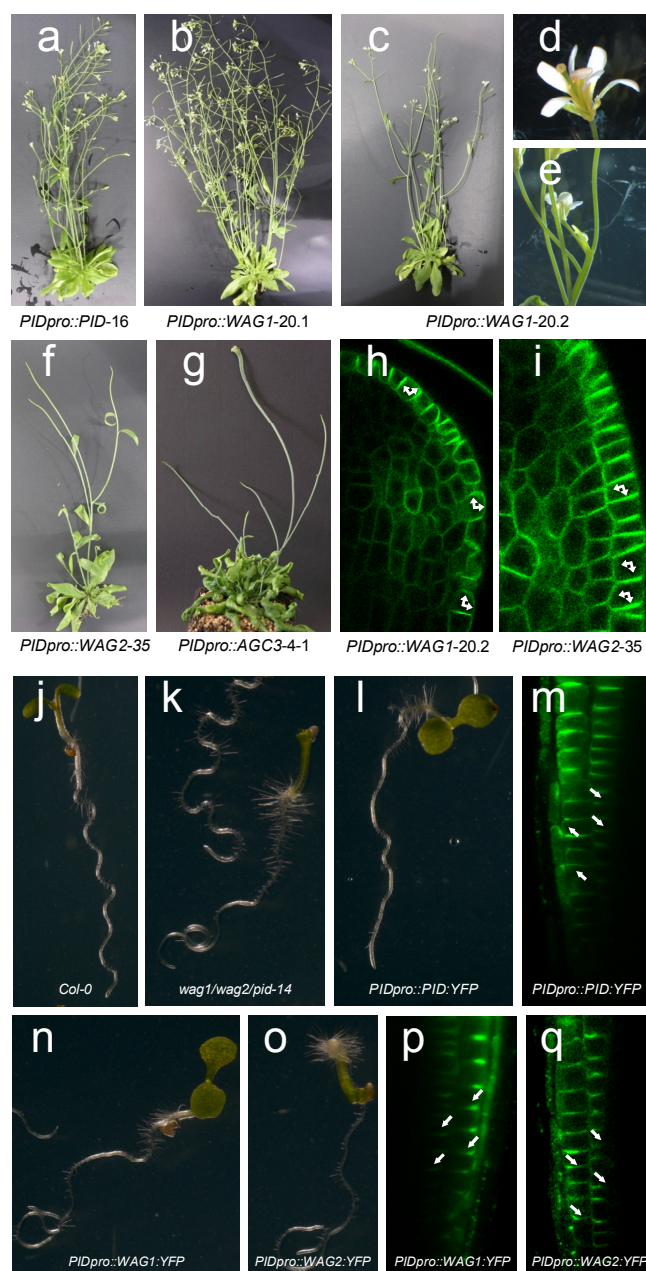


Figure 4 Promoter swap analysis of the AGC3 kinases showing that PID and WAG1 but not WAG2 or AGC3-4 can complement the *pid-14/wag1/wag2* inflorescence phenotypes.

(a-g) Adult phenotype of *wag1/wag2/pid-14* T2 plants transgenic for *PIDpro::PID:YFP* (a), *PIDpro::WAG1:YFP* (b-e), *PIDpro::WAG2:YFP* (f), *PIDpro::AGC3-4:YFP* (g).

(h-i) Subcellular localization of PIN1:GFP in inflorescence apex of *wag1/wag2/pid-14* plants transgenic for *PIDpro::WAG1:YFP* (h), *PIDpro::WAG2:YFP* (i). The polarity of PIN1:GFP is indicated by white arrows.

(j-q) Root morphology of wild type (j), *wag1/wag2/pid-14* (k), or *wag1/wag2/pid-14* containing *PIDpro::PID:YFP* (l), *PIDpro::WAG1:YFP* (n), *PIDpro::WAG2:YFP* (o), and whole mount

Figure 4 (*continued*)

immunolocalisation of PIN2 in 5 days old seedling roots of *wag1/wag2/pid-14* containing *PIDpro::PID:YFP* (m), *PIDpro::WAG1:YFP* (p), *PIDpro::WAG2:YFP* (q). PIN2 polarity is indicated by white arrows.

indicate that WAG1 and AGC3-4 but not WAG2 partially complement *pinoid* function during embryogenesis.

Because of the overlapping expression patterns of WAGs and PID kinases in the root tip and the observed reduced gravitropism in the *pid-14/wag1/wag2* (Figure 3 and Supplemental figure 1) mutant we test if WAG expression could restore root growth. Transgenic lines containing *PIDpro::PID:YFP* in the *pid-14/wag1/wag2* mutant background, showed WT root growth following the gravity axis in vertical plates (Figure 4j-l). Restoration of gravitropic growth correlated with the restoration of PIN2 apical localization in the epidermal cell layer close to the meristem (Figure 4m). Interestingly, *PIDpro::WAG1:YFP* or *PIDpro::WAG2:YFP* transgenic lines showed a reduced gravitropic growth and mislocalization of PIN2 in epidermal cells of the root meristem, similar to what is observed in the *pid-14/wag1/wag2* mutant background (Figure 3j, Figure 4n-q). Our data indicate that the WAGs can not replace PID when expressed under control of the *PID* promoter.

WAG2 mediated localization of PIN proteins

The partial complementation observed indicates that WAG2 and AGC3-4 might have different effect on the polarity of PIN proteins than PID and WAG1. To test this possibility, we established transgenic lines expressing *PID:mRFP1*, *WAG1:YFP* and *WAG2:YFP* under control of the strong *Cauliflower Mosaic Virus 35S* promoter. *PID* overexpression mainly has effect on young seedling development, causing agravitropic growth and eventually collapse of the main root meristem, as a result of a general basal-to-apical shift in PIN polarity that the drains organizing auxin maximum [17]. Interestingly overexpression of *WAG1:YFP* and *WAG2:YFP* resulted in the same phenotypic characteristics as overexpression of *PID* or *PID:mRFP1* (Figure 5d-i), and correlating with an basal-to-apical shift in PIN2 and PIN1 localization in respectively the lower cortex cells (Figure 5e) or the central cylinder (Supplemental figure 2). The results

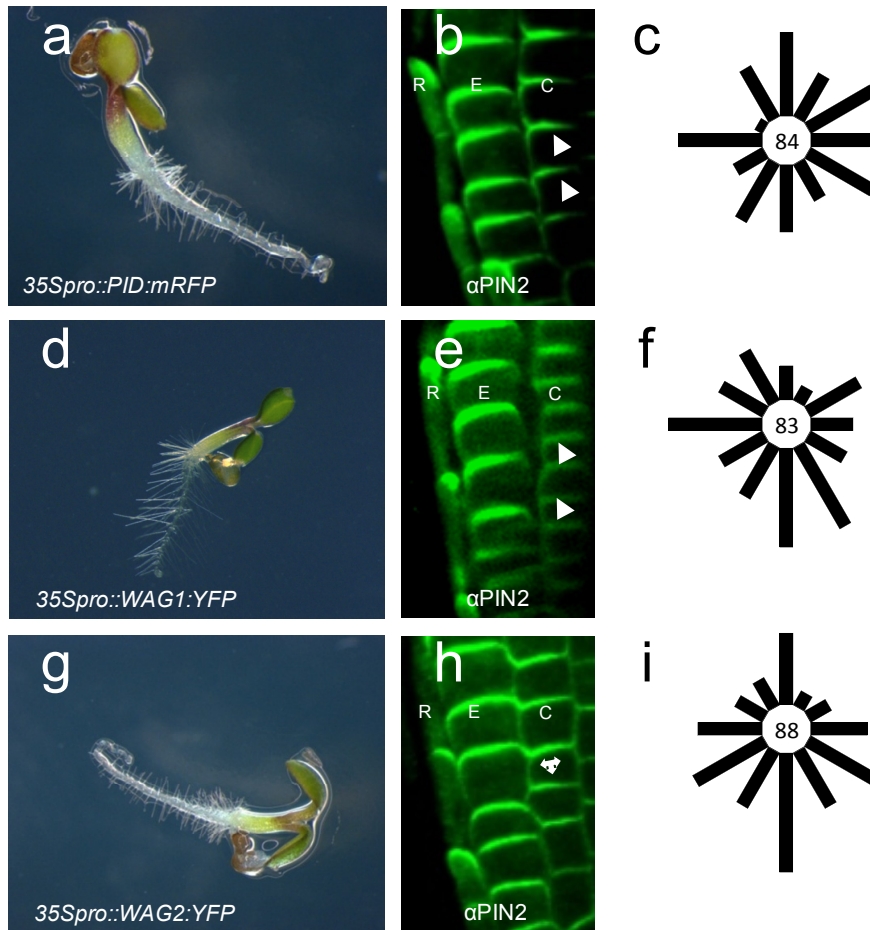


Figure 5 Overexpression of PID, WAG1 and WAG2 in young seedlings shows that the three AGC3 kinases act redundantly in apical PIN polar targeting.

(a, d, g) Morphology of 5 days old *35Spro::PID:mRFP* (a), *35Spro::WAG1:YFP* (d), and *35Spro::WAG2:YFP* (g). (b, e, h). Whole mount immunolocalisation of PIN2 in 3 days old *35Spro::PID:mRFP* (b), *35Spro::WAG1:YFP* (e), and *35Spro::WAG2:YFP* (h) seedlings. (c, f, i) Quantification of the gravitropic response of 3 days old *35Spro::PID:mRFP* (c), *35Spro::WAG1:YFP* (f), and *35Spro::WAG2:YFP* (i) seedlings roots grown on vertical plates, by categorizing the angle of the root with the gravity axis in intervals of 30°, from which percentages were calculated. The number at the center represents the number of roots measured.

indicate that in roots PID, WAG1 and WAG2 act in the similar manner on PIN polar targeting, resulting in asymmetric recruitment of PIN proteins to the apical plasma membrane.

AGC3 kinase mediated PIN localization is required for phototropic growth

The capacity of plants to direct their growth towards a unidirectional light source, or phototropism, allows them to position their leaves for optimal light perception. Until now, few component involved in the phototropic growth have been identified. The blue light photoreceptor PHOTOTOPIN1 initiates a complex signal transduction cascade at the light side of the hypocotyl that leads to differential PIN3-dependent lateral transport of auxin lateral, resulting in the establishment of an auxin maximum in the epidermis at the dark side of the hypocotyl [14;35]. Since PID and WAGs are able to phosphorylate PINHL(Figure 1e), we tested loss and gain-of function mutants for defects in phototropic response. Dark-germinated seedlings were exposed for 4 hours to a unidirectional low-intensity light source, and hypocotyl bending was quantified by measuring the angle of the hypocotyl tip with the seedlings axis (Supplemental figure 3). Whereas *pid-14* or *wag2* loss of function mutants responded like wild type seedlings, *wag1* and

Table 2. Phototropic response of AGC3 kinase loss- and gain-of-function mutants

Line	Av °	SD	n
Col-0	68	20	81
<i>wag2</i>	63	22	43
<i>wag1</i> *	54	22	62
<i>wag1/wag2</i> *	53	13	53
<i>pin3</i> *	26	18	60
<i>35Spro::PID 21</i> *	8	12	23
<i>phot1</i> *	3	6	23

*** Significant difference from Col-0 ANOVA (0.05)**

wag1/wag2 double mutant showed a slight but significant reduction in phototropic response compare to the wild type (Col-0) seedlings (Table 2 and Supplemental figure 3). The delay in phototropic response in these mutants was not as strong as that in *pin3* (Table 2 and Supplemental figure 3), suggesting that *WAG1* might be important in the primary response, probably by regulating *PIN3* dependent lateral transport. Furthermore, *35Spro::PID 21* was unable to respond to directional light to the same extent as *phot1* (Table 2 and Supplemental figure 3), suggesting that PID overexpression overrules PHOT1-induced differential changes in PIN3 polarity in the hypocotyl.

Discussion

Polar auxin transport (PAT) is an active and directed process that is tightly regulated throughout plant development. Despite the extensive efforts in the characterization of the regulatory network of PAT, the molecular and cellular mechanism of PIN-mediated auxin transport is still poorly understood [36]. Nevertheless, an essential role for phosphorylation has recently been established in the regulation of the subcellular polar localization of PIN proteins [19;36]. PID and the protein phosphatase 2A (PP2A) are until now the only known determinants of the establishment of PIN polarity and directionality of auxin gradients [19]. Here we present evidence that AGC3 kinases are key components in the regulation of PIN polarity through direct phosphorylation, and their function is essential for plant development and growth.

AGC3 kinases dependent phosphorylation control PIN subcellular localization

A central question in plant developmental biology is how cells are capable to establish PIN polarity required for the generation of auxin gradients and maxima that control plant development. Currently, it is known that PIN polarity depends on its primary structure and on cell specific sorting machineries capable to identify and read these intrinsic PIN signals [10]. The discovery of PID as key regulator in establishing apical sub cellular localization of PIN proteins through direct phosphorylation has provided a plausible molecular mechanism of the signals that determine PIN polarity [18;19]. The apical-to-basal switch of PIN1 in the epidermal cell layer of the shoot apical meristem in loss-of-function *pid* mutants, the observed opposite effect with PID overexpression in the root, and the direct phosphorylation of the hydrophilic loop provide evidence for a direct effect of PID in the regulation of PIN proteins. However, PIN2 remains apical in the root epidermis in *pid* mutants, suggesting that other components might be involved. Our results show that WAG1, WAG2 and PID protein kinases act redundantly in the regulation of PIN2 apical polarity. The observed apical-to-basal switch of PIN2 localization on the root epidermis in *pid-14/wag1/wag2* mutant plants together with the *in vitro* phosphorylation supports this hypothesis. Whether all three kinases phosphorylate the same residues on the PIN hydrophilic loop still needs to be determined. Moreover,

overexpression of *WAG1* and *WAG2* in the root leads to apicalization of PIN1 in the stele, causing root collapse as has been described previously for PID [18]. Interestingly, in *WAG2* overexpression lines PIN2 subcellular localization in the cortex cell layer is rather apolar than apical, suggesting that PID and WAG1 phosphorylation signals act differently than WAG2 on the establishment of PIN polarity in this cell type.

Redundant and differential action of AGC3 kinases in programmed and adaptive plant development

Here we investigated the possible role of the three PID-like AGC3 protein kinases (*WAG1*, *WAG2* and *AGC3-4*) as regulators of polar auxin transport. Like PID, the three kinases are plasma membrane-associated and can phosphorylate the PINHL *in vitro*. Moreover, detailed analysis of loss- and gain-of-function mutant lines showed that *WAG1* and *WAG2* act redundantly with PID in instructing apical polar targeting of PIN proteins. However, promoter swap complementation experiments where the four AGC3 kinases were placed in the PID expression domain in the *pid-14/wag1/wag2* triple mutant background suggested that *WAG2* and *AGC3-4* may also act in parallel pathways and thus have different effect on PIN polarity in these tissues.

The differential action by *WAG1* and *WAG2* can also be observed in the *pid-14/wag* double and triple mutant phenotypes. For example, the effect of the *pid-14/wag1* double mutation on cotyledon development is mild compared to the *pid-14/wag2* double, where seedlings without cotyledons were observed, a phenotype that is fully penetrant for the *pid-14/wag1/wag2* triple mutant. Another example for a possible differential action of PID and *WAG2* has been identified during fruit development, where a shift in PIN3 polarity from apical to apolar coincides with repression of *PID* and induction of *WAG2* by the *INDEHISCENCE (IND)* transcription factor, resulting in an auxin minimum that specifies the dehiscence zone [6]. All these results raise the question how a differential action of similar kinases can be brought about. Recent data suggest that all four AGC3 kinases phosphorylate the same residues in the PIN hydrophilic loop (Huang *et al.*, in prep), which is in line with the redundant rather than the differential action of the kinases. The differential action of the kinases is therefore more likely to depend on cell-type of tissue-specific factors, such as binding proteins, or on the differential stability or activity

of the kinases. For one thing, WAG2 was found to be much more active in *in vitro* phosphorylation reactions than the other AGC3 kinases, and might thus induce a higher overall phosphorylation of PIN proteins. Since phosphorylation of PIN proteins is supposed to be reversible [19] and dynamic polarity switches are thought to be important for proper phyllotactic patterning [37], this higher phosphorylation activity might thus preclude dephosphorylation and thus lead to defective inflorescence development, as observed in the promoter swap experiments.

One of the kinases for which the functional analysis needs to be finalized is AGC3-4. Data by Cheng and coworkers suggest that the *pid/wag1/wag2/agc3-4* quadruple loss-of-function mutant shows the same phenotype as the *pid/wag1/wag2* triple mutant [28]. However, our preliminary analysis of an *agc3-4* mutant allele, with a T-DNA insertion in the first exon, suggests that homozygous mutant progeny can not be obtained, possibly due to problems during gametophyte development. This suggests that AGC3-4 is involved in different developmental processes as the other AGC3 kinases, and may explain its lack of complementation in the promoter swap experiment. Future research should reveal the exact role of this kinase.

Based on the phenotypes of the *pid* loss-of-function mutant in the embryo and inflorescence, the PID kinase has initially been considered as regulator of programmed plant development. However, the strong wavy root phenotype of the *wag1/wag2* double mutant [23] and the recent observation that *pid* mutant roots are affected in gravitropic growth indicate a role for the AGC3 kinases in adaptive plant development. This role is further corroborated by the reduced phototropic response of the *wag1* single and *wag1/wag2* double mutants, and the agravitropic roots of the *pid-14/wag1/wag2* triple mutant. It is likely that environmental signals act on these kinases through their upstream regulators, such as the calcium binding proteins TCH3 (Chapter 2) and PBP1 (Chapter 3), and the phosphoinositide dependent kinase (PDK1, Chapter 4).

In conclusion, our findings indicate that the AGC3 kinases act both redundantly and differentially in programmed plant development as well as in developmental plasticity in response to environmental stimuli, and that they orient plant development by instructing the subcellular distribution of the PIN auxin efflux carriers.

Materials and Methods

Molecular cloning and constructs

Molecular cloning was performed following standard procedures [38]. Primers used for cloning are listed in Table 1. Bacteria were grown on LC medium supplemented with 100 µg/ml carbenicillin (Cb) or 10 µg/ml gentamicin for *E. coli* strain DH5α containing *pDONR207*, *pART7* or *pGEX*-based plasmids, or 50 µg/ml kanamycin (Km) for in *E. coli* strain DH5α or *Agrobacterium tumefaciens* strain AGL1 containing *pGreenII*-based binary vectors [39]. For AGL1 20 µg/ml rifampicin was included in the LC medium. The construct *pGEX-PIN2HL* construct was described previously [19;34]. For *pART7*-based destination vectors the recombination cassette was inserted in frame with the *YFP*, *CFP* or *mRFP1* coding region between the *CaMV 35S* promoter and, the *CaMV 35S* terminator. For the *pGEX*-based destination vector, the recombination cassette was inserted in frame with the *GST* coding region. For the *pGreenII*-based destination vector, the recombination cassette in frame with the *YFP* coding region and the *CaMV 35S* terminator was excised from the *pART7*-based destination vector and cloned into *pGreenII0179*. The coding regions of *PID* and *AGC3-4* were amplified from *Arabidopsis thaliana* ecotype Columbia (Col-0) cDNA from siliques using respectively primer sets attB1 PIN3HL - attB2 PIN3HL, attB1 PIN7HL - attB2 PIN7HL, PID attB F - PID -Stop attB R, and AT2 attB F - AT2 -Stop attB R. The genomic clones for *WAG1* and *WAG2* comprising respectively 3205bp and 3402bp upstream from the ATG, were amplified from *Arabidopsis thaliana* Col-0 genomic DNA using respectively primer sets attB1 WAG1pWAG1 3 F - WAG1 -Stop attB R, and attB1 WAG2p 2 F - WAG2 -Stop attB R. Coding regions for *WAG* genes were PCR amplified from *Arabidopsis thaliana* Col-0 genomic DNA using respectively primer sets WAG1 attB F - WAG1 -Stop attB R, and WAG2 attB F - WAG2 -Stop attB R. Expression vectors *pGEX-PID*, *pGEX-WAG1*, *pGEX-WAG2*, *pGEX-AGC3-4*, *pART7-PID:CFP*, *pART7-PID:mRFP*, *pART7-WAG1:YFP*, *pART7-WAG1:CFP*, *pART7-WAG2:YFP*, *pART7-WAG2:CFP* and *pART7-AGC3-4:CFP* were constructed using the Gateway Technology (Invitrogen). BP reactions were performed in *pDONR207* according to manufacturer's instructions (Invitrogen). LR reactions were performed in either the *pGEX*-based destination vector for N terminal

fusions with the Glutathione-S-transferase (GST), or the *pART7*-based destination plasmids (Galvan-Ampudia and Robert, unpublished). Overexpression cassettes containing the genes of interest were digested with *Not I* and cloned into *pGreenII* binary vectors for *Agrobacterium*-mediated transformation of *Arabidopsis thaliana*. Binary vectors *pGreenII0179 WAG1pro::WAG1:YFP* and *pGreenII0179 WAG2pro::WAG2:YFP* were cloned using the *pGreenII0179YFP* destination vector (Galvan-Ampudia, unpublished). The promoter region of *PID* (3065bp upstream of the start codon) was amplified from *Arabidopsis thaliana* Col-0 genomic DNA using the primer set PID prom XhoI F - PID prom XhoI R and cloned into the *pGEM-T* Easy vector (Promega). From this plasmid the *PID* promoter fragment was excised as a *Xho I* fragment and cloned into the *pGreenII0179YFP* destination vector (Galvan-Ampudia, unpublished). Expression vectors *pGreenII0179 PIDpro::PID:YFP*, *pGreenII0179 PIDpro::WAG1:YFP*, *pGreenII0179 PIDpro::WAG2:YFP* and *pGreenII0179 PIDpro::AGC3-4:YFP* were constructed using the Gateway technology (Invitrogen).

Table 1: Primer list

PID attB F	5'GGGGACAAGTTTGTACAAAAAAGCAGGCTTCAGCATGTTACGAGAATCAGACGGT3'
PID -Stop attB R	5'GGGGACCACTTTGTACAAAGAAAGCTGGGTCAAAGTAATCGAACGCCGTGG3'
AT2 attB F	5' GGGGACAAGTTTGTACAAAAAAGCAGGCTTCAGCATGGCTAATTCTAGTATCTTT 3'
AT2 -Stop attB R	5' GGGGACCACTTTGTACAAAGAAAGCTGGGTCAAATAATCAAAATAATTAGA 3'
attB1 WAG1pWAG1 3 F	5'GGGGACAAGTTTGTACAAAAAAGCAGGCTTATATGATGTCGTAAGTGTATT3'
WAG1 attB F	5'GGGGACAAGTTTGTACAAAAAAGCAGGCTTCAGCATGGAAGACGACGGTTATTAC3'
WAG1 -Stop attB R	5'GGGGACCACTTTGTACAAAGAAAGCTGGGTCTAGCTTTTACCCACATAATG3'
attB1 WAG2p 2 F	5'GGGGACAAGTTTGTACAAAAAAGCAGGCTTAGGATGTGTTGTGTCCTTTGT3'
WAG2 attB F	5'GGGGACAAGTTTGTACAAAAAAGCAGGCTTCAGCATGGAACAAGAAGATTCTAT3'
WAG2 -Stop attB R	5'GGGGACCACTTTGTACAAAGAAAGCTGGGTCAACGCGTTTGCRACTCGCGTA3'
PID prom XhoI F	5'TACTCGAGCCGAACCAATCTAGCAATA3'
PID prom XhoI R	5'ATCTCGAGCGCCGGGAAAATCGAAGTTAAATCAAGA3'
PIDex1 F1	5'TCTCTCCGCCAGGTA AAAA3'
PIDex2 R1	5'CGCAAGACTCGTTGGAAAAG3'
N502056 F	5'TCTCGCAGCTCAAGCCTAAC3'
N502056 R	5'CACCAATCTACACCGCTTCCG3'
N570240 F	5'TCTTCTACGACGAAGCGACGG3'
N570240 R	5'CTATCAAGTCTCCAATGTCTTCTTT3'
N588841 F	5'GCCGATTTTACAAGGATCAGGT3'
N588841 R	5'CCCATGAAGGAAAGGGAAGA3'

attB recombination sites are underlined

Protein purification

The *E. coli* Rosetta strain (Novagen) was transformed with the constructs encoding GST-tagged PID, WAG1, WAG2, AGC3-4 and PIN2HL. Single colonies were grown overnight at 37°C in liquid LC medium containing carbenicillin (100 µg/ml) and chloramphenicol (34 µg/ml). Cultures were diluted 1/20 in 100 ml of fresh LC medium containing the same antibiotics and grown at 37°C until OD600 was 0.8, then after addition of IPTG at 1 mM final concentration, cultures were grown at 30°C for 4 hr. Bacteria were pelleted by centrifugation at 4000 x g for 20 min at 4°C and stored at -20°C.

For the purification of GST-tagged proteins, frozen bacterial pellets were resuspended in of Extraction Buffer (150 mM NaCl, 2 mM KCl, 2 mM KH₂PO₄, 10 mM Na₂HPO₄, 2 mM EDTA, 2 mM EGTA, 10 mM DTT) and incubated on ice for 10 min. After sonication for 2 min, Triton X-100 was added to a final concentration of 1 % and the mixture was incubated for 5 min on ice, followed by centrifugation at 15,000 x g for 20 min at 4°C. Supernatants were added to 400 µl of pre-equilibrated 50% Glutathione Sepharose 4B beads (GE Amersham) and incubated for 1 hr. Beads were washed three times with Extraction Buffer. Purified proteins were recovered with Elution buffer (10 mM reduced glutathione, 50 mM Tris-HCl pH 8.0) and analyzed by SDS-PAGE, blotted on a PDVF membrane (Millipore, USA) and immunodetected using anti-GST (Molecular Probes) according to the manufacturer's instructions.

***In vitro* phosphorylation assays**

GST-tagged proteins were purified as described above. *In vitro* phosphorylation assays were performed in a final volume of 20 µl with 1X kinase buffer (25 mM Tris-HCl pH 7.5, 5 mM MgCl₂, 2 mM CaCl₂ and 1 mM DTT), 1 µg of purified GST-tagged kinase, 2 µg GST-PIN2HL, 100 µM ATP and 1 µCi [γ -³²P] ATP (3000 Ci/mM) (GE Amersham). Reactions were incubated at 30°C for 30 min and stopped by adding 5 µl of 5X SDS loading buffer (0.3125 M Tris-HCl pH 6.8, 10% SDS, 50% glycerol, 7.5 M β -mercaptoethanol and 0.125% bromophenol blue) and boiled for 5 min. Samples were separated by SDS-PAGE. After electrophoresis gels were washed 3 times with 5% of

TCA and 1% Na₂H₂P₄O₇, Coomassie stained, dried and exposed to a phospho-imager screen (Molecular Dynamics).

Protoplast transfection

Protoplasts were isolated from *Arabidopsis thaliana* Col-0 cell suspension culture and 10 µg plasmid DNA was introduced by PEG-mediated transfection as described originally by Axelos and co-workers [40] and adapted by Schirawski and co-workers [41]. Following transfection, the protoplasts were incubated for at least 16h. Images were obtained by laser scanning confocal microscopy.

Confocal microscopy

For the protoplasts experiments, a Leica DM IRBE confocal laser scanning microscope was used with a 63X water objective, digital zoom and 51% laser intensity. The fluorescence was visualized with an Argon laser for excitation at 514 nm (YFP) and 457 nm (CFP) with 525-545 nm and 465-495 nm emission filters, respectively. Whole mount immunolocalisations of PIN1 and PIN2 were done as previously described [2;19;42] using anti-PIN1 and anti-PIN2 antibodies that were kindly provided by Jiri Friml and Christian Luschnig, respectively.

Arabidopsis thaliana roots and shoot apical meristems were observed using a 40X oil objective with a ZEISS Axioplan microscope equipped with a confocal laser scanning unit (MRC1024ES, BioRad, Hercules, CA). Fluorescence was monitored with a 522-532 nm band pass emission filter (488 nm excitation). All images were recorded using a 3CCD Sony DKC5000 digital camera. The images were processed by ImageJ (<http://rsb.info.nih.gov/ij/>).

***Arabidopsis* lines, plant growth and transformation**

The *pid-14* (SALK_049736), *wag1* (SALK_002056), *wag2* (SALK_070240), and *phot1* (SALK_088841) were obtained from NASC [43]. The *pid-14* mutant contains a T-DNA inserted in the intron and shows developmental defects similar to those reported for strong *pid* alleles [30]. The *wag1* and *wag2* mutants contain a T-DNA inserted in the coding region and have been previously characterized as null mutants [23]. For the

detection of the T-DNA, gene-specific primers and insertion-specific primer LB1a were used (PIDex1 F1 - PIDex2 R1 for *pid-14*, N502056 F - N502056 R for *wag1*, N570240 F - N570240 R for *wag2*, and N588841 F - N588841 R for *phot1*). The *pin3.3* loss-of-function mutant was kindly provided by Jiri Friml [14]. *Arabidopsis* seeds were surface-sterilized by incubation for 10 min in a 50% commercial bleach solution and rinsed five times with sterile water. Seeds were vernalized for 5 days in dark at 4°C and germinated (21°C, 16 h-photoperiod and 42 $\mu\text{mol}/\text{m}^2/\text{s}$) on solid MA medium supplemented with antibiotics when required [44]. Two- to three-weeks old plants were transferred to soil and grown at 21°C and 70% relative humidity with a 16 hr photoperiod (140 $\mu\text{mol}/\text{m}^2/\text{s}$). *Arabidopsis thaliana* Col-0 was transformed by the floral dip method as described [45]. Primary transformants were selected on medium supplemented with 20 $\mu\text{g}/\text{ml}$ hygromycin (Hm) for pGreenII0179 constructs or 30 $\mu\text{g}/\text{ml}$ phosphinothricin (PPT) for pGreenII0229 and 100 $\mu\text{g}/\text{ml}$ timentin to inhibit the *Agrobacterium* growth. For further analysis, single locus insertion lines were selected by germination on 20 $\mu\text{g}/\text{ml}$ Hm or 30 $\mu\text{g}/\text{ml}$ PPT.

Biological assays

For the phenotypic analysis of the crosses, about 400 seeds were plated in triplicate, germinated and grown for one week on solid MA medium. The number of cotyledon defects was counted and the penetrance of the phenotypes was calculated based on a 1:3 segregation ratio for homozygous *pid-14* seedlings.

Phototropic assays were performed by germinating seedlings in dark for 5 days on 60° inclined petri dishes, followed by exposing them for four hours to unilateral light (4.94 $\mu\text{mol}/\text{m}^2/\text{s}$). Hypocotyl bending was determined from digital images, using the Sony DKC 5000 3CCD camera, as the angle of the tip relative to the main axis of the seedling. Processing of the data was done using the Custom Software Application ImageJ (freeware available from the NIH at <http://rsb.info.nih.gov/ij/>). Statistical differences were calculated using ANOVA.

Accession Numbers

The *Arabidopsis* Genome Initiative locus identifiers for the genes mentioned in this chapter are as follows: *PID* (At2g34650), *WAG1* (At1g53700), *WAG2* (At3g14370), *AGC3-4* (At2g26700), *PHOT1* (At3g45780), *PIN2* (At5g57090).

Acknowledgments

The authors thank Gerda Lamers, Ward de Winter and Werner Helvesteyn for their help with respectively microscopy, tissue culture and technical assistance. This work was funded through grants from the Chinese Science Council (F.H.) and the Research Council for Earth and Life Sciences (ALW 813.06.004) and from the Netherlands Organisation for Health Research and Development (ZON 050-71-023), and with financial aid from the Dutch Organization of Scientific Research (NWO).

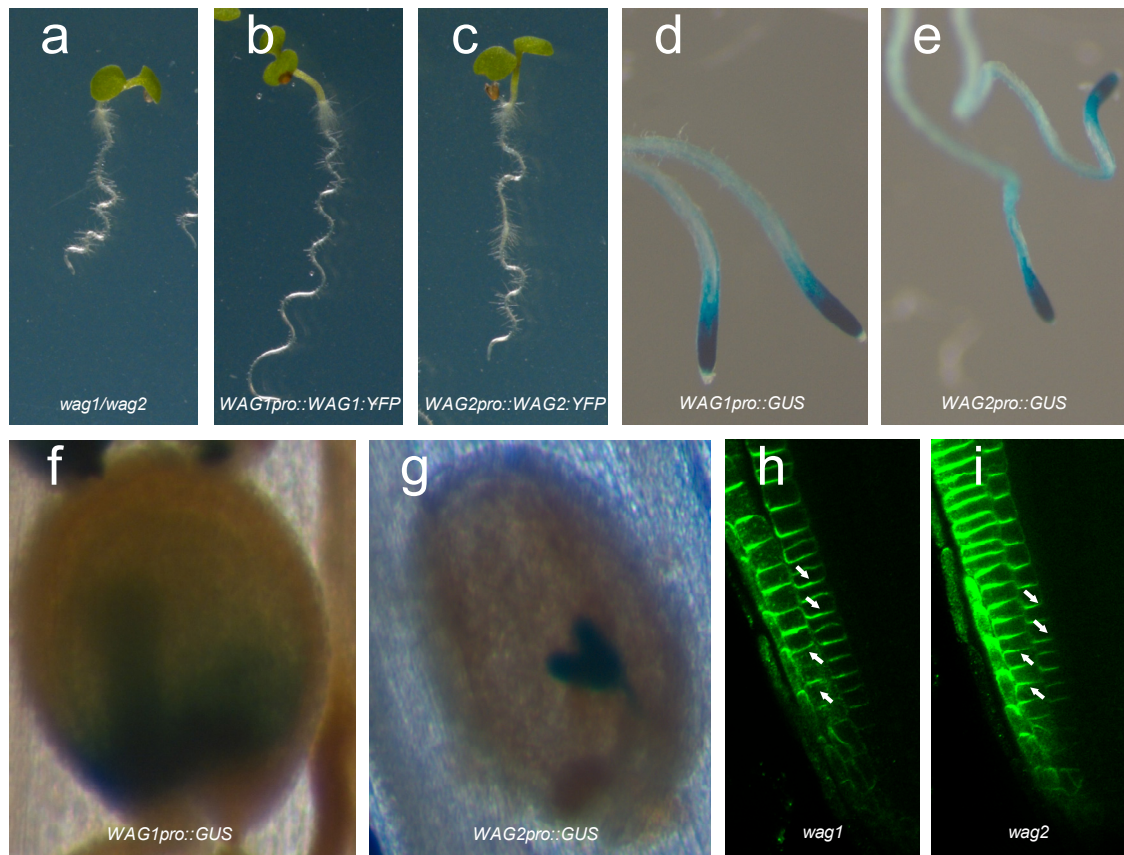
Reference List

1. Benková E, Michniewicz M, Sauer M, Teichmann T, Seifertová D, Jürgens G, Friml J (2003). **Local, efflux-dependent auxin gradients as a common module for plant organ formation.** *Cell*. 115(5), 591-602.
2. Friml J, Vieten A, Sauer M, Weijers D, Schwarz H, Hamann T, Offringa R, Jürgens G (2003). **Efflux-dependent auxin gradients establish the apical-basal axis of *Arabidopsis*.** *Nature*. 426(6963), 147-153.
3. Okada K, Ueda J, Komaki MK, Bell CJ, Shimura Y (1991). **Requirement of the Auxin Polar Transport System in Early Stages of *Arabidopsis* Floral Bud Formation.** *Plant Cell*. 3(7), 677-684.
4. Reinhardt D, Mandel T, Kuhlemeier C (2000). **Auxin regulates the initiation and radial position of plant lateral organs.** *Plant Cell*. 12(4), 507-518.
5. Reinhardt D, Pesce ER, Stieger P, Mandel T, Baltensperger K, Bennett M, Traas J, Friml J, Kuhlemeier C (2003). **Regulation of phyllotaxis by polar auxin transport.** *Nature*. 426(6964), 255-260.
6. Sorefan K, Girin T, Liljegren SJ, Ljung K, Robles P, Galván-Ampudia CS, Offringa R, Friml J, Yanofsky MF, Ostergaard L (2009). **A regulated auxin minimum is required for seed dispersal in *Arabidopsis*.** *Nature*. 459(7246), 583-586.
7. Tanaka H, Dhonukshe P, Brewer PB, Friml J (2006). **Spatiotemporal asymmetric auxin distribution: a means to coordinate plant development.** *Cell Mol. Life Sci*. 63(23), 2738-2754.
8. Petrášek J, Mravec J, Bouchard R, Blakeslee JJ, Abas M, Seifertová D, Wisniewska J, Tadele Z, Kubes M, Covanová M, Dhonukshe P, Skupa P, Benková E, Perry L, Krecek P, Lee OR, Fink GR, Geisler M, Murphy AS, Luschnig C, Zazimalova E, Friml J (2006). **PIN Proteins Perform a Rate-Limiting Function in Cellular Auxin Efflux.** *Science*. 312, 914-918.
9. Vieten A, Sauer M, Brewer PB, Friml J (2007). **Molecular and cellular aspects of auxin-transport-mediated development.** *Trends Plant Sci*. 12(4), 160-168.
10. Wisniewska J, Xu J, Seifertová D, Brewer PB, Ruzicka K, Blilou I, Rouquié D, Benková E, Scheres B, Friml J (2006). **Polar PIN localization directs auxin flow in plants.** *Science*. 312(5775), 883.
11. Aida M, Vernoux T, Furutani M, Traas J, Tasaka M (2002). **Roles of PIN-FORMED1 and MONOPTEROS in pattern formation of the apical region of the *Arabidopsis* embryo.** *Development*. 129(17), 3965-3974.

12. Luschnig C, Gaxiola RA, Grisafi P, Fink GR (1998). **EIR1, a root-specific protein involved in auxin transport, is required for gravitropism in *Arabidopsis thaliana*.** *Genes Dev.* 12(14), 2175-2187.
13. Muller A, Guan C, Galweiler L, Tanzler P, Huijser P, Marchant A, Parry G, Bennett M, Wisman E, Palme K (1998). **AtPIN2 defines a locus of *Arabidopsis* for root gravitropism control.** *EMBO J.* 17(23), 6903-6911.
14. Friml J, Wisniewska J, Benková E, Mendgen K, Palme K (2002). **Lateral relocation of auxin efflux regulator PIN3 mediates tropism in *Arabidopsis*.** *Nature.* 415(6873), 806-809.
15. Friml J, Benkova E, Blilou I, Wisniewska J, Hamann T, Ljung K, Woody S, Sandberg G, Scheres B, Jurgens G, Palme K (2002). **AtPIN4 mediates sink-driven auxin gradients and root patterning in *Arabidopsis*.** *Cell.* 108(5), 661-673.
16. Weijers D, Sauer M, Meurette O, Friml J, Ljung K, Sandberg G, Hooykaas P, Offringa R (2005). **Maintenance of embryonic auxin distribution for apical-basal patterning by PIN-FORMED-dependent auxin transport in *Arabidopsis*.** *Plant Cell.* 17(9), 2517-2526.
17. Benjamins R, Quint A, Weijers D, Hooykaas P, Offringa R (2001). **The PINOID protein kinase regulates organ development in *Arabidopsis* by enhancing polar auxin transport.** *Development.* 128(20), 4057-4067.
18. Friml J, Yang X, Michniewicz M, Weijers D, Quint A, Tietz O, Benjamins R, Ouwwerkerk PBF, Ljung K, Sandberg G, Hooykaas PJJ, Palme K, Offringa R (2004). **A PINOID-dependent binary switch in apical-basal PIN polar targeting directs auxin efflux.** *Science.* 306(5697), 862-865.
19. Michniewicz M, Zago MK, Abas L, Weijers D, Schweighofer A, Meskiene I, Heisler MG, Ohno C, Huang F, Weigel D, Meyerowitz EM, Luschnig C, Offringa R, Friml J (2007). **Phosphatase 2A and PID kinase activities antagonistically mediate PIN phosphorylation and apical/basal targeting in *Arabidopsis*.** *Cell.* 130(6), 1044-1056.
20. Bennett SRM, Alvarez J, Bossinger G, Smyth DR (1995). **Morphogenesis in Pinoid Mutants of *Arabidopsis thaliana*.** *Plant Journal.* 8(4), 505-520.
21. Sukumar P, Edwards KS, Rahman A, DeLong A, Muday GK (2009). **PINOID kinase regulates root gravitropism through modulation of PIN2-dependent basipetal auxin transport in *Arabidopsis thaliana*.** *Plant Physiol.*
22. Ma J, Khanna R, Fukasawa-Akada T, Poisso J, Deitzer GF, Watson JC (1998). **PK3At (Accession No. AF082391): An *Arabidopsis* homolog of the PsPK3 protein kinase from *Pisum sativum* L.** *Plant Physiol.* 118, 712.

23. Santner AA, Watson JC (2006). **The WAG1 and WAG2 protein kinases negatively regulate root waving in *Arabidopsis***. *Plant J.* 45(5), 752-764.
24. Boonsirichai K, Guan C, Chen R, Masson PH (2002). **Root gravitropism: an experimental tool to investigate basic cellular and molecular processes underlying mechanosensing and signal transmission in plants**. *Annu. Rev. Plant Biol.* 53:421-47., 421-447.
25. Massa GD, Gilroy S (2003). **Touch modulates gravity sensing to regulate the growth of primary roots of *Arabidopsis thaliana***. *Plant J.* 33(3), 435-445.
26. Oliva M, Dunand C (2007). **Waving and skewing: how gravity and the surface of growth media affect root development in *Arabidopsis***. *New Phytol.* 176(1), 37-43.
27. Galvan-Ampudia CS, Offringa R (2007). **Plant evolution: AGC kinases tell the auxin tale**. *Trends Plant Sci.* 12(12), 541-547.
28. Cheng Y, Qin G, Dai X, Zhao Y (2008). **NPY genes and AGC kinases define two key steps in auxin-mediated organogenesis in *Arabidopsis***. *Proc. Natl. Acad. Sci. USA.* 105(52), 21017-21022.
29. Zourelidou M, Muller I, Willige BC, Nill C, Jikumaru Y, Li H, Schwechheimer C (2009). **The polarly localized D6 PROTEIN KINASE is required for efficient auxin transport in *Arabidopsis thaliana***. *Development.* 136(4), 627-636.
30. Bennett SRM, Alvarez J, Bossinger G, Smyth DR (1995). **Morphogenesis in *pinoid* mutants of *Arabidopsis thaliana***. *Plant Journal.* 8(4), 505-520.
31. Christensen SK, Dagenais N, Chory J, Weigel D (2000). **Regulation of auxin response by the protein kinase PINOID**. *Cell.* 100(4), 469-478.
32. Furutani M, Vernoux T, Traas J, Kato T, Tasaka M, Aida M (2004). **PIN-FORMED1 and PINOID regulate boundary formation and cotyledon development in *Arabidopsis* embryogenesis**. *Development.* 131(20), 5021-5030.
33. Bhalerao RP, Eklof J, Ljung K, Marchant A, Bennett M, Sandberg G (2002). **Shoot-derived auxin is essential for early lateral root emergence in *Arabidopsis* seedlings**. *Plant J.* 29(3), 325-332.
34. Abas L, Benjamins R, Malenica N, Paciorek T, Wisniewska J, Moulinier-Anzola JC, Sieberer T, Friml J, Luschnig C (2006). **Intracellular trafficking and proteolysis of the *Arabidopsis* auxin-efflux facilitator PIN2 are involved in root gravitropism**. *Nat. Cell Biol.* 8(3), 249-256.
35. Liscum E, Briggs WR (1995). **Mutations in the *NPH1* locus of *Arabidopsis* disrupt the perception of phototropic stimuli**. *Plant Cell* 7(4), 473-485.

36. Kleine-Vehn J, Friml J (2008). **Polar targeting and endocytic recycling in auxin-dependent plant development.** *Annu. Rev. Cell Dev. Biol.* 24:447-73., 447-473.
37. Heisler MG, Ohno C, Das P, Sieber P, Reddy GV, Long JA, Meyerowitz EM (2005). **Patterns of auxin transport and gene expression during primordium development revealed by live imaging of the *Arabidopsis* inflorescence meristem.** *Curr. Biol.* 15(21), 1899-1911.
38. Sambrook J, Fritsch F., Maniatis T. (1989) **Molecular cloning - A laboratory Manual.** Edited by C.Nolan. Cold Spring Harbor Laboratory press, NY, USA.
39. Hellens RP, Edwards EA, Leyland NR, Bean S, Mullineaux PM (2000). **pGreen: a versatile and flexible binary Ti vector for *Agrobacterium*-mediated plant transformation.** *Plant Mol. Biol.* 42(6), 819-832.
40. Axelos M, Curie C, Mazzolini L, Bardet C, Lescure B (1992). **A protocol for transient gene-expression in *Arabidopsis thaliana* protoplasts isolated from cell-suspension cultures.** *Plant Physiology and Biochemistry.* 30(1), 123-128.
41. Schirawski J, Planchais S, Haenni AL (2000). **An improved protocol for the preparation of protoplasts from an established *Arabidopsis thaliana* cell suspension culture and infection with RNA of turnip yellow mosaic tymovirus: a simple and reliable method.** *Journal of Virological Methods.* 86(1), 85-94.
42. Friml J, Benkova E, Mayer U, Palme K, Muster G (2003). **Automated whole mount localisation techniques for plant seedlings.** *Plant J.* 34(1), 115-124.
43. Alonso JM, Stepanova AN, Lisse TJ, Kim CJ, Chen H, Shinn P, Stevenson DK, Zimmerman J, Barajas P, Cheuk R, Gadrinab C, Heller C, Jeske A, Koesema E, Meyers CC, Parker H, Prednis L, Ansari Y, Choy N, Deen H, Geralt M, Hazari N, Hom E, Karnes M, Mulholland C, Ndubaku R, Schmidt I, Guzman P, Aguilar-Henonin L, Schmid M, Weigel D, Carter DE, Marchand T, Risseeuw E, Brogden D, Zeko A, Crosby WL, Berry CC, Ecker JR (2003). **Genome-Wide Insertional Mutagenesis of *Arabidopsis thaliana*.** *Science.* 301(5633), 653-657.
44. Masson J, Paszkowski J (1992). **The Culture Response of *Arabidopsis-Thaliana* Protoplasts Is Determined by the Growth-Conditions of Donor Plants.** *Plant Journal.* 2(5), 829-833.
45. Clough SJ, Bent AF (1998). **Floral dip: a simplified method for *Agrobacterium*-mediated transformation of *Arabidopsis thaliana*.** *Plant J.* 16(6), 735-743.

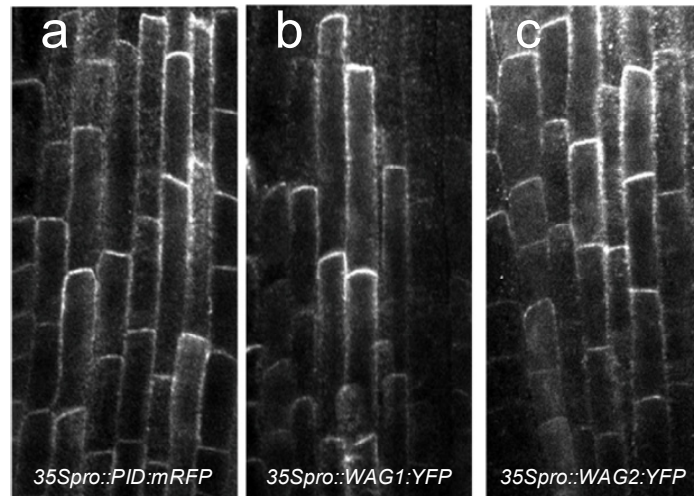


Supplemental figure 1 WAGs expression pattern.

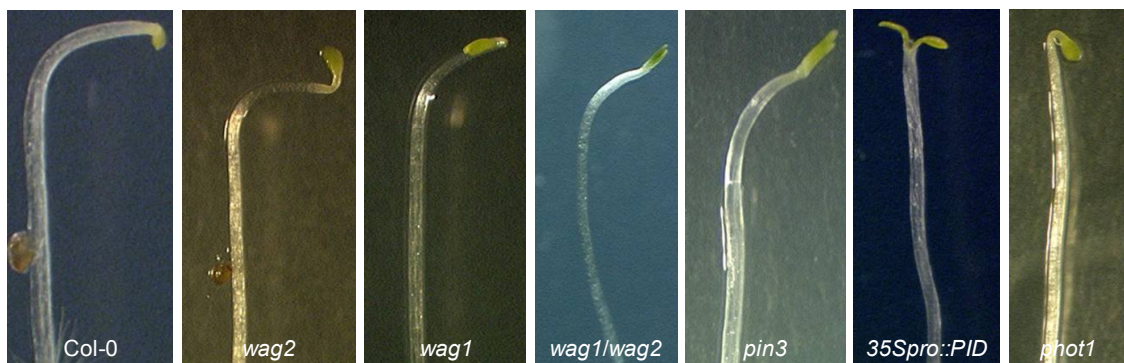
(a-c) The short and wavy root phenotype of the *wag1/wag2* double mutant (a) is complemented by either the *WAG1pro::WAG1:YFP* (b) or the *WAG2pro::WAG2:YFP* (c) transgene.

(d-g) Expression pattern of *WAG1pro* (d and f) or *WAG2pro* (e and g) driving the *GUS* reporter gene in 7 days old seedlings root tip (d and e) and late heart stage embryos (f and g).

(h-i) Whole mount immunolocalisation of PIN2 in roots of *wag1* and *wag2* single mutants.



Supplemental Figure 2 Apical PIN1 localization in primary roots of seedlings overexpressing AGC3 kinases. (a-c) Whole mount immunolabeling of PIN1 in three days old seedling roots overexpressing *PID:mRFP* (a), *WAG1:YFP* (b) or *WAG2:YFP* (c).



Supplemental Figure 3 Phototropic response of AGC3 kinase loss- and gain-of-function mutants. Representative picture of indicated mutants in phototropic assays. Dark grown seedlings were germinated 5 days in dark and exposed to 4 hrs of directional light.

Supplemental table 1. Percentage of embryo defects in T2 transformant lines.

Genotype	Number of cotyledons				n
	0	1	2	3	
<i>wag1/wag2/pid14±</i>	21		79		121
<i>wag1/wag2/pid14/PIDpro::PID:VENUS:YFP-16</i>			76	24	92
<i>wag1/wag2/pid14/PIDpro::WAG1:YFP-20</i>	7	4	64	25	75
<i>wag1/wag2/pid14±/PIDpro::WAG2:YFP-47</i>	26	1	73		82
<i>wag1/wag2/pid14±/PIDpro::AGC3-4:YFP-9</i>	15		84	1	82

SUMMARY

Plant development follows strict programs producing uniform body plans and organs, however, it can be flexible during vegetative growth. In view of the predominantly sessile nature of plants, this flexible development is crucial to enable adaptation to changes in the environment. Plants have developed mechanisms to constantly monitor their surroundings in order to be able sense changes in their environment. The initial observations of Darwin on the growth responses of canary grass coleoptiles have set the basis in plant developmental biology on the understanding of how environmental signals, such as light and gravity, modulate plant growth and architecture by causing changes in the distribution of the plant hormone auxin (indole-3-acetic acid). Now it is well-established that auxin is transported from cell-to-cell in a polar fashion from its sites of synthesis to its sites of action. This polar auxin transport (PAT) generates auxin gradients and maxima that mediate tropic growth responses, embryo development, meristem maintenance and organ positioning.

The distribution of auxin within the tissues is controlled by three types of plasma membrane (PM) proteins, the AUX1/LAX auxin influx carriers, the P glycoprotein (PGP) type of ABC transporters, and the PIN auxin efflux carriers. The PIN proteins are considered to be the primary drivers of transport that determine the direction of auxin flow through their asymmetric subcellular distribution. The PIN proteins cycle via actin-mediated vesicle transport between PM and endosomal compartments, and this cyclic vesicle transport is essential for polarity establishment. Although the exact mechanism of PIN polarity establishment is still elusive, the first identified component in this pathway is the plant AGC protein serine/threonine kinase PINOID (PID). PID instructs apical (shoot meristem facing) PIN polarity, and acts antagonistically with protein phosphatase 2A (PP2A) in determining the phosphorylation status of the PIN proteins.

PID belongs to the plant-specific AGCVIII group of protein kinases (named after protein kinase A (PKA), cyclic GMP-dependent protein kinase (PKG) and protein kinase C (PKC)), which have unique structural features. In *Chapter 1* is present an extensive bioinformatic analysis of these protein kinases and propose a classification for these subfamily. Only for the blue light receptors phototropins (PHOTs, AGC4) and the PID-related kinases (AGC3) a role in auxin-mediated plant development has been well-established. On one hand, light-activated phototropins induce rapid Ca^{2+} release into the

cytosol and initiate differential auxin transport leading to auxin accumulation in the cell layers at the dark side of the hypocotyl. On the other hand, PID, and possibly other AGC3 kinases, direct PAT by determining the correct polar localization of PIN proteins during embryo development and organ formation in the shoot apical meristem.

Although none of the AGC3 kinases has been directly connected to phototropic growth, the observation that the activity of PID is regulated by interacting calcium-binding proteins, named TOUCH3 (TCH3)(*Chapter 2*) and PINOID BINDING PROTEIN1 (PBP1)(*Chapter3*), suggests that these kinases might be downstream components of the phototropin signal-transduction pathway. Based on our analysis, we propose that those AGCVIII kinases that play an essential role in plant development, recapitulate plant evolution. Phototropins represent the most ancient AGCVIII kinase forms that regulate highly conserved processes in plants like optimization of light perception and AGC3 kinases co-evolved with PIN auxin transporters in multicellular plants during their colonization of land, and act together, possibly downstream of the phototropins, to orient plant development by establishing the directionality of auxin transport.

Chapter 2 presents a detailed study of the in vivo interaction between PID and TCH3. Using loss- and gain-of-function mutant lines, we confirm in vitro observations that TCH3 is a negative regulator of the PINOID kinase activity. This regulation occurs directly by inhibition of the kinase activity, as shown in phosphorylation assays, and by sequestration of PID from the plasma membrane. Interestingly, auxin treatment also results in rapid transient re-localization of the membrane-associated kinase to the cytosol.

Chapter 3 describes the functional and genetic analysis of the PID-PBP1 interaction to elucidate the regulatory role of PBP1, also named KRP2 (for KIC-related protein2), as it is part of a small protein family that includes the close PBP1 homolog PBP1H/KRP1 and KIC (KCBP-interacting Calcium binding protein). In vitro experiments show that PID contains two major PBP1-binding sites and that PBP1 not only enhances PID kinase activity but also changes its substrate recognition signature. Using *Arabidopsis thaliana* protoplasts we tested the effect of PBP1 on PID membrane localization. Our results show that PBP1 sequester PID from the PM into the cytosol. Moreover, we characterized combinations of *Arabidopsis* loss- and gain-of-function

mutant lines of PBP1, PBP1H and PID. Our results indicate that PBP1 and PBP1H act redundantly to enhance PID kinase activity during embryo development, and that they partly suppress root growth, possibly through their stimulatory effect on PID. PBP1 overexpression partially inhibits auxin-induced calcium-dependent sequestration of PID from the plasma membrane, suggesting that apart from enhancing the activity of the PID kinase, PBP1 also influence PID subcellular localization. These data confirm previous *in vitro* data, indicating a role for PBP1 and PBP1H as positive regulators of PID kinase activity, and extend the function of these small EF-hand proteins to that of regulators of subcellular PID localisation.

As a PIN polarity determinant, PID is an excellent target for the regulation of the direction of transport by external stimuli through upstream regulators, such as 3-phosphoinositide-dependent kinase 1 (PDK1). PDK1-dependent phosphorylation is a conserved eukaryotic mechanism for the regulation of many signal transduction pathways downstream of AGC protein kinases. PDK1 phosphorylates PID on two well-conserved residues of the activation loop (Ser 288 and Ser 290) resulting in enhanced kinase activity towards a generic substrate *in vitro*. PDK1 is a conserved gene among eukaryotes that regulates and activates other kinases by phosphorylation. As in mammals and yeast, plant PDK1 activates and phosphorylates the activation loop of different AGC protein kinases. In **Chapter 4** we describe the effect of PDK1-dependent phosphorylation of PID at the cellular level, and show that PDK1 causes a change in the subcellular localization of PID from PM to endomembrane structures and microtubules (MT) in *Arabidopsis* cell suspension derived protoplasts. Furthermore, the PDK1 phosphorylation sites in PID were shown to be required for this relocalization. Finally, we provide evidence *in planta*, showing that in osmotic stressed *Arabidopsis* roots, PID is recruited to similar structures as in protoplasts. We present a model in which stress responses initiate a lipid signaling cascade and PDK1-dependent activation of PID, one of the major regulators of polar auxin transport, proposing a direct molecular link between stress responses and auxin-mediated plant development and growth.

AGC3 protein kinases have being implicated to the regulation of polar auxin transport. In *Arabidopsis* loss-of-function single mutants of *WAG1* and *WAG2*, the closes homologues of PID, result in weak root waving phenotype, but double mutants show a

constitutive root waving. Root growth is a highly complex mechanism which is the result of the interaction between gravitropism, thigmotropism and circumnutation. Interestingly, *wag* mutants respond normally to gravity stimulation, indicating that they are involved in root growth, possibly through the regulation of PAT. In **Chapter 4** is described the functional characterization of AGC3 kinases as regulators of PAT. We show that all four AGC3 kinases are plasma membrane associated proteins and are able to phosphorylate the hydrophilic loop of PIN proteins. Furthermore, multiple combinations of double and triple loss-of-function mutants have strong and different pleiotropic defects in plant development. Most important, such developmental defects correlate with changes in PIN polarity in different stages of development. Gene complementation experiments show that AGC3 kinases have partial overlapping functions during plant development. Moreover, we present evidence showing that WAG2 sort PIN proteins at different location than WAG1 and PID. Consistently, we show that WAGs control the early events of phototropism, probably through the regulation of PAT. Our results provide compelling data that AGC3 kinases are partially redundant in regulating PIN polarity through direct phosphorylation and that are essential in the regulation of PAT through plant development and growth.

SAMENVATTING

De ontwikkeling van planten verloopt enerzijds strikt geprogrammeerd, en dit zorgt er onder andere voor dat jonge nakomelingen hetzelfde basale lichaamsplan en bloemen een uniform patroon hebben. Anderzijds, met name gedurende de vegetatieve groei is de ontwikkeling van een plant meer flexibel. Deze flexibiliteit stelt planten in staat zich snel aan veranderingen in hun omgeving aan te passen, wat zeer belangrijk is voor hun sessiele levenswijze. Het plantenhormoon auxine (3-indolazijnzuur) speelt een centrale rol bij zowel de geprogrammeerde als de flexibele ontwikkeling van planten, waarbij ontwikkelingsprocessen gestuurd worden door maxima en minima van dit hormoon gegenereerd door polair cel naar cel transport. De richting van dit polaire auxine transport (PAT) wordt bepaald door asymmetrisch op het plasmamembraan geplaatste membraaneiwitten, de PIN familie van efflux carriers en de P-glycoproteïne (PGP) type ABC transporters. Voor de PIN carriers is een sterke correlatie gevonden tussen hun polaire lokalisatie op het plasmamembraan en de richting van PAT. Daarbij leidt fosforylering van deze PIN eiwitten in hun grote centrale hydrofiele loop door het PINOID (PID) proteïne kinase tot targetting van deze eiwitten naar het apicale (naar de scheut apex gerichte) deel van het plasmamembraan, terwijl defosforylering door PP2A-type proteïne fosfatases leidt tot ophoping van PIN efflux carriers op het basale (naar de wortelpunt gerichte) deel van het plasmamembraan.

Met de in dit proefschrift beschreven onderzoek is de regulatie van PIN polariteit door PID verder onderzocht. PID behoort tot de plant-specifieke klasse van AGCVIII proteïne kinases, vernoemd naar analoge kinases (proteïne kinase A, G en C) die onder andere betrokken zijn bij groeihormoon signaaltransductie in dieren. **Hoofdstuk 1** beschrijft een gedetailleerde *in silico* analyse van de AGCVIII kinase familie. Van de 23 familieleden in *Arabidopsis* is alleen voor de fototropines (AGC4: PHOT1 en PHOT2) en voor PID en een tweetal PID-gerelateerde kinases (AGC3: PID, WAG1, WAG2) tot nu toe een rol in auxine-afhankelijke ontwikkeling van planten beschreven. Fototropines zijn blauwlichtreceptoren die een signaaltransductieketen activeren die uiteindelijk leidt tot accumulatie van auxine aan de donkere zijde van de stengel, waardoor de scheut naar het licht groeit (fototropie). Voor PID is de functie bekend, en mede gezien hun associatie met het plasmamembraan lijkt het zeer waarschijnlijk dat ook de drie andere AGC3 kinases de polaire lokalisatie van PIN eiwitten bepalen. Analyse van beschikbare

plantengenoomsequenties laat zien dat phototropines de oorspronkelijke AGCVIII kinases waren in eencellige algen, en dat de AGC3 subfamilie pas later is ontstaan tegelijkertijd met de PIN auxine efflux carriers in multicellulaire planten gedurende de kolonisatie van het land. Activering van fototropines leidt tot verhoging van het cytosolisch calcium. Het feit dat de AGC3 kinases binden met, en gereguleerd worden door de calciumbindende eiwitten TOUCH3 (TCH3) en PINOID BINDING PROTEIN 1 (PBP1) maakt het aantrekkelijk om te speculeren dat deze kinases betrokken zijn bij het veranderen van PIN polariteit na activering van de fototropines door blauw licht.

Hoofdstuk 2 beschrijft een detailanalyse van de *in vivo* interactie tussen PID en TCH3. De analyses bevestigen de eerdere conclusie dat TCH3 een negatieve regulator is van het PID kinase, en laten zien dat de regulatie niet alleen verloopt via directe inhibitie van kinase activiteit, maar ook via sequestratie van het kinase weg van de PIN phosphoryleringstargets op het plasmamembraan. Interessant genoeg leidt incubatie van PID:VENUS wortels met auxine ook tot sequestratie van PID van het plasmamembraan, en het feit dat dit voorkomen kan worden met calcium transport inhibitor of een calmoduline inhibitor, suggereert dat TCH3 bij deze sequestratie betrokken is.

Hoofdstuk 3 beschrijft een vergelijkbare analyse voor de interactie tussen PID en PBP1. *In vitro* experimenten laten zien dat PID twee bindingsplaatsen voor PBP1 bezit, en dat PBP1 binding niet alleen de activiteit van PID verhoogt, maar ook de specificiteit van het kinase verandert. De nauw verwante homoloog van PBP1 in *Arabidopsis*, PBP1H, bindt ook aan PID en genetische analyses laten zien dat beide eiwitten redundant werken als positieve regulatoren van PID gedurende embryogenese en wortelgroei. In tegenstelling tot TCH3 lijkt PBP1 juist de associatie van PID met het plasmamembraan te stabiliseren. Naast hun directe positieve effect op de PID kinase activiteit, lijken de EF-hand eiwitten PBP1 en PBP1H dus te zorgen voor een optimale specificiteit en lokalisatie van PID ten opzichte van de PIN targets.

Naast TCH3 en PBP1 was het 3-fosfoinositide-afhankelijke kinase 1 (PDK1) eerder geïdentificeerd als regulator van PID. PDK1 is geconserveerd in eukaryoten als positieve regulator van AGC kinase signaaltransductie. Ook in *Arabidopsis* blijkt PDK1 een aantal AGCVIII kinases te activeren waaronder PID. PID is zelfactiverend, maar fosforylering door PDK1 op twee geconserveerde serine residuen (Ser 288 en Ser 290) in

de activeringsloop van het kinase resulteerde in verhoogde kinase activiteit in vitro. In **hoofdstuk 4** is het effect van de fosforylering van PID door PDK1 op cellulair niveau onderzocht. In *Arabidopsis* protoplasten leidt PDK1-afhankelijke fosforylering van PID tot relokalisatie van het kinase van het plasmamembraan naar endomembraanstructuren en microtubuli. Het feit dat in de epidermis van *Arabidopsis* wortels PID wordt gerekruteerd naar vergelijkbare structuren na het toedienen van osmotische stress, een signaal dat geacht wordt PDK1 te activeren en dat leidt tot kortere wortels, suggereert dat deze signaaltransductieroute een functie heeft in de modulering van PAT en dus van groei onder invloed van stress factoren.

Tot slot beschrijft **hoofdstuk 5** het onderzoek naar de rol van de drie andere AGC3 kinases in *Arabidopsis* als regulatoren van PAT. Het onderzoek laat zien dat alle vier de kinases geassocieerd zijn met het plasma-membraan, en dat ze in staat zijn de hydrofiele loop van PIN2 te fosforyleren. Dubbel en triple combinaties tussen *pid*, *wag1* en *wag2* verlies-van-functie mutanten laten zien dat de kinases redundant werken, en dat ontwikkelingsdefecten correleren met veranderingen in PIN polariteit in verschillende stadia van ontwikkeling. WAG1 blijkt daarbij een sturende rol te spelen bij fototrope groei, wat klopt met onze eerdere hypothese dat de AGC3 kinases mogelijk door fototropines worden aangestuurd. Een complementatieexperiment waarbij de vier AGC3 kinases in het PID domein in de *pid wag1 wag2* verlies-van-functie mutant tot expressie zijn gebracht toont echter aan dat WAG2 en AGC3-4 in de scheut anders werken dan PID en WAG1, omdat de eerste twee kinases geen complementatie van de triple mutant geven. Of WAG2 en AGC3-4 in de scheut apex inderdaad een ander effect hebben op de PIN polariteit, of dat de kinases in deze weefsels instabiel zijn of co-regulatoren missen zal nader onderzoek moeten uitwijzen.

Het onderzoek in dit proefschrift laat zien dat niet alleen PID, maar ook de andere drie AGC3 kinases betrokken zijn bij de regulering van PAT door fosforylering van PIN auxine efflux carriers, en dat de kinases niet alleen betrokken zijn bij geprogrammeerde ontwikkeling, maar dat zij mede door hun bindende eiwitten en regulatoren belangrijke schakels zijn in de modulatie van plantenontwikkeling door omgevingssignalen.

Curriculum vitae

Carlos Samuel Galván Ampudia was born on June 12, 1978 in Monterrey, State of Nuevo Leon, Mexico. He attended the Colegio Madrid high school at Mexico City. In 1996, he started the study of Biology at the Universidad Nacional Autonoma de Mexico (UNAM). In 1999, he started his research training in the Plant Molecular Biology department at the Biotechnology Institute (UNAM), under the supervision of Dr. Federico E. Sanchez, and his project involved the functional characterization of Src homology 3 (SH3) domains in *Arabidopsis thaliana*. In 2002, he obtained his BSc in Biology with specialization in bioinformatics and biochemistry. In March 2002, he joined the team of Dr. Remko Offringa, at the Molecular and Developmental Genetics department, Institute of Biology, Leiden University, the Netherlands. He was involved in the molecular and biochemical characterization of the PINOID calcium/calmodulin regulated protein kinase. In 2003, he obtained his MSc in Biology (cum laude). In July 2003, he started as a PhD student in the group of Dr. Remko Offringa on an ALW/NWO funded project (813.06.004) concerning the characterization of plant AGC protein kinases and their role in the regulation of transport of the plant hormone auxin in *Arabidopsis thaliana* (this thesis). During this time he was also involved in the Horizon breakthrough project (050.71.172) concerning the development and validation of a novel randomized peptide-based kinase target microarray (the Pepchip Kinase Sitefinder) as a generic tool in kinomics, in collaboration with PEPSCAN[©] (Lelystad) and Biomolex[©] (Oslo). From September 2008 on, he works as a post-doc in the Plant Physiology department at the Swammerdam Institute for Life Sciences (SILS), Amsterdam University. Under the supervision of Dr. Christa Testerink, he focuses on the characterization of lipid regulated signaling in the crosstalk between environmental stress and plant development.

Publications list

International journals

Sorefan K., Girin T., Liljegren S.J., Ljung K., Robles P., **Galvan-Ampudia C.S.**, Offringa R., Friml J., Yanofsky M.F., and Østergaard L. (2009). A regulated auxin minimum is required for seed dispersal in *Arabidopsis*. *Nature*. 459(7246), 583-586.

Galvan-Ampudia CS, Offringa R (2007). Plant evolution: AGC kinases tell the auxin tale. *Trends Plant Sci.* 12(12), 541-547.

Benjamins R, **Galvan Ampudia CS**, Hooykaas PJ, Offringa R. (2003). PINOID-mediated signaling involves calcium-binding proteins. *Plant Physiol.* 132: 1623-1630.

Contribution to books

Kemel Zago M, **Galvan Ampudia CS** and Offringa R (2007). Signaling in Auxin-Dependent Plant Development. *Plant Cell Monogr.* Ed Laszlo Bögre, Gerrit Beemster. Springer-Verlag Berlin Heidelberg.